

**THE INFLUENCE OF MATERNAL NICOTINE  
EXPOSURE ON NEONATAL RAT TRACHEA  
DEVELOPMENT AND ALVEOLI STATUS.**

**BY**  
**ZELDA VERGOTINE**

The logo of the University of Western Cape, featuring a classical building with a pediment and columns, rendered in a light blue color.

submitted in partial fulfilment of the requirements for the degree of  
M.Sc. in the Department of Physiological Sciences, University of  
Western Cape.

**PROMOTER: Prof. G.S.Maritz**

**CO-PROMOTER: Prof. G.Van Der Horst**

**November 2000**

I *Zelda Verigotine* ..... hereby cede to the University of the Western Cape the entire copyright that may in future subsist in any research report or thesis submitted by me to the University in partial fulfilment of the requirements for the degree of Magister Scientiae in the department of *Physiology* .....



**DEDICATION:**

**I dedicate this document to my sister Ashlene, who passed away on 8 November 1989. YOU ARE ALWAYS IN MY THOUGHTS.**

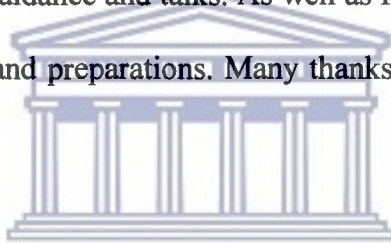
## **Acknowledgements:**

I would like to take this opportunity to express my heartfelt gratitude to the following persons for their assistance during the research and writing of my thesis:

Thank You, Father for giving me the necessary endurance, strength and patience to complete this thesis.

My parents, both who have come a long way with me. This thesis is also yours. Thank you, for your constant support and advice.

Mrs. P.Delport, for all the guidance and talks. As well as for your assistance with all the histological specimens and preparations. Many thanks, for being just across the pathway.



Mr. R.Salie, who assisted me so kindly with the transmission electron microscopy section. Many thanks, for the long chats and “Happy Thoughts”.

Mr. Weitz, for the use of the processing machine at Botany.

Mr. B.Julies and Mr. G.Malgas, thank you both for your assistance at the EM Unit. I have learned so much from both of you.

Prof. G.S.Maritz , Prof. G.Van der Horst , all staff as well as postgraduate students of the Department of Physiological Sciences.

Ms. B.Nicolaai (Boela), for your assistance in taking photos for light microscopy section. Thank you, for being the friend that's always full of ideas.

Heidi Dames, Deidre Clarke (Dee), Ashley Pretorius (Ash). We've all come a long way. I feel blessed with such great friendships. Thank you, for your constant encouragement and faith that this will also come to completion.

Mr. S.Majiet, for strengthening my faith, giving me hope but mostly for your friendship and belief in me.



## **ABSTRACT**

The aim of this study was to determine the effect of maternal nicotine exposure on the status of the rat tracheal development as well as the rat lung of 7 to 42 day old offspring. Wistar dams were injected subcutaneously, using a dosage of 1 mg nicotine/kg body mass/day, and treatment commenced 7 days after conception. The morphological and morphometric data were used to evaluate any damage or change in the structure of the trachea and lungs due to maternal nicotine exposure. Three techniques were used namely, light microscopy, scanning electron microscopy and transmission electron microscopy. Both morphological status and morphometric data were obtained from the sample animals.

The basic haematoxylin and eosin stain was used to view the histological structure of the trachea. Large patches of hyaline cartilage, with chondrocytes embedded in the matrix and surrounded by a perichondrium, were identified. At postnatal days 21 and 42, the nicotine exposed animals appeared to have ruptured chondrocytes within the cell matrix. Significant developmental changes of the chondrocytes in the nicotine exposed animals were evident for postnatal day 7, which includes volume and density changes when compared to the control.

The surface morphology of the tracheal epithelium, the tracheal cartilage and alveoli when exposed to nicotine were compared to the control animals. At postnatal day 42 the nicotine exposed rat pups showed areas of damage to the lacunae within the tracheal cartilage. The alveolar surface of the nicotine exposed pups (7 to 42 days of

age) showed an increasing level of alveolar fenestrations when compared to controls.

Chondrocytes contained well-developed Golgi apparatus, mitochondria, endoplasmic reticulum (ER), nucleus, lipid bodies and cytoplasm at 21 days postnatally. The cytoplasm of the chondrocytes of 21 day old rat pups, also appeared to be similar when compared to that of the 42 day old rats. Changes in the volume density of the ER, of the chondrocytes, for days 7 and 21 old control rat pups were found to be significantly higher ( $P < 0.05$ ) than that of the nicotine exposed rat pups of the same ages. The volume density of the lipid bodies of day 7 old control rat pups was lower than that of postnatal day 7 of the nicotine exposed group ( $P < 0.05$ ).

This study implies that exposure to nicotine during pregnancy and lactation has a damaging effect on the tracheal cartilage, supportive functionality. There is also the possible indication of irreversible change of surface morphology of the tracheal epithelium. The availability of endoplasmic reticulum within the chondrocytes components could have a possible effect in the metabolic activities, which includes the energy supply required for growth and development. This could in turn also effect the capacity of the chondrocytes to synthesize the components of the matrix of the cartilage. As for the alveoli, nicotine exposure showed to have a continuous damaging effect on the lung structure, throughout it's developmental status.

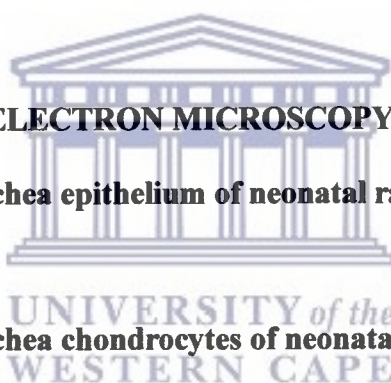
# CONTENTS

HEADING	PAGE(S)
<b>ACKNOWLEDGEMENTS</b>	
<b>ABSTRACT</b>	
<b>CHAPTER 1 : AN OVERVIEW OF PRE- AND POSTNATAL TRACHEA AND LUNG DEVELOPMENT</b>	
<b>1.1 INTRODUCTION</b>	<b>1</b>
<b>1.2 OVERVIEW OF NORMAL TRACHEA AND LUNG DEVELOPMENT IN THE HUMAN</b>	<b>3</b>
1.2.1 Morphogenesis of the human airway epithelium	4
<b>1.3 OVERVIEW OF NORMAL TRACHEA AND LUNG DEVELOPMENT IN THE RAT</b>	<b>6</b>
1.3.1 Development of the rat airways	6
1.3.2 Morphogenesis of the rat airway epithelium	9
<b>1.4 OVERVIEW OF THE CELLULAR MAKE-UP OF THE TRACHEA EPITHELIUM</b>	<b>10</b>
<b>1.5 TRACHEA AND BRONCHIAL CARTILAGE</b>	<b>14</b>
1.5.1 Collagen synthesis	15
1.5.2 Type I collagen	16
1.5.3 Type II collagen	17
<b>1.6 CARTILAGE SYTHESIS AND GROWTH</b>	<b>17</b>
<b>1.7 TRACHEA CARTILAGE MORPHOLOGY</b>	<b>18</b>



<b>1.8</b>	<b>THE BASIS OF CARTILAGE DAMAGE AND HEALING PROCESSES</b>	<b>23</b>
<b>1.9</b>	<b>THE REPAIR RESPONSE OF CARTILAGE TO DAMAGE</b>	<b>25</b>
<b>1.10</b>	<b>ALVEOLAR DEVELOPMENT</b>	<b>26</b>
<b>1.11</b>	<b>EFFECTS OF SMOKE AND NICOTINE ON AIRWAY AND LUNG DEVELOPMENT</b>	<b>27 - 32</b>
1.11.1	Nicotine	27
1.11.2	Smoking	30
<b>1.12</b>	<b>AIMS OF THE PURPOSED STUDY</b>	<b>32</b>
<b>CHAPTER 2:</b>	<b>MATERIALS AND METHODS</b>	
<b>2.1</b>	<b>Experimental animals</b>	<b>33</b>
2.1.2	Trachea tissue excision and preparation	34
<b>2.2</b>	<b>LIGHT MICROSCOPY</b>	<b>37</b>
<b>2.3</b>	<b>SCANNING ELECTRON MICROSCOPY</b>	<b>37</b>
<b>2.4</b>	<b>TRANSMISSION ELECTRON MICROSCOPY</b>	<b>37</b>
2.4.1	Animals	37
2.4.2	Tissue preparation	37
<b>2.5</b>	<b>MORPHOMETRIC DATA</b>	<b>37</b>

<b>CHAPTER 3:</b>	<b>RESULTS</b>	
<b>3.1</b>	<b>LIGHT MICROSCOPY OF THE DEVELOPING RAT</b>	<b>38 - 48</b>
	<b>TRACHEA</b>	
3.1.1	Morphological Status	38
3.1.2	Morphometric Data	44
<b>3.2</b>	<b>SCANNING ELECTRON MICROSCOPY</b>	<b>49 - 65</b>
3.2.1	Trachea Cartilage	51
3.2.2	Trachea Epithelium	56
3.2.3	Alveolar Surface	61
<b>3.3</b>	<b>TRANSMISSION ELECTRON MICROSCOPY</b>	<b>65 - 79</b>
<b>3.3.1</b>	<b>Morphology of trachea epithelium of neonatal rats: Effects of maternal nicotine exposure</b>	<b>65</b>
<b>3.3.2</b>	<b>Morphology of trachea chondrocytes of neonatal rats: Effects of maternal nicotine exposure</b>	<b>69</b>
<b>3.3.3</b>	<b>Morphometric Data</b>	<b>75</b>
<b>CHAPTER 4:</b>	<b>DISCUSSION</b>	<b>80</b>
<b>REFERENCES</b>		<b>94</b>
<b>APPENDIX A</b>		<b>112</b>
<b>APPENDIX B</b>		<b>114</b>
<b>APPENDIX C</b>		<b>117</b>



Depression of fetal breathing movements has been found to result in disturbed growth of airways and alveoli (Wang et al., 1983). Maternal malnutrition is also known to inhibit animal lung growth, and epidemiological data indicates a relationship between adult airway function and birth weight suggesting that intrauterine nutrition in humans may be more important than previously recognized (Shaheen and Barker, 1994; Barker et al., 1991 and Helms, 1995).

To compare the human and rat airway development with respect to diseased states, a description of the normal development and morphology of both systems need to be discussed. In order to establish a background for the investigation of the trachea and alveoli it is necessary therefore to firstly describe the normal development in the following phases:

- (a) Overview of the prenatal and postnatal development of the airways
- (b) Tracheal and bronchial cartilage
- (c) Alveolarisation



The latest available research data concerning the consequences of smoking and nicotine exposure during pregnancy on the fetus and the neonate airway and lung development will also be discussed.

## **1.2 OVERVIEW OF THE NORMAL TRACHEA AND LUNG DEVELOPMENT IN THE HUMAN**

The airways of the human lung begin their development 22 – 26 days postfertilization as a central diverticulum budding from the foregut and lined by epithelium of endodermal origin. In humans the diverticulum forms two small ventrolateral buds (lung primordia) during the following 4 weeks. The trachea then becomes separated from the esophagus by the rostral extension of an epithelial derived septum that forms at the root of the lung buds. As the two ventrolateral buds grow, they become invested by mesenchyme derived from splanchnic mesoderm. The latter condenses and differentiates around the growing bronchial tree to form cartilage, muscle, blood vessels, lymphatics and other connective tissue elements (Jeffery et al., 1992).

The adult pattern of the airways branching is complete by the 18<sup>th</sup> week of gestation (Hislop et al., 1986). However, after birth the size of the tracheobronchial tree increases and the distal (smallest) airways will grow until at least 8 years of life. The airway mucosa of the newborn is not fully developed as the mucus-secreting cells and connective tissue elements, whilst present, must still mature (Jeffery et al., 1992).

The airway epithelium includes the surface epithelium which lines all airways (nose to alveolus) and it is continuous with that forming the tubulo-acinar submucosal mucus-secreting glands which develop from the surface in utero (Jeffery, 1990). The stratified squamous epithelium, which lines much of the larynx, gives way to one which is pseudostratified, ciliated and columnar with secretory cells when the trachea is reached. In man, this type of epithelium persists throughout the major bronchi,

becoming simple cuboidal more peripherally within the lungs. Normally, ciliated cells predominate, interspersed by mucus-secreting (goblet) cells which are found regularly in the tracheobronchial tree but rarely in bronchioles of less than 1mm diameter (Jeffery, 1990).

### 1.2.1 Morphogenesis of the human airway epithelium

There are two types of surface secretory cells known to secrete mucus: the mucous (goblet) and the less frequently found epithelial 'serous' cells (Jeffery, 1990). Histochemically, the presence of intracellular mucus has been demonstrated in the human fetal trachea by the 13<sup>th</sup> week of gestation (Bucher and Reid, 1961 & De Haller, 1969) when ciliated cells are already present. The mucus-secreting cells are sparse or gathered into small groups of cells. The goblet-shaped cells are infrequent, and are distended by their intracellular secretion, which then compresses the nucleus to its base. Like ciliated cells, mucus-secreting cells appear first in the proximal airways and then subsequently develop in the more peripheral airways (Sturgess, 1985). The mucus-secreting cells increase in number and peaks in the middle of gestation when they represent approximately 30 – 35% of the cells lining the luminal surface (Wharton et al., 1978).

Towards the end of the second term of gestation there is a relative decrease in the number of mucus-secreting cells, these being replaced by numerous ciliated cells. There are more mucus secreting cells present in the proximal than in the peripheral airways, during the third term of gestation (Lallemand, 1991). The antiprotease

enzyme antileucoprotease (ALP), present in adult serous gland and Clara cells of human bronchi, has recently been identified in the surface epithelium of the human trachea and bronchi by 20 weeks gestation (Willems et al., 1988). As the submucosal glands of the second term of fetal development are not fully mature and secrete little mucus, the fetal surface secretory cells are probably an important source of the ALP required for the protection of airway epithelium against proteolysis. In addition, the mucus-secreting cells fulfil a role as progenitors of ciliated and other epithelial cell types for the development of the fetal trachea of the hamster (Mc Dowell et al., 1985), monkey (Plopper et al., 1986), and human airways (Gaillard et al., 1989).

Airway submucosal glands appear in the human trachea at about the 13<sup>th</sup> week of gestation. They appear in proximal airways and then progressively more peripherally and reach the main carina some 7 days later. Development of each gland starts within the surface epithelium, by the division of surface basal cells, to form a sharply defined cluster of cells with dark nuclei (Bucher and Reid, 1961). Although the branching pattern of the submucosal glands is complete at birth, the overall density of glands in the airways wall remains higher than that in adults and contains a larger proportion of mucous cells than would be found in the adult (Jeffery et al., 1992).

The relative percentage of serous cells increases during the first two years of postnatal growth. During development the submucosal glands which firstly comprises solely of mucous acini contain both neutral and acidic glycoproteins (Lallemand, 1991: Bucher & Reid, 1961 & De Haller et al., 1969). During development the number of surface

epithelial secretory cells is relatively high, particularly during the beginning of the second trimester (Lallemand, 1991).

### **1.3 OVERVIEW OF THE NORMAL TRACHEA AND LUNG DEVELOPMENT IN THE RAT**

#### **1.3.1 Development of the rat airways**

Fetal lung development is divided into three stages namely, the pseudoglandular, the canalicular and the terminal sac stages. Profound changes that takes place over a period of weeks in man (Wigglesworth, 1987), have been found to occur over a few days, and sometimes hours, in the rat (Kauffman, 1980). Therefore, as a means to simplify the study of these rapid changes that occur in the development of the rat airways, some detail of the various stages of fetal lung development will be discussed.

Cell proliferation is the highest (for epithelium and mesenchyme) during the pseudoglandular stage in the rat (O' Hare and Townes, 1970). During the canalicular period of the rat lung, proliferation of the mesenchyme occurs together with the development of a rich blood supply within it (Thurlbeck, 1975). Flattening of the epithelium lining airways also occurs, which are irregularly thinned with cellular continuity only maintained at their bases (Thurlbeck, 1975). During this period other changes which occur are the thinning of the interstitium, rapid development of capillaries and the angulation of vessels between alveolar epithelial cells (Kauffman, 1980).

In the terminal sac stage, the proportion of dividing epithelial cells decreases and the resting cells remain quiescent until the early postnatal growth period (Kauffman, 1980). At this stage, similar to the fetal lamb, the potential air spaces are filled with “ fetal pulmonary fluid ” (Farrel, 1982). At birth the conducting airways occupy a relatively large percentage of lung volume when compared to the mature lung. At this stage a number of different levels of conducting airways may be identified, viz.:

- (a) bronchi – airways with cartilage and seromucous glands.
- (b) bronchioles – those airways lacking the above structures.

Epithelia of the peripheral airways flatten and form straight smooth-walled channels (Burri, 1974).

By day 4 the distal parts of the conducting channels show that cuboidal epithelial cells start thinning out, showing a blood-air barrier typical of the gas exchange region. Many morphological differences in the blood-air barrier are evident between days 4 and 7 rats. The initially smooth septa show “ buds” protruding into the air space. These buds (ridges or crests) form secondary septa. From day 10 to day 13, respiratory bronchioli become evident, which are lined by a flattened epithelium. Elastic fibers are well developed and are usually found at the mouth of the developing alveoli. After day 13 an expansion and thinning out of the alveolar septa occurs. An increase of the gas exchange surface area is also an indication of “septal stretching”. During this development, formation of secondary septa seems to be due to growth of mesodermal derivatives (Burri, 1974).



Tracheal development in the rat begins at mid-gestation (Day 11; term 21 days) with the formation of the tracheal groove, a longitudinal diverticulum of endodermal epithelium that evaginates from the floor of the pharynx and tubular foregut. Paired lung buds (primary bronchial buds) forms at the caudal end of the tracheal groove (Morse et al., 1979;Witschi, 1962).

During day 11 to 12 the formation of a longitudinal tracheoesophageal septum divides the combined tracheal groove and developing foregut into two structures, the trachea and esophagus. The lung buds remain as simple, unbranched epithelial pouches. As development proceeds from day 12 to 13, the trachea and esophagus grow apart, surrounded by independently organized populations of mesenchymal cells. Near this time, the primary bronchial buds give rise to secondary (lobar) buds of pulmonary epithelium that establishes the lobar pattern of the right and left lungs and marks the formation of extrapulmonary bronchi. Until about day 13 - 14, the cranial trachea and developing larynx do not become independent of the pharynx. Between days 14 - 16, the development of smooth muscle and pre-cartilage formation begins within the tracheal mesenchyme, which precedes the differentiation of the mucociliary epithelium. Progressive branching of the bronchial tree and positional changes of the growing lobes are characteristic of further development of the pulmonary lobes. These changes occur in relation to the surrounding organs and the developing pleura cavity (Mc Ateer, 1984).

Epithelial differentiation is first evident at day 17, with the formation of ciliated cells as the first mature epithelial cell type to differentiate. Cartilage ring formation has advanced and cellular organization is evident, with closely spaced polygonal chondroblasts surrounded by concentric layers of elongated fibroblastic cells. The cartilage matrix is not yet apparent. At day 18, the principal features of the tracheal wall micro-anatomy are established and persist through parturition. The cartilage rings are well advanced and separated from the subjacent epithelium by a distinct region of fibroblastic mesenchyme (primitive submucosal connective tissue). A hyaline matrix now separates the chondrocytes. Cell surface characteristics of the tracheal epithelium indicate that secretory cells differentiate at about day 19 - 20 (McAteer, 1984).

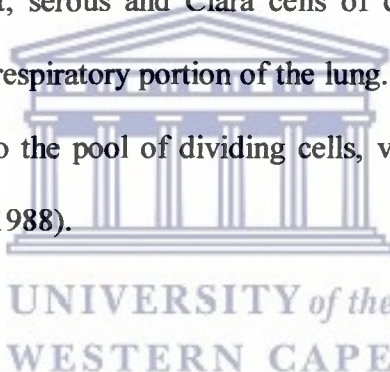
The time of the appearance of the remaining mature cell types of the mucociliary epithelium has not been determined. However, the tracheal epithelium in the rat has been found to be immature at birth. Important changes still take place in the morphology and distribution of cell types during the neonatal period (Jeffery & Reid, 1977; Smolich et al., 1976).

### 1.3.2 Morphogenesis of the rat airway epithelium

At least eight epithelial cell types are recognized in the lining epithelium of conducting airways and three in the epithelium lining of the alveoli. In animals the surface epithelium is simple columnar at the level of the trachea and bronchus, which normally has only two layers of nuclei, one basal and one superficial with all cells reaching the basement membrane (Bindreitter et al., 1968, Blenkinskopp, 1967 & Rhodin, 1966).

In conducting airways, there are three types of secretory cells, distinguished both by the nature of their secretory granules and the airway level at which each occur. Serous and goblet cells normally occur in the proximal airways only (Jeffery and Reid, 1975), while Clara cells are usually found distally, limited to the small bronchioles of most but not all species (Pack et al., 1981 & Plopper et al., 1980). The majority of the epithelial cell types in proximal airways have been thought to arise following the division and differentiation of basal cells (Blenkinskopp, 1967, Bolduc and Reid, 1976, Condon, 1941 & Rhodin, 1966).

The surface epithelial cells of the lower respiratory tract which have a capacity to divide are the basal, goblet, serous and Clara cells of conducting airways and the alveolar type II cells of the respiratory portion of the lung. The number and proportion of each, which contribute to the pool of dividing cells, varies with airway level and species (Ayers and Jeffery, 1988).



#### **1.4 OVERVIEW OF THE CELLULAR MAKE-UP OF THE TRACHEAL EPITHELIUM**

There are at least three different cell types in the tracheal epithelium as is represented in Figure 1. The basal cells (Bc) form a layer next to the basement membrane. Goblet cells (Gc) represent the mucus-producing cell of the epithelium. They reach from the basement membrane to the surface of the epithelium. Ciliated cells (Ci) are predominant, they all face the surface and generally reach the basement membrane. A

fourth cell type, which is frequently noticed in the human epithelium, is the intermediate cell (Ic) found to be located just above the basal cell layer (Rhodin, 1966).

### **Basal cells (Bc)**

Bc are polygonal or slightly elongated in shape and rests on the thin basement membrane. The lateral surfaces make contacts with neighboring basal cells, and also with the basal processes of the goblet cells. These contacts may be in the form of thin cytoplasmic processes making a membrane-to-membrane contact, but more often than not these contacts take the shape of desmosomes (Rhodin, 1966).

The nucleus occupies a large portion of the Bc. The cytoplasm is characterized by a multitude of fine tonofilaments, which traverse the cell in many directions and often converge on the desmosomes. Mitochondria are sparse, and those present are small and spherical and scattered about in the cell. Ribosomes are sparse; Golgi complex is vestigial, if at all present. Some granular structures with high electron density may represent lysosomes. Bc gives rise to other cells of the epithelium (Rhodin, 1966).

### **Intermediate cells (Ic)**

Ic are found, infrequently, just above the basal cell layer with a more elongated or spindle shape. Mitoses can often be seen within this incomplete cell layer. These cells are derived from the Bc (Rhodin, 1966).

### **Goblet cells (Gc)**

The goblet cells (Gc) are the mucous producing cells in the trachea. In the mucosa of the trachea, the Gc has a more elongated shape than elsewhere, probably because of the rather extreme depth of the epithelium. The base of the goblet cell tapers off considerably, and most of the time it is seen to bend around basal and intermediate cells. The nucleus is located toward the base of the cell. It is shaped round or slightly oval, and it's rarely compressed as it is in the intestinal goblet cells or in the mucus-producing cells of the tracheal lamina propria. The Golgi complex of the goblet cell is rather prominent, just above the nucleus. Secretory granules are formed within the Golgi region (Caro and Palade, 1964).

The cytoplasm of the Gc is rich in ribosomes, which gives it a dark and electron-dense appearance compared to the basal and ciliated cells. Ribosomes are frequently attached to membranes or sacs, forming the granular endoplasmic reticulum, which is engaged in early elaboration of the secretory products (Caro and Palade, 1964). Mitochondria are sparse and oval in shape. Lysosomes occur throughout the cytoplasm and seem to be more abundant towards the end of the secretory cycle (Rhodin, 1966).

### **Ciliated cells (Ci)**

Ciliated cells are the most common in the human tracheal epithelium. On average, there are about five Ci for each mucus-producing cell. The Ci extends from the basement membrane to the luminal surface of the epithelium. The nucleus of the Ci is oval, it is located toward the tapered end of the cell. The cytoplasm is electron lucent



Figure 1: Longitudinal section of the pseudostratified ciliated tracheal epithelium composed mainly of four cell types: basal cells (Bc), intermediate cells (Ic), goblet cells (Gc), and ciliated cells (Ci). (Rhodin, 1966)



(appearing lighter) compared to the Gc and contains scattered ribosomes and occasional short profiles of the granular endoplasmic reticulum (Porter, 1961). Within this area, there is always an abundance of mitochondria, which are long and even show connections with other mitochondria (Rhodin, 1966).

A large number of lysosomes are found in the Ci, which seems to be associated with processes involving lysis (Novikoff, 1961). The luminal surface of the Ci is provided with an average of 200 cilia. In addition, microvilli protrude from the surface in between the cilia at varying lengths (Rhodin & Dalhamn, 1956).

## **1.5 TRACHEA AND BRONCHIAL CARTILAGE**

A distinctive feature of the airways is the presence of cartilagenous support within the walls. In the trachea and first-order bronchi, cartilage is present as plates that do not encircle the airway. Once the airways penetrate the parenchyma of the lung, cartilage is present as incomplete rings that are part of the bronchiolar walls down to the ninth-order branches (Krahl, 1964). The appearance of bronchial cartilage has not yet received detailed study, but appears similar to hyaline cartilage found elsewhere in the body (Hance and Crystal, 1975).

The cartilage contains Type II collagen in the form of fine, nonbanded fibrils associated with an amorphous proteoglycan matrix. The perichondrium contains, in part, Type I collagen that appears as banded fibrils. These fibrils fuse with the continuous bronchovascular framework, firmly attaching the cartilage within the walls

of the airway (Pras and Glynn, 1973). The structural importance of cartilage is underscored by the consequences of congenital absence of cartilage. Without the added support given by cartilage, airway closure produces tension emphysema in the affected segments of the individual lungs (Hance and Crystal, 1975).

#### 1.5.1 Collagen synthesis

Collagen is an important structural component throughout the lung, including the tracheobronchial tree, vascular tree, parenchyma and pleura. Approximately 30 to 40% of collagen in the lung are in the large airways, large blood vessels and septae dividing major lung segments (Fulmer and Crystal, 1975). The remainder is present in the various subcompartments of parenchyma, including alveolar interstitium, basement membrane, small blood vessels and transitional airways. The fundamental unit of collagen is the tropocollagen molecule, which by its capacity to copolymerize with other tropocollagen molecules and to interact with a variety of other connective tissue elements is capable of forming structures such as cartilage, basement membrane, and various fibrils that form the pleura and the skeleton of the lung parenchyma (Hance and Crystal, 1975).

Tropocollagen is a rod-shaped molecule (1.5 x 300 nm) composed of 3  $\alpha$  chains in a right-handed helical arrangement (Piez and Miller, 1974). The right-handed “triple helical” tropocollagen is, in turn, wound in a left-handed “super coil” during fibril formation (Traub and Piez, 1971). Tropocollagen is heterogeneous; the 4 types found in the body are distinguishable by the  $\alpha$  chains composing them, but they do share



certain structural features. Every  $\alpha$  chain has a molecular weight (MW) of 95,000 to 100,000 daltons and each is composed of approximately 1,050 amino acids (Piez and Miller, 1974). More than 1,000 of these amino acids occur in repetitive triplets of the form, (glycine – X – Y)<sub>n</sub>. Although the amino acids represented by X and Y are variable, there is a high content of alanine, proline, lysine, hydroxyproline and hydroxylysine (Gallop et al., 1972). The latter 2 amino acids are especially characteristic of collagen. At the N – and C - terminal ends of each  $\alpha$  chain there are regions of approximately 20 amino acids that do not have the glycine – X - Y sequence (Piez and Miller, 1974).

These regions known as “ teleopeptides “ do not take part in helix formation but they do have an important role in crosslink formation both within and between tropocollagen molecules (Traub and Piez, 1971). It is the uniqueness of each tropocollagen that allows it to perform its structural function in a different way, depending on the requirements of a given tissue. For this discussion only the two types of tropocollagen that appear in cartilage will be detailed.

### 1.5.2 Type I collagen

Type I collagen is the most ubiquitous collagen in the body, found most abundant in skin, bone, tendon and a number of other tissues (Bornstein and Piez, 1966; Miller, 1973 and Trelstad, 1974). Type I collagen constitutes a significant proportion of the collagen in the large bronchi and blood vessels. In addition, Type I collagen is also synthesized by lung parenchyma, indicating a role in support of the interstitium

(Bradley et al., 1974). Type I collagen readily forms fibrils that have high tensile strength. These fibrils are tightly packed, leaving little room for ground substance (Grant and Prockop, 1972). Due to its ubiquity of Type I collagen, it is not surprising that more than one cell type is capable of its synthesis.

### 1.5.3 Type II collagen

Type II collagen has been identified only in cartilaginous tissue (Miller et al., 1974). This is true for lung, where Type II collagen has been found only in the trachea and bronchi. It is the major collagen synthesized by these structures (Bradley et al., 1974). Type II collagen does not form prominent fibrils within these tissues, but rather is found in association with large amounts of proteoglycan (Strawich et al., 1971). These proteoglycan-collagen complexes are maintained by strong ionic interactions that may be fostered by the presence of a considerable amount of carbohydrate attached to Type II collagen (Miller, 1971). The chondroblast cells have been found to be responsible for the synthesis of Type II collagen in adult tissue (Mayne et al., 1973) and thus the chondroblasts in the tracheal and bronchial cartilage are probably responsible for its synthesis in lung.

## 1.6 **CARTILAGE SYNTHESIS AND GROWTH**

Cartilage is capable of both interstitial (endogenous) growth, i.e., growth within the substance of the cartilage and appositional (exogenous) growth, i.e., growth at the surface of the cartilage (Tortora & Anagostakos, 1990).

In the process of interstitial growth, the cartilage increases rapidly in size through the division of existing chondrocytes and continuous deposition of increasing amounts of intercellular matrix by the chondrocytes. The formation of new chondrocytes and their production of new intercellular matrix cause the cartilage to expand from within, thus the term interstitial growth. Chondrocytes that have recently divided are close to each other and may even be in the same lacuna. This growth pattern occurs while the cartilage is young and pliable, as during childhood and adolescence (Tortora & Anagnostakos, 1990).

In the process of appositional growth, the activity of the inner chondrogenic layer of the perichondrium increases. The deeper cells of the perichondrium, the fibroblasts, divide. As differentiation occurs, the chondroblasts become surrounded with intercellular matrix and become chondrocytes. As a result, the matrix is deposited on the surface of the cartilage, increasing in size. It follows then, that the cells, which have just become chondrocytes, are close to the perichondrium. They appear flatter and smaller, and in smaller lacunae than more deeply located cells (Figure 1.1 A). This growth pattern starts later than interstitial growth and continues throughout life (Tortora & Anagnostakos, 1990).

## **1.7 TRACHEAL CARTILAGE MORPHOLOGY**

Cartilage consists of homogeneous appearing matrix in, which are small spaces, called lacunae, that contain chondrocytes. The cartilage is completely surrounded by a fibrous irregularly arranged dense connective tissue, the perichondrium. Chondrocytes are

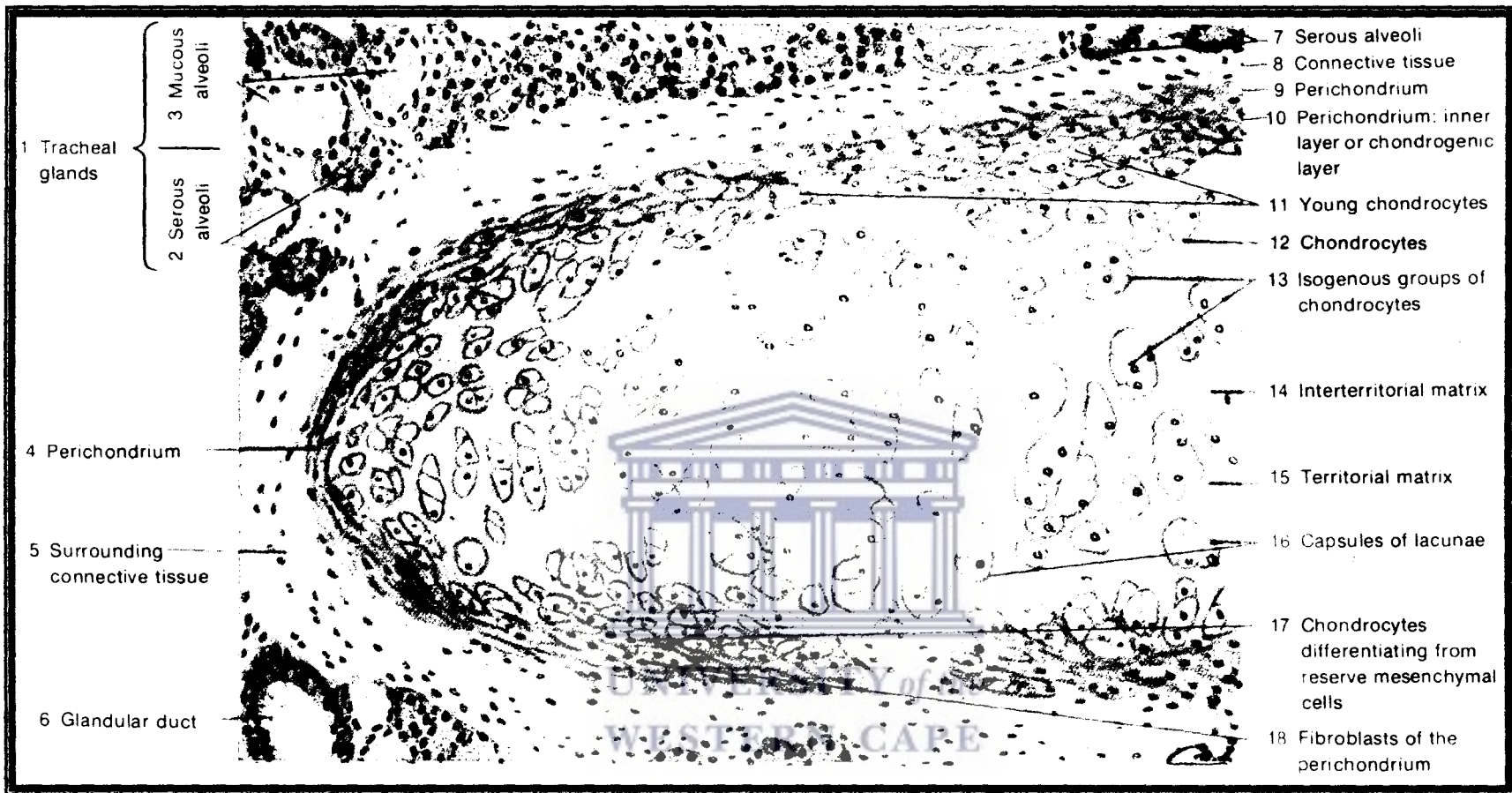


Figure 1.1 (A): A perichondrium of dense connective tissue surrounds the entire cartilage plate. It's inner layer is the chondrogenic area, here chondrocytes are being formed by proliferation and differentiation of mesenchymal cells. (di Fiore, 1981)

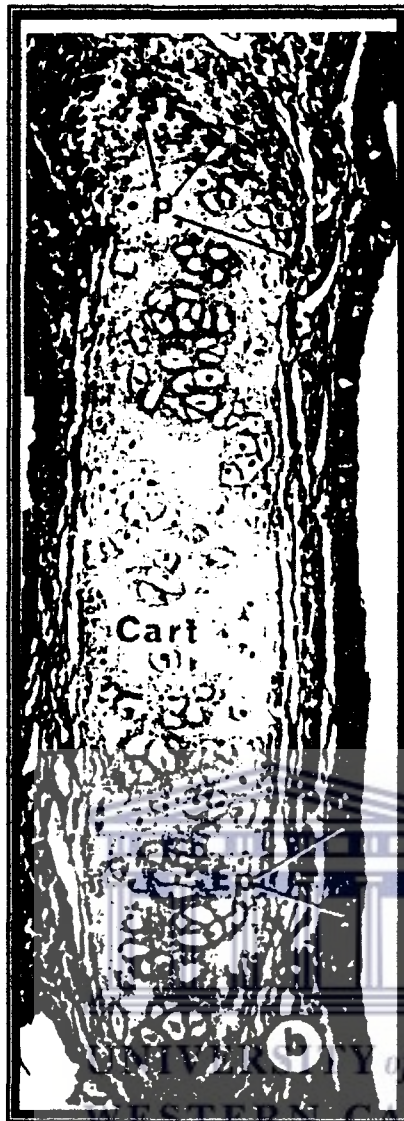


Figure 1.1 (B): Hyaline cartilage (**Cart**) in trachea appears as an avascular expanse of tissue surrounded by a perichondrium (**P**) and outer layer of epithelium (**Ep**) (Rhodin, 1975).

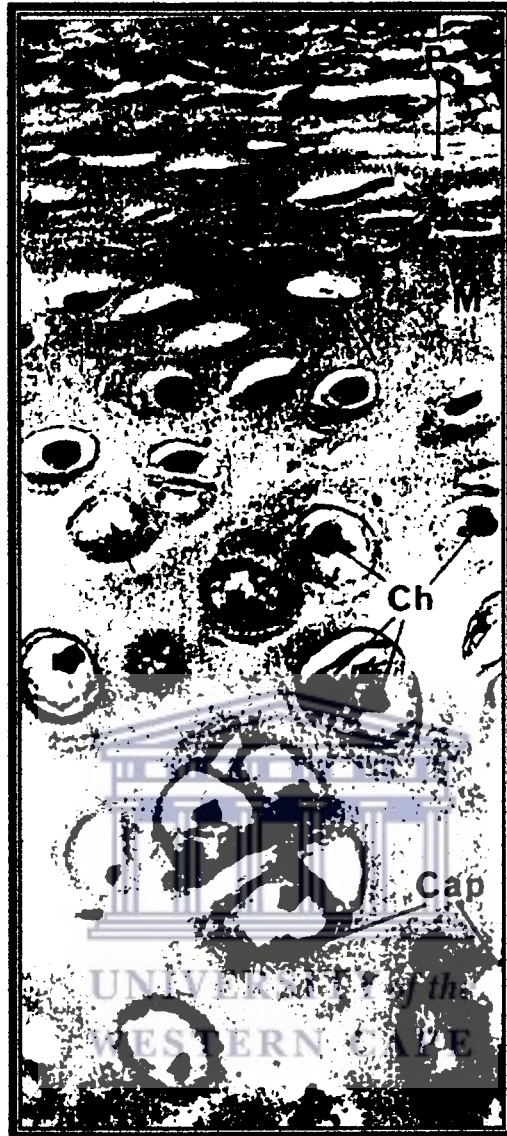


Figure 1.1 (C): Cartilage in trachea consists of a homogeneous appearing matrix (M), in, which lacunae with a capsule (Cap) contains chondrocytes (Ch). Cartilage surrounded with a fibrous capsule-like cover, the perichondrium (P) (Rhodin, 1975).

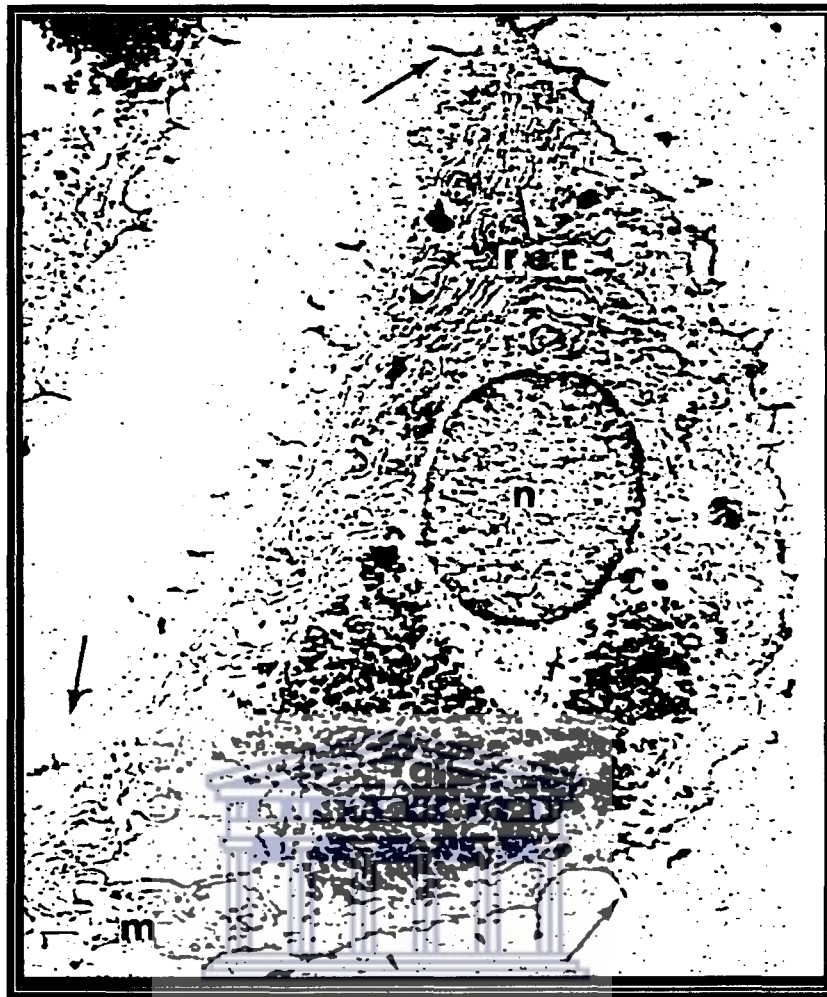


## **1.8 THE BASIS OF CARTILAGE DAMAGE AND HEALING PROCESSES**

Cartilage, have been documented as lacking regenerative power. Mainly due to the fact that it is avascular and thus its reparative process differs significantly from the three-phase response of necrosis (i.e. death of cell or group of cells as result of disease or injury), inflammation, and repair that occurs in vascularized tissues (Chen et al., 1999).

Cartilage undergoes the initial phase of necrosis in response to damage, but there is less cell death, given its relative insensitivity to hypoxia (Mankin, 1982). The second phase namely inflammation, is largely absent, a response primarily mediated by the vascular system. The third phase of repair is also severely limited, given the lack of inflammatory responses. There is a lack of the vascular proliferation and recruitment of undifferentiated mesenchymal cells that normally proliferate and modulate the repair response (Chen et al., 1999). The burden of repair thus falls on the existing chondrocytes in a process termed intrinsic repair (Mankin, 1982). Although cells of immature cartilage is capable of mitotic activity, unstimulated chondrocytes in mature cartilage have little potential for replication (Mankin, 1962).

An extrinsic repair mechanism depends on differentiation and proliferation of mesenchymal stem cells (Campbell, 1969). Some mesenchymal cells are found scattered irregularly throughout adult connective tissue, most frequently around the blood vessels. Here mesenchymal cells differentiate into fibroblasts that assist in wound healing. Adult connective tissue exists in the newborn that has differentiated from mesenchyme and does not change after birth. It mainly forms all other kinds of



UNIVERSITY of the

Figure 1.2: A transmission electron micrograph of a single chondrocyte is illustrated. Cell organelles, such as rough-surfaced endoplasmic (rer), mitochondria (m), glycogen (gi), and the cell nucleus (n) are present in this section. The cartilage matrix have a fine granular appearance with the chondrocyte having numerous cytoplasmic projections (arrows) at its surface (Kessel, R.G. and Kardon, R.H, 1979).



connective tissue. Mesenchymal cells are found in the perichondrium, which is a layer of dense collagenous connective tissue surrounding the cartilage (Tortora and Anagnostakos, 1990). However studies have shown that the population of mesenchymal stem cells declines with increasing age (Buckwalter et al., 1993). This decline therefore constitutes another limiting factor in cartilage healing.

### **1.9 THE REPAIR RESPONSE OF CARTILAGE TO DAMAGE**

The initial necrosis of chondrocytes is followed by increased mitotic and metabolic activities of the surviving chondrocytes within 48 to 72 hours. There are enhanced rates of type II collagen and matrix molecule synthesis by the surviving chondrocytes, which proliferate and form clusters in the periphery of the injured zone. This increased metabolic and mitotic activity is only for a limited time, after which the synthesis rates fall back to normal (Mankin, 1982 & Mankin et al., 1994).

Proliferating chondrocytes do not migrate into the area of damage. Newly synthesized matrix remains mainly in the periphery and does not fill the defect. Due to no inflammatory response that is initiated or undifferentiated mesenchymal cells bind to the damaged cartilage and as a result the overall repair response remains suboptimal (Mankin, 1982 & Mankin et al., 1994). As the cartilaginous matrix deterioration progresses, the inability of the surviving chondrocytes to repair the damaged tissue and prevent further damage may result in further degradation of the surrounding surface (Chen et al., 1999)

## 1.10 ALVEOLAR DEVELOPMENT

Two patterns of lung alveolarization have been described (Boyden and Tompsett, 1965 & Emery, 1970). These are the

- (1) evagination of gas exchange units from the walls of terminal bronchioles, transforming these conducting airways into respiratory airways, and also
- (2) involves the budding of new septa from the saccule walls of immature lungs.

At birth, the lung parenchyma of man and of rodents have been found to consists of large, thick-walled saccules with few recognizable alveoli (Thurlbeck, 1975).

In man, the alveolar stage occurs from 32 weeks to term (Wigglesworth, 1987). During this phase immature alveoli forms with a double capillary network (Dornan & Meban, 1985). Approximately three hundred million alveoli develop during the first 8 to 10 years of life, with little or no alveolarization occurring after this time (Thurlbeck, 1975). It was indicated, however, that most alveolar formation and capillarisation occurs within the first postnatal year, much sooner than previously thought (Motoyama et al., 1988). The neonatal lung undergoes remarkable immediate functional transformations so that by the end of the first few minutes of life, it is serving as an adequate organ of gas exchange. At birth, the basic formation of the cartilaginous airways is complete, though the number of generations of conducting airways decrease through the conversion of alveolarization of a few non- respiratory bronchioles into respiratory bronchioles (Murray, 1986). Alveolar size continues to increase until growth of the chest wall ceases with attainment of adult thoracic size (Farrell, 1982).

In the rat, the actual process of alveolar formation mainly involves the following three headings:

- (1) formation and growth of secondary septa;
- (2) capillarisation of the secondary septa;
- (3) maturation of the immature septa and capillary remodeling.

Between day 4 and day 13 after birth, sacculle walls and interstitial cells observed at birth undergo major structural and functional changes. True alveoli with a thin single capillary layer begin to appear. The interalveolar septa begin to appear in various stages of development. Ranging from small evaginations to long, thin, well developed septa. Lipid-filled cells seem to predominate in the interstitium of alveolar corners and at the base of forming septa (Vaccaro & Brody, 1978).

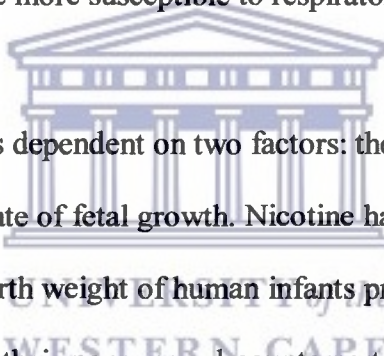
## **1.11 EFFECTS OF SMOKING AND NICOTINE ON AIRWAY AND LUNG DEVELOPMENT**

### **1.11.1 Nicotine**

Nicotine, a major alkaloid in tobacco smoke, has been implicated as the one which produces adverse effects on fetal growth (Murrin et al., 1987). It readily gains access to the fetal compartment via the placenta, with fetal tissue concentrations generally 15% higher than maternal blood levels (Koren, 1995). Nicotine is thus rapidly absorbed by the infant and accumulates in the respiratory tract after absorption, where it may interfere with lung development and maturation to an extent that increases susceptibility to damage such as emphysema (Maritz et al., 1993).

(5) alveolarisation of the neonatal lung (Dolley, 1995), which explains the increased radial alveolar count (RAC) of lung tissue of the nicotine exposed rat pups due to the adverse effect of the maternal nicotine exposure on elastogenesis in neonatal lung.

(6) the integrity of the fetal alveolar Type II pneumocyte (Maritz & Thomas, 1995), by use of histochemical techniques showed abnormal lung morphology for the nicotine exposed animals. The type II pneumocytes that were exposed to nicotine during development were also noted to have no microvilli on their alveolar surface. These histological findings seen with fetal nicotine exposure during a time of rapid lung remodeling and growth may possibly be the reason for the offspring of smoking mothers to be more susceptible to respiratory insult in early life.



The birth weight of a baby is dependent on two factors: the gestational age of the fetus at time of delivery and the rate of fetal growth. Nicotine has been shown to affect both these factors. The average birth weight of human infants prenatally exposed to nicotine is 100 to 320 g lighter than their nonexposed counterparts (Becerra and Smith, 1988; Butler et al., 1972). There seems to be a dose–response effect of nicotine on the birth weight, because the type of cigarette smoked has as much an impact as the number of cigarettes smoked per day.

### 1.11.2 Smoking

Morrow et al., (1988) evaluated the effects of cigarette smoking on umbilical and uterine blood flow velocities. They found smoking a 1mg nicotine cigarette produced increases in maternal blood pressure and heart rate and increases in fetal heart rate. This suggested that fetal hemodynamics might change in response to maternal smoking, it is however not clear if this effect is caused by nicotine or carbon monoxide (Morrow et al., 1988) and whether this may have an influence on fetal and neonatal lung growth and development.

Maternal smoking has been implicated in long-term deficits in infant mental development and adverse behavioral problems in children such as deficit disorder (Lambers & Clark, 1996). There are animal studies that support the effects of nicotine on the developing cerebrum. Arbeille *et al.*, (1992) studied the nicotine-induced changes in cerebral blood flow in the ovine fetus. They found a significant increase in resistance was noted by the end of gestation in the cerebral arteries, which translate into arterial vasoconstriction and increased impedance. A higher rate of stillbirth (61% compared with 10% in controls) was also noted. This increase in resistance would lead to a reduction of cerebral perfusion.

Exposure to cigarette smoke appear to affect the airways by:

- (1) stimulating mucous discharge, where initiation of these changes can begin from the first insult. In rats, inhalation of cigarette smoke for 1 day stimulated the discharge of mucus in the extrapulmonary airways namely the upper, middle and lower

trachea as well as the main bronchi. By the third day the number of secretory cells in both the extra- and intrapulmonary airways (subsegmental bronchi) was increased. The intracellular distribution of glycoproteins was reduced from cells containing neutral glycoproteins to those containing a combination of acid and neutral glycoproteins (Jones et al., 1978 & Jeffery and Reid, 1981). This suggests changes in glycoprotein metabolism in the goblet cells.

(2) inhibiting active ion transport, a function of the normal epithelium, which plays an important role in the control of the quantity and composition of the respiratory tract mucus. It has been shown that transepithelial water flux follows ion movement in the airways and this water contributes not only to the volume of respiratory fluids but is important to the hydration of mucus (Phipps and Denas, 1982). In dogs, a decrease in the transepithelial electrical potential difference resulted after exposure of ten to twelve puffs of cigarette smoke (Welsh, 1983).

(3) by increasing the permeability of the large airways in guinea pigs. This increase in permeability was concentration dependent with effects beginning with twenty puffs. At ultrastructural level, progressive disruption of epithelial tight junctions resulted, with the maximum effect observed at 200 puffs (Boucher et al., 1980). In guinea pigs receiving 100 puffs of cigarette smoke, the maximum increase in permeability was observed 0.5 hours after exposure. After this time, there was a steady return towards normal (Hubert et al., 1981). This change in permeability was associated with an increase in tracheal wet/dry weight ratio and a decrease in the number of goblet cells/mm of epithelium.

(4) causing tracheobronchial epithelial changes associated with mucous cell and glandular hyperplasia, during chronic exposure to tobacco smoke (Auberbach et al., 1979).

(5) cytotoxic effects of tobacco smoke consist of inhibition of growth, inhibition of oxidative metabolism, cilia and membrane damage (Verra et al., 1995).

### **1.12 AIMS OF THE PROPOSED STUDY**

Data on the effects of maternal nicotine exposure and smoking on the development of the alveolar region of the lung have been widely researched. However, no information is available regarding the possible effects that maternal nicotine exposure could have on tracheal development. This particular study therefore deals mostly with the structural aspects of trachea development, which give more information on the sites of the upper airways most sensitive to nicotine exposure. The aim of this study is therefore to investigate the effect of maternal nicotine exposure on neonatal rat trachea in particular and also the alveoli status by:

1. investigating the cellular characteristics of the trachea. These include the cells of the hyaline cartilage as well as the tracheal epithelium. Morphometric analysis of the chondrocytes is emphasized.
2. investigating at ultrastructural level the cell organelles of the developing tracheal chondrocytes and tracheal epithelium.

To investigate the above-mentioned aspects the following techniques were employed namely, light microscopy, scanning and transmission electron microscopy.



## **CHAPTER 2**

### **MATERIALS AND METHODS**

#### **2.1 Experimental animals**

The animals used in this particular study were white Wistar rats, bred in the laboratory animal unit of the department of Physiological Sciences, University of Western Cape. A standard diet of Epol rat cubes was fed as required. Tap water was supplied daily. To ensure good animal hygiene the cages and animal room were maintained at optimal conditions of cleanliness.

Litters were obtained for study by allowing mating to take place overnight (12 hours) and removing the sires on the following morning. Females were then randomly assigned to control and experimental groups. The rats were weighed on a weekly basis. A significant increase in body mass was an indication of the animal being pregnant. These animals were then placed in separate cages from day 7 to end of gestation, an average of 22,5 days. The experimental group received subcutaneous injections of 1mg nicotine/kg body mass/day (diluted in distilled water) between 9h00 and 10h00. The control group animals received saline injections and were allowed to develop normally without being given nicotine treatment, thus creating a measure against which the experimental group could be compared.

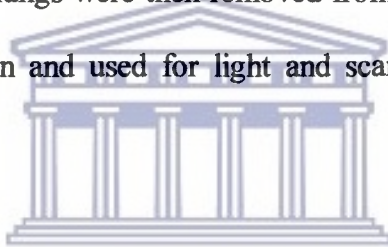
Disposable plastic 23 gauge 1,0 ml syringes were used for all the injections. Only gamma-irradiated syringes were used as to minimize occurrence of infection as a result of the daily injections. At all times, care was taken when handling the rats, as



not to inflict pain or unduly excite the animal. The day of birth of the pups was designated day 0. A minimum of 3 pups were randomly selected from each litter, both the experimental and control group. For this study, pups were sampled on days 7, 14, 21, 42 after birth.

### **2.1.2 Trachea tissue excision and preparation**

Animals were killed on predetermined days, 24 hrs after their last exposure. The trachea tissue samples were obtained by an incision in the thorax to expose the lungs as well as the whole trachea. The trachea was removed with the lungs after, which a longitudinal cut was made down the trachea, including the branches (of trachea) into the lungs (Figure 2.1). The lungs were then removed from the trachea and were then fixed with buffered formalin and used for light and scanning electron microscopy investigation.



For the light microscopy investigation, the samples were fixed in buffered formalin for 24 hrs, whereafter it was washed in running tap water for 30 minutes. Each sample was then placed in a labeled plastic cassette. A Shandon tissue processor was programmed for dehydration and wax impregnation using the following program in Table 2.1.

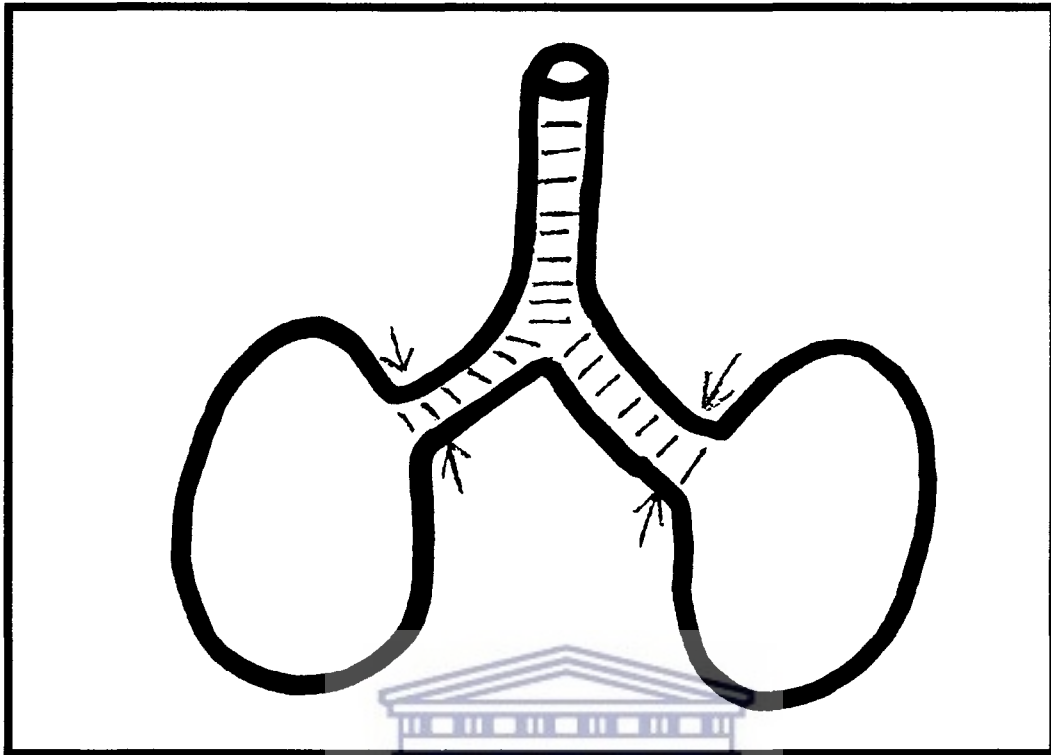


Figure 2.1: View of trachea and lungs when removed. The arrows indicated (↓) the cut-off points for dissecting the whole trachea.



<b>1</b>	<b>70% ethanol</b>	<b>1 hour</b>
<b>2</b>	<b>80% ethanol</b>	<b>1h 30 minutes</b>
<b>3</b>	<b>90% ethanol</b>	<b>2 hours</b>
<b>4</b>	<b>96% ethanol</b>	<b>2 hours</b>
<b>5</b>	<b>96% ethanol</b>	<b>2 hours</b>
<b>6</b>	<b>100% ethanol</b>	<b>2 hours</b>
<b>7</b>	<b>100% ethanol</b>	<b>1h 30 minutes</b>
<b>8</b>	<b>Xylene</b>	<b>1h 30 minutes</b>
<b>9</b>	<b>Xylene</b>	<b>2 hours</b>
<b>10</b>	<b>Wax bath</b>	<b>2 hours</b>
<b>11</b>	<b>Wax bath</b>	<b>1h 30 minutes</b>

Table 2.1: Protocol for dehydration and wax impregnation of trachea tissue.

Then the tissue was embedded in paraplast wax using a Tissue Tek II system. Before cutting of sections, the wax embedded samples were refrigerated at 4°C for a minimum of 3 hrs. A rotary microtome was used to get down to the correct tissue plane, by initially cutting thick sections of 10µm. After this, 4µm sections were cut in ribbons consisting of 3 to 4 sections. These ribbons were then flattened out in a waterbath at 45°C and picked up on clean microscope slides and fixed overnight at 37°C in an incubator.

These slides were stored in slide retaining boxes for later staining, while the cassettes were stored in a cool, dry cupboard for later use. For staining purposes, the

appropriate slides were removed from storage, then labeled on the frosted end with a graphite pencil and then fixed by placing in a hot – air oven at 80° C for 20 minutes.

## **2.2 LIGHT MICROSCOPY**

Refer to Appendix A for the reagents and procedure used.

## **2.3 SCANNING ELECTRON MICROSCOPY**

Refer to Appendix B for the preparations for scanning ultramicroscopy.

## **2.4 TRANSMISSION ELECTRON MICROSCOPY**

### **2.4.1 Animals**

Treatment of animals is the same as stipulated in Section 2.1. After the removal, the trachea tissue samples were cut into smaller pieces with razor blades and then processed as follows:

### **2.4.2 Tissue Preparation**

The tissue samples were treated with 2 fixatives, namely gluteraldehyde, which forms cross-links between protein molecules as well as the unsaturated lipids within the tissue. Osmium was also used as it stains cell membranes, lipid inclusions and nucleoproteins, thus enhancing contrast. A phosphate buffer was used as the fixative vehicle.

Refer to Appendix C for the reagents and procedures used for fixation, embedding and microtomy.

## **2.5 MORPHOMETRIC DATA**

Refer to Weibel, 1963 for the procedure used to collect the morphometric data.

## **CHAPTER 3**

### **RESULTS**

#### **3.1 LIGHT MICROSCOPY OF THE DEVELOPING RAT TRACHEA**

##### **3.1.1 Morphological Status:**

It is important to first describe the morphology of the hyaline cartilage illustrated in Figure 3 (a). The hyaline cartilage has distributed throughout a homogenous substance, the matrix, with numerous ovoid spaces termed lacunae which contain the chondrocytes, which may be singly or isogenous grouped. Each chondrocyte has granular cytoplasm and a nucleus, which appear to fill their lacunae. The matrix between the groups of cells is termed interterritorial (intercellular) matrix and stains lightly compared to the territorial matrix. A perichondrium of dense connective tissue surrounds the entire cartilage plate. Its inner layer is the chondrogenic area, here chondrocytes are formed by proliferation and differentiation of mesenchymal cells (di Fiore, 1981).

Heamatoxylin and eosin sections of the trachea of 7 day old control (Figure 3.1) and the nicotine exposed rats pups (Figure 3.2) show the hyaline cartilage with chondrocyte cells. The numerous chondrocytes (c) contained within the lacunae that are embedded in the matrix and surrounded by a perichondrium (p) represent the main component of the trachea cartilage. The trachea cartilage has a layer of connective tissue and then a layer of epithelium on the luminal side of the trachea. The perichondrium is a fibrous capsule-like covering with an outer part, which is more fibrous and the inner part being more

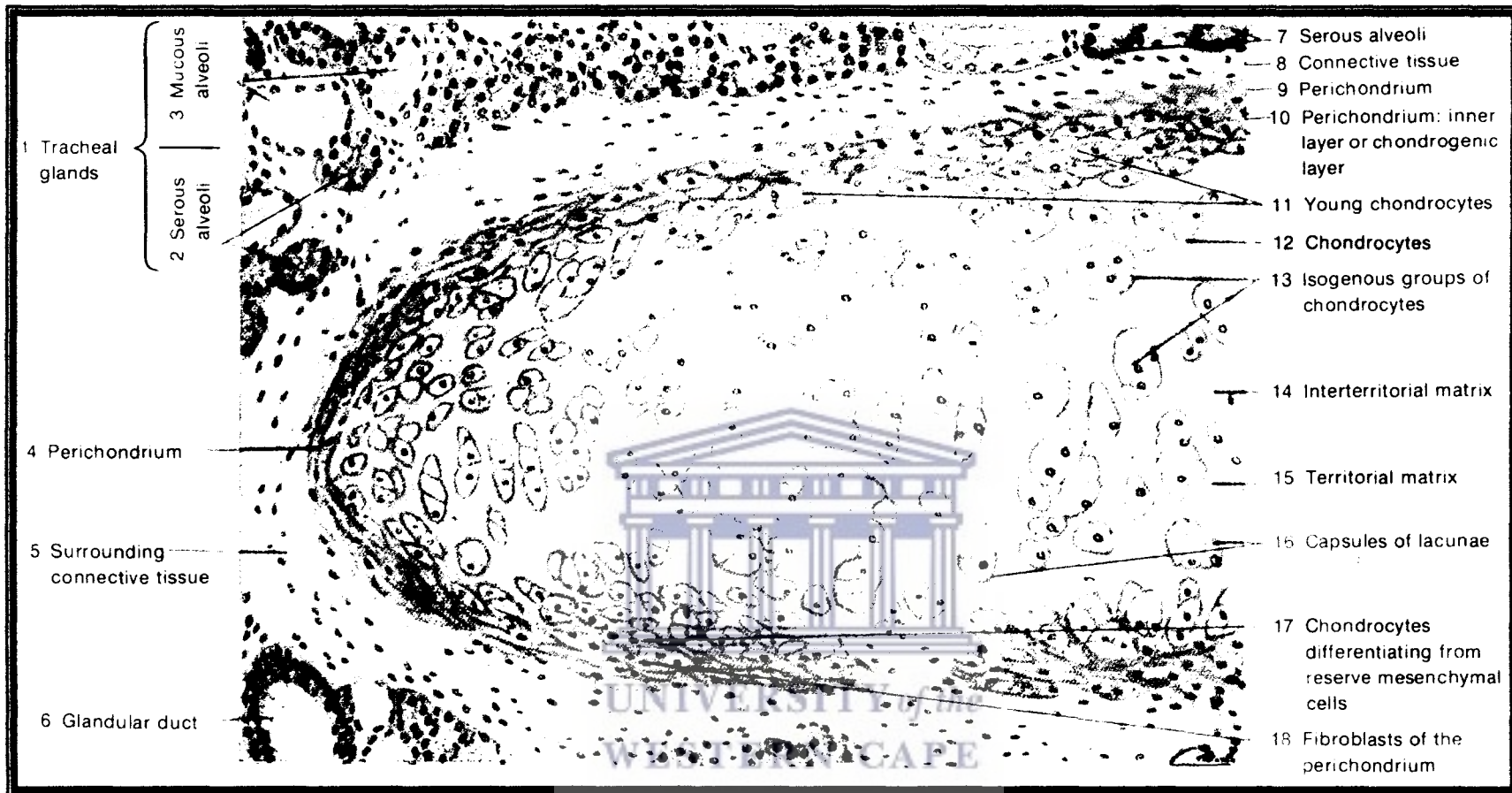


Figure 3 (a): Hyaline cartilage of trachea. (di Fiore, 1981)

cellular. At day 7 the chondrocytes of the control rats (Figure 3.1) appear dense and are arranged in semi-circulars. In comparison to the day 7 old experimental rats (Figure 3.2) with randomly arranged chondrocytes that appear sparse.

At day 14 the trachea cartilage of the control (Figure 3.3) and nicotine exposed (Figure 3.4) rats consisted of chondrocytes (c) embedded within the matrix, surrounded with a perichondrium (p) and then with a layer of epithelium (e). Notable differences are the darkly stained nuclei of the nicotine exposed rats (Figure 3.4) when compared to that of the control (Figure 3.3).

At day 21, a closer view of the cartilagenous surface shows closely situated lacunae with their chondrocytes (c) in all lacunae. The nuclei of the chondrocytes are clearly visible and appear spherical in the control (Figure 3.5) and nicotine exposed rat pups (Figure 3.6). In the trachea of the experimental animals, the cytoplasm of the chondrocytes in the areas of damage appears to be less dense. In addition, the chondrocytes close to the area of damage appear to be bigger with less of the solidified ground substance i.e. matrix that contains the collagenous fibers than elsewhere in the trachea cartilage (Figure 3.6).

At day 42, the control rat trachea shows the trachea cartilage with the lacunae closely situated together, containing chondrocytes (c) with spherical nuclei, appearing well intact within it's matrix (Figure 3.7 & 3.9). In the case of the experimental animals, widespread areas of damage occurred. Few nuclei are viewed within the area of damage (Figure 3.8 & 3.10). The areas of damage show that the matrix between adjacent lacunae is ruptured. This may increase the susceptibility of the hyaline cartilage rings to damage.



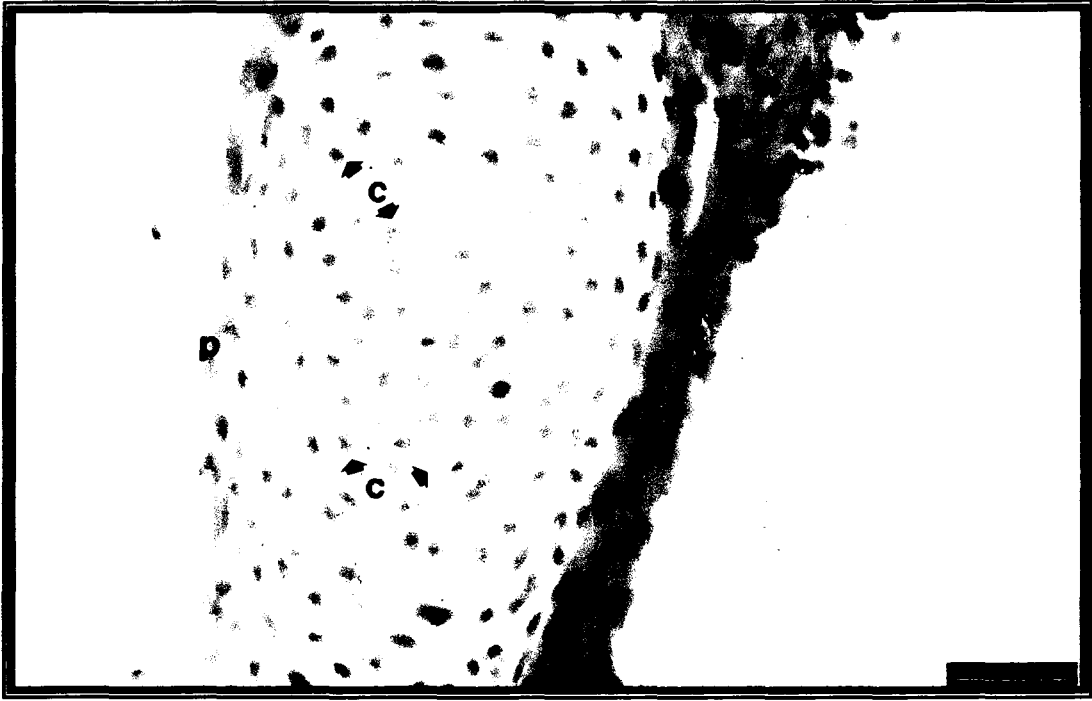


Figure 3.1: Trachea of a 7 day old control rat. Bar = 80 $\mu$ m  
Chondrocytes (c) within the matrix, surrounded with a perichondrium (p).

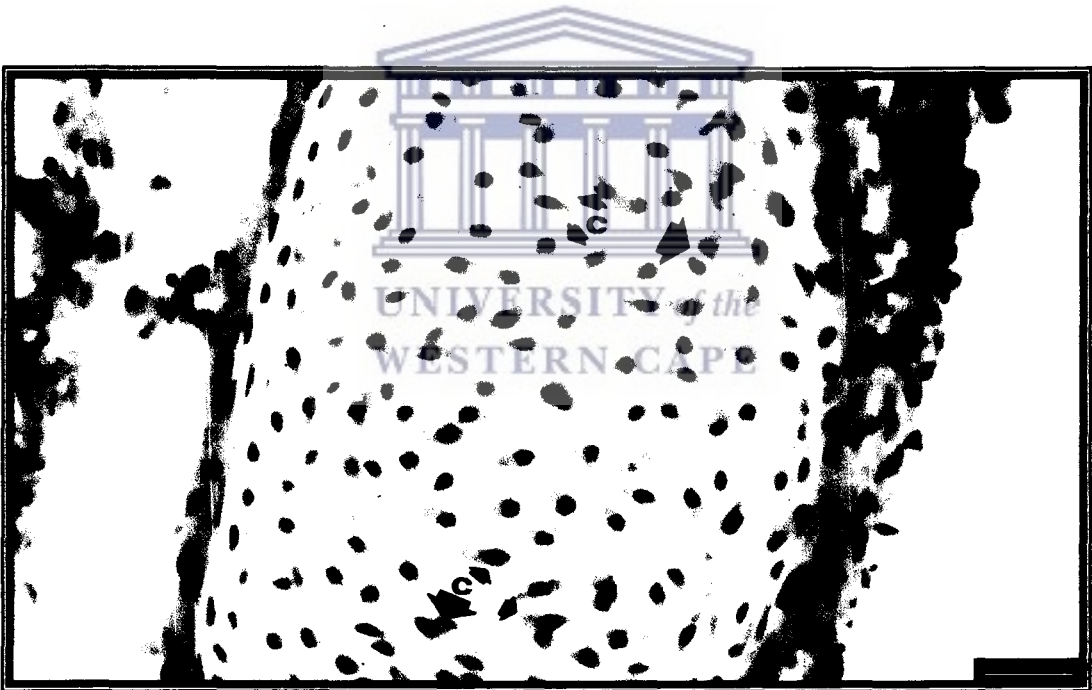


Figure 3.2: Trachea of a 7 day old nicotine exposed rat. Bar = 80 $\mu$ m  
Chondrocytes (c) within matrix and surrounded with a perichondrium (p) and epithelium (e).

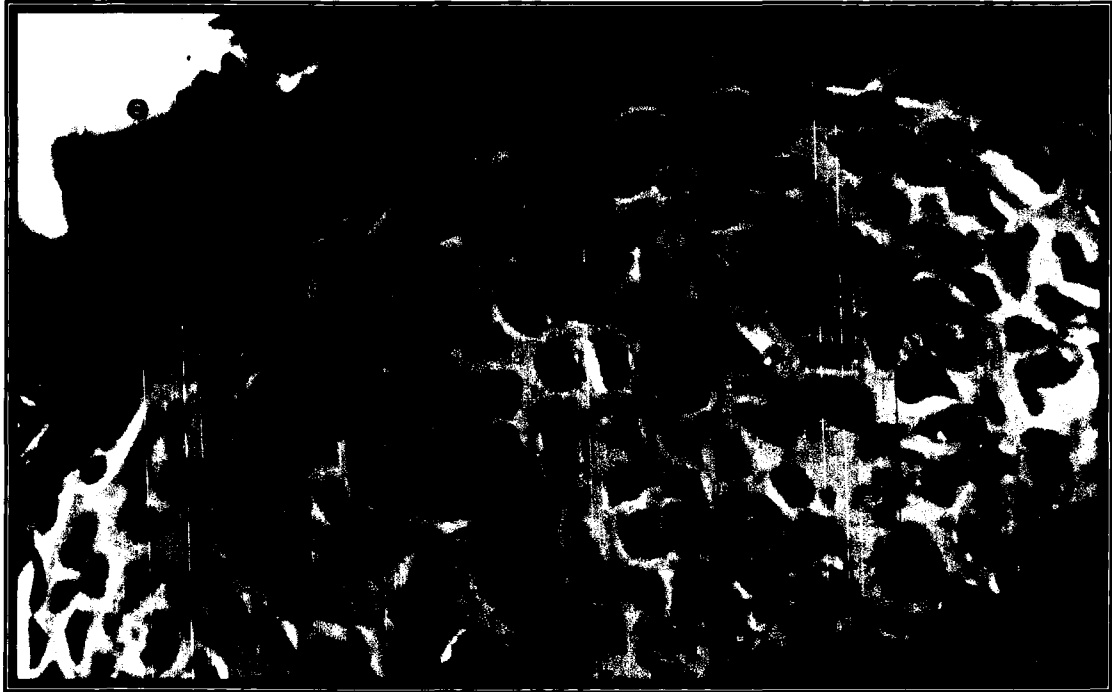


Figure 3.3: Trachea of a 14 day old control rat. Bar = 40 $\mu$ m  
Trachea cartilage with chondrocytes (c) surrounded with a perichondrium (p) and epithelium (e).

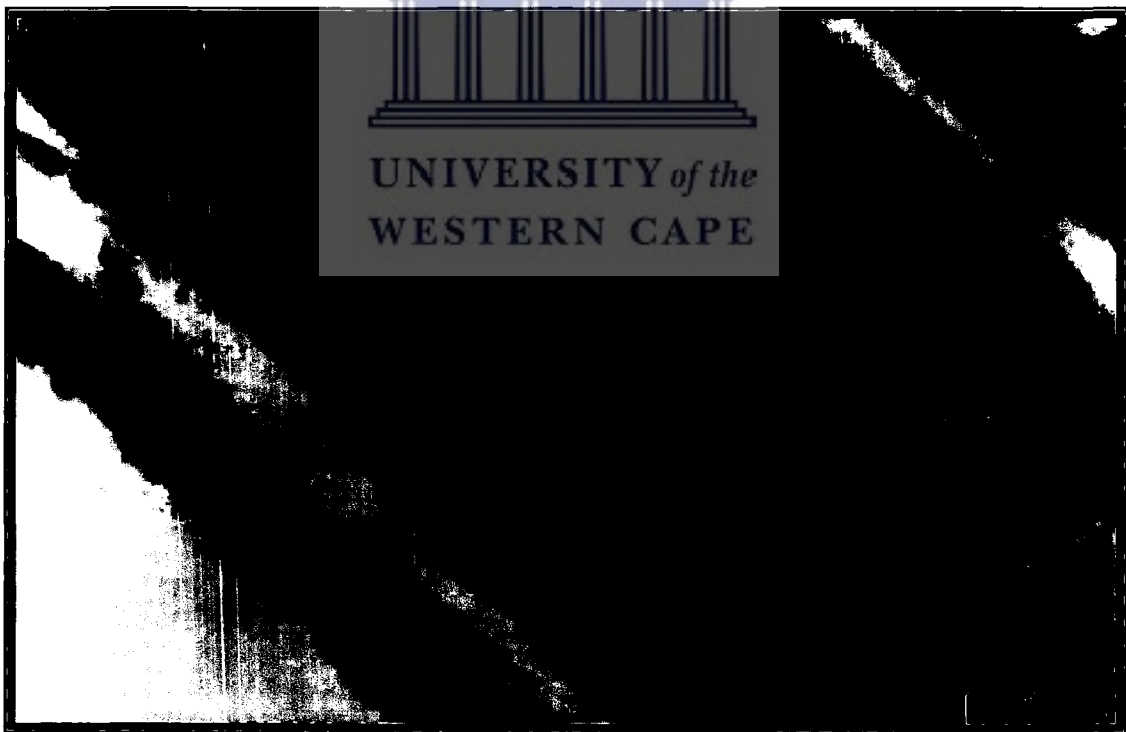


Figure 3.4: Trachea of a 14 day old nicotine exposed rat. Bar = 40 $\mu$ m.  
Chondrocytes (c) surrounded with a perichondrium (p).

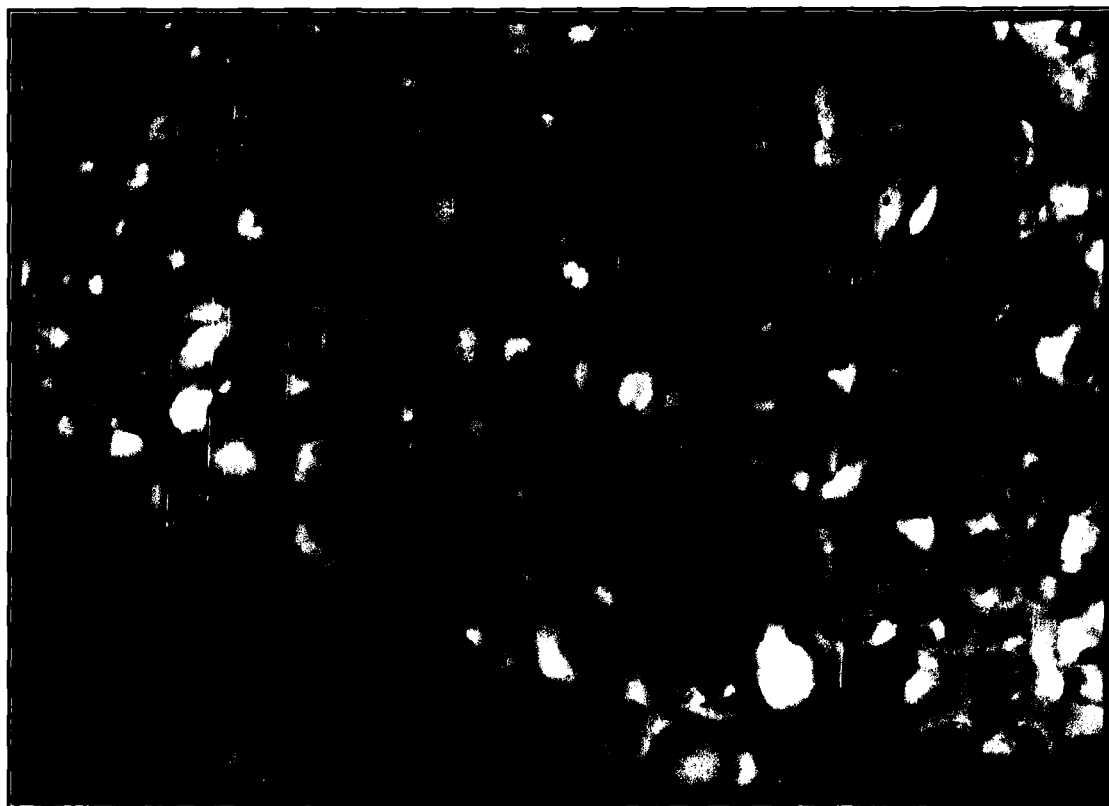


Figure 3.5: Trachea of a 21 day old control rat.  
Lacunae containing chondrocytes (c) embedded within the matrix.

Bar = 40 $\mu$ m



Figure 3.6: Trachea of a 21 day old nicotine exposed rat.  
Areas of damage within the trachea cartilage indicated with arrows ( $\blacklozenge$ ).

Bar = 40  $\mu$ m.

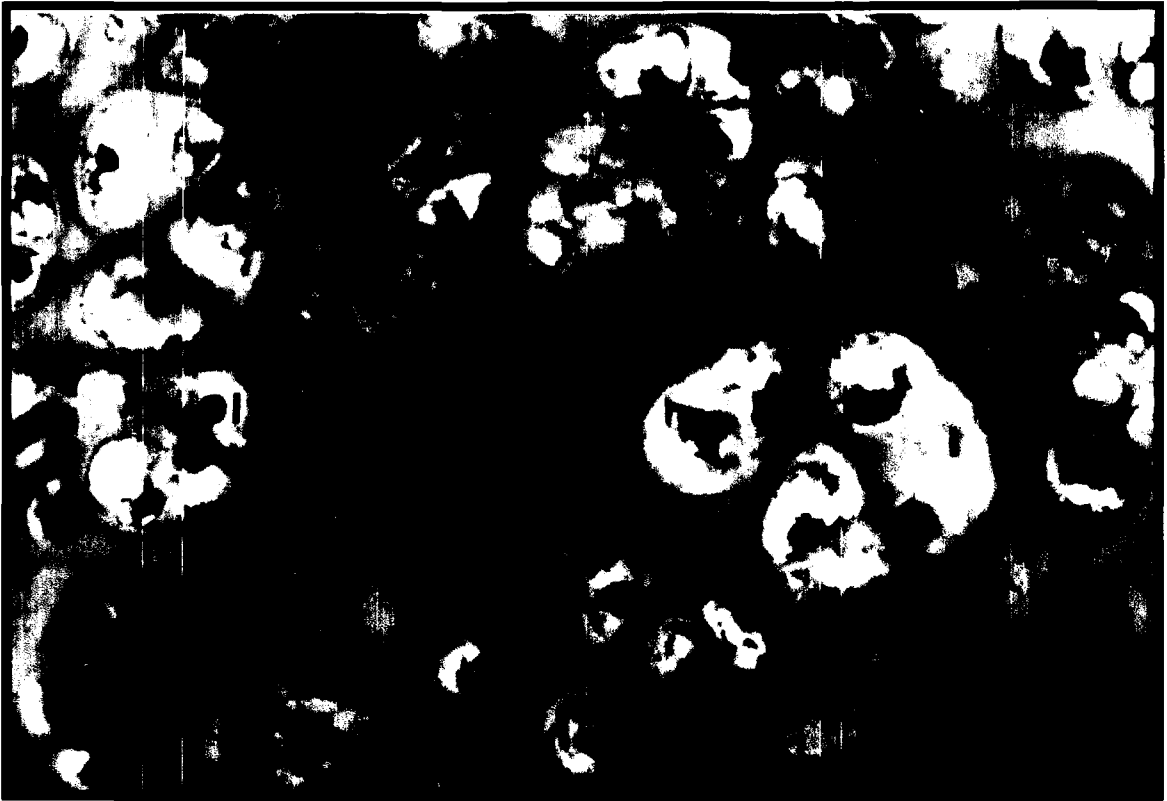


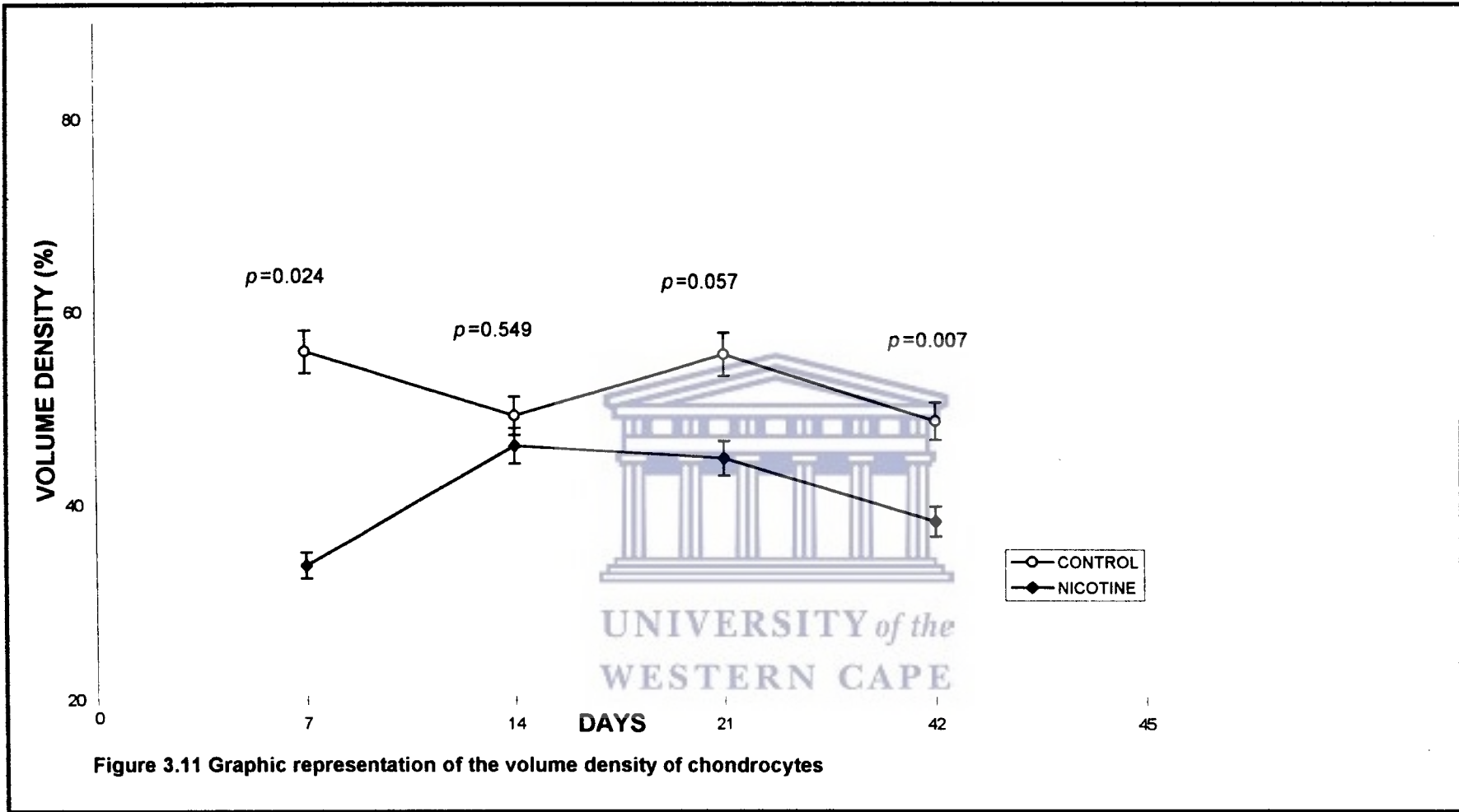
Figure 3.9: Trachea of a 42 day old control rat.  
Trachea cartilage with chondrocytes (c) contained within lacunae (l).

Bar = 40 $\mu$ m



Figure 3.10: Trachea of a 42 day old nicotine exposed rat.  
Chondrocytes (c) appear ruptured within areas of damage indicated with arrows (♦).

Bar = 40 $\mu$ m



### **3.2 SCANNING ELECTRON MICROSCOPY**

Scanning electron microscopy was used to determine whether maternal nicotine exposure during pregnancy and lactation had any influence on the surface morphology of the trachea epithelium and trachea hyaline cartilage rings. It's effects on hyaline cartilage and on the alveoli was also investigated. The data presented in figures 3.11 – 3. 21 are described below.

The wall of the trachea consists of a mucosa, submucosa and adventitia (Figure 3 (b)). The mucosa consists of pseudostratified ciliated epithelium with goblet cells and a lamina propria of fine connective tissue with diffuse lymphatic tissue. In the deep part of the lamina propria, elastic fibers become concentrated to form a longitudinal elastic membrane. The submucosa consists of loose connective tissue with mixed glands whose ducts pass through the lamina propria to open in the lumen of the trachea (di Fiore, 1981).

The plate of hyaline cartilage is surrounded by its perichondrium of dense fibrous tissue, which merges internally with the submucosa and externally with the adventitia. The usual relationship of cartilage to perichondrium is seen, with larger lacunae and chondrocytes in the interior of the plate becoming progressively flattened toward the perichondrium, and the matrix gradually blending with the connective tissue. Numerous blood vessels and nerves course in the adventitia and supply smaller branches to the outer layers (di Fiore, 1981).

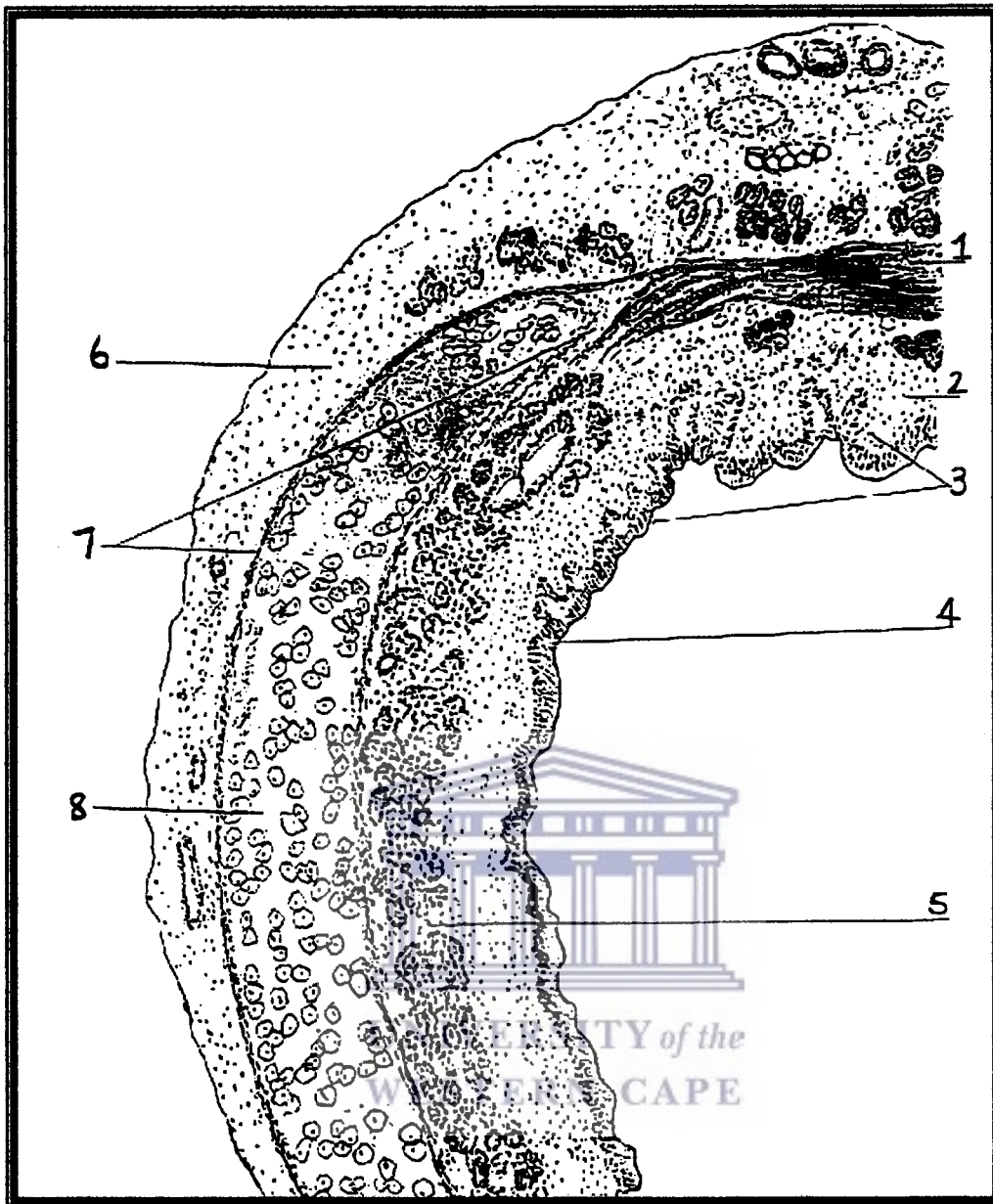


Figure 3 (b): Trachea surface overview (transverse section). The wall of the trachea consists of a mucosa (3), submucosa (5) and adventitia (6). The mucosa (3) consists of the pseudostratified ciliated columnar epithelium (4) and a lamina propria (2). The trachea cartilage (8) is surrounded by the perichondrium (7), where between their ends lies the tracheal muscle (1). (di Fiore 1981)



### 3.2.1 Trachea Cartilage

The following features were evident in the trachea cartilage of both the control (Figure 3.11 & 3.13) and nicotine exposed (Figure 3.12 & 3.14) rat pups. In preparation of the samples, it was evident that the chondrocytes (CH) were washed out of their normal ovoid spaces called the lacunae (LH) and was illustrated by light microscopy. The epithelial (EP) constituents of ciliated cells, non-ciliated cells as well as goblet cells, which is separated from underlying connective tissue by a basal membrane. Located between the submucosa and the adventitia is a C-shaped plate of hyaline cartilage, which is surrounded by a thin fibrocellular sheet, called the perichondrium (P). The cartilaginous trachea zones were found to occupy large areas. The cartilage cells, or chondrocytes (CH) are in the lacunae, which is embedded in a cartilage matrix (M).

No notable differences in the surface morphology occur between the 14 day old control (Figure 3.11) and experimental rat pups (Figure 3.12). However, at postnatal day 42 in the control animals (Figure 3.13) the sites of chondrocytes (CH) appear to be homogenous whilst that of the nicotine exposed (Figure 3.14) rat pups, show areas of damage to the lacunae. Similar damage was also evident with light microscopy, where area of damage within the matrix occurred in the hyaline cartilage at postnatal day 21 and 42.

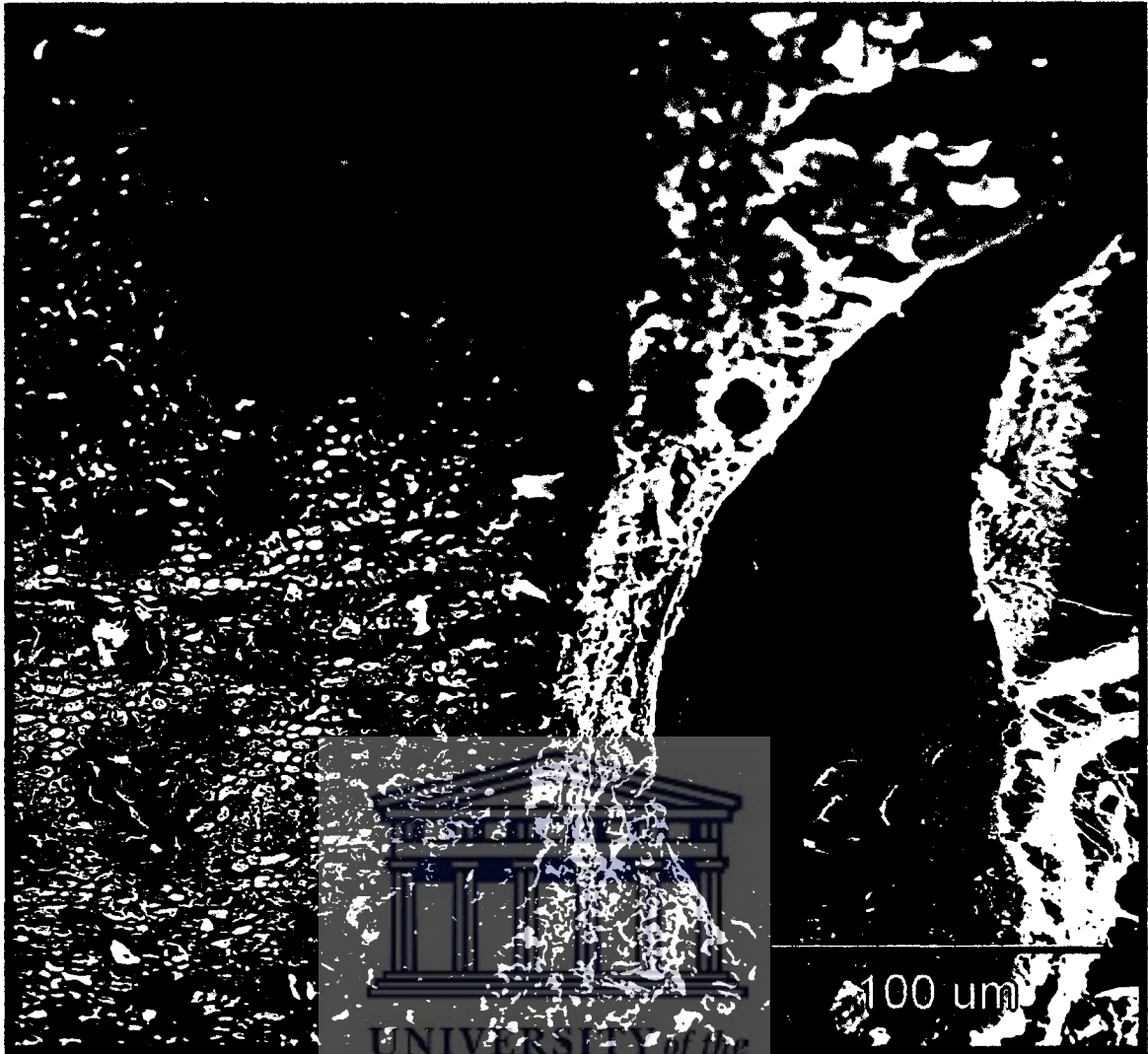


Figure 3.11: Trachea cartilage of a 14 day old control rat. **PE** Bar =100  $\mu\text{m}$

Lacunae, which normally contain chondrocytes (**CH**) embedded in matrix surrounded by a perichondrium (**P**) and a layer of trachea epithelial surface (**EP**).

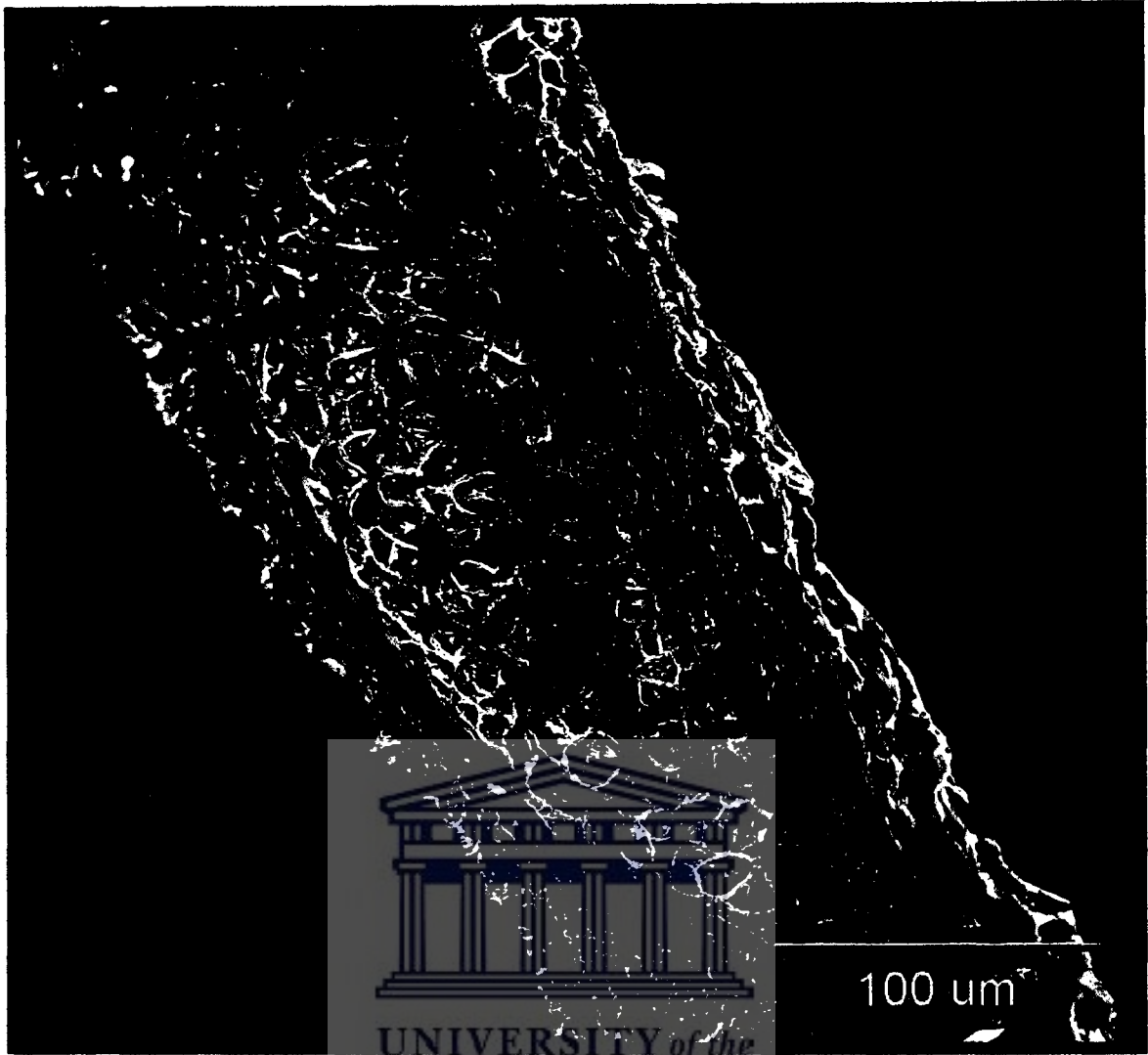


Figure 3.12: Trachea cartilage of a 14 day old nicotine exposed rat. Bar =100  $\mu$ m

Lacunae, which normally contain chondrocytes (CH) embedded in matrix (M) surrounded by a perichondrium (P) and a layer of trachea epithelial surface (EP).



Figure 3.13. Trachea cartilage of a 42 day old control rat pup.

Bar = 100 $\mu$ m

Lacunae (L) which normally contain chondrocytes (CH) embedded in matrix (M), surrounded by a perichondrium (P) and a layer of trachea epithelial surface (EP).

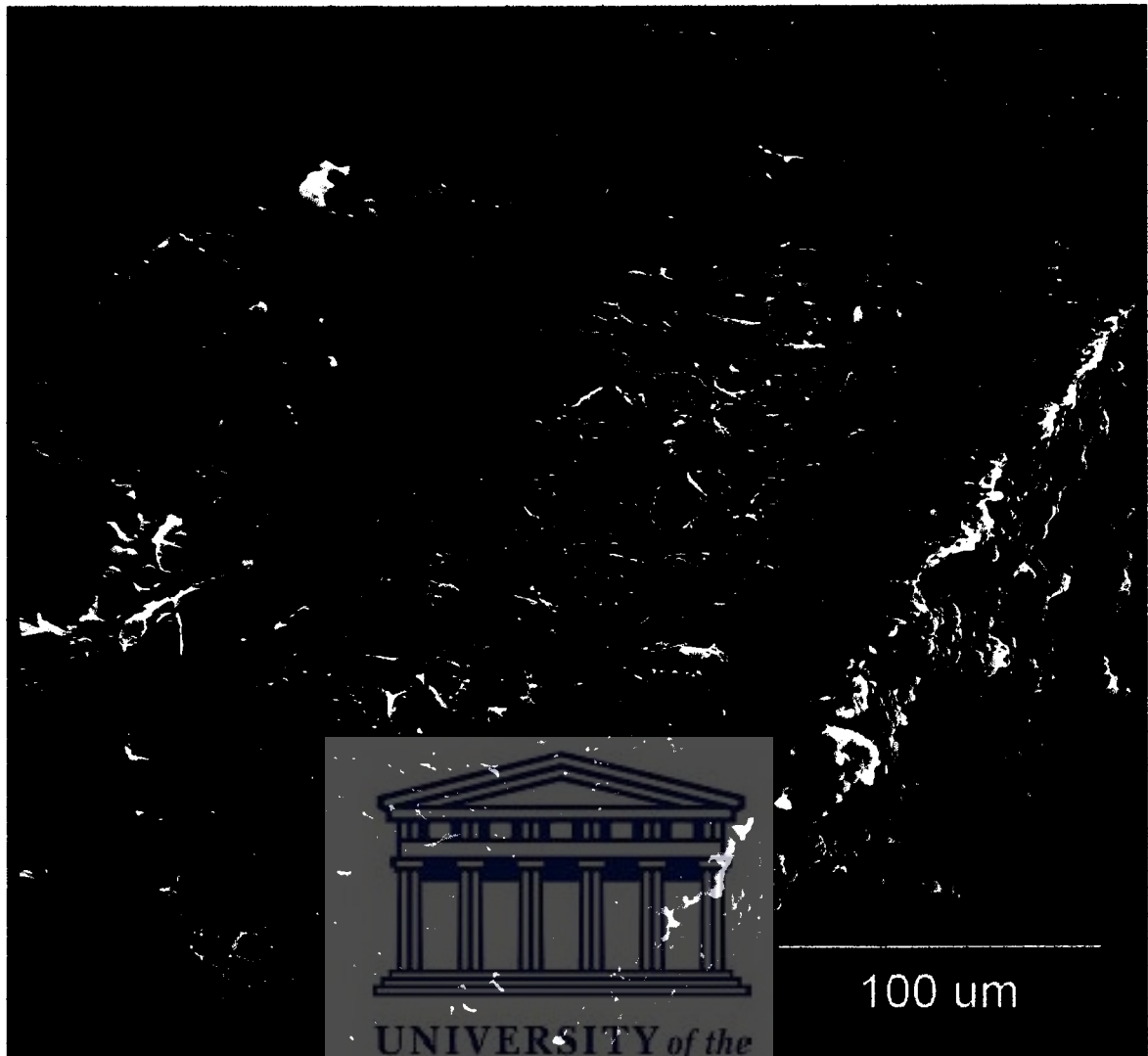
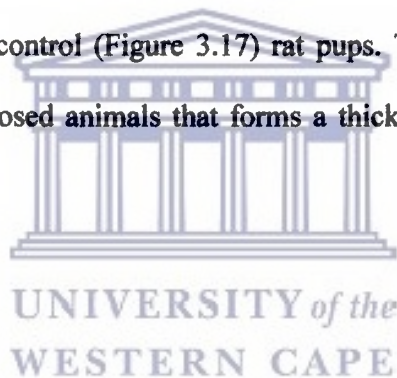


Figure 3.14: Trachea cartilage of a 42 day old nicotine exposed rat. Bar = 100 $\mu$ m  
Lacunae (L) which normally contain chondrocytes (CH) embedded in matrix (M),  
surrounded by a perichondrium (P) and a layer of trachea epithelial surface (EP). Areas  
of damage are encircled.

### 3.2.2 Trachea Epithelium

Figures 3.15 & 3.17 and Figures 3.16 & 3.18 are micrographs of the surface morphology of the trachea epithelium of 14 and 42 day old control and experimental rats, respectively.

At postnatal day 14 the trachea epithelium of control animals (Figure 3.15) and the nicotine exposed rat pups (Figure 3.16) displayed numerous ciliated cells as well as the secreting cells e.g., goblet cells. Numerous microvilli occur on the surface of the goblet cells of both the 14 day old control and nicotine exposed (Figure 3.16) rat pups. As for the 14 day old control animals, the goblet cells of the 42 day old rat pups showed numerous prominent microvilli. However, the microvilli of the goblet cells of 42 day old nicotine exposed (Figure 3.18) animals is less prominent than on the postnatal day 14 than that of the 42 day old control (Figure 3.17) rat pups. This is due to more mucus secretion in the nicotine exposed animals that forms a thick coverage over the ciliated cells (Figure 3.16 & 3.18).



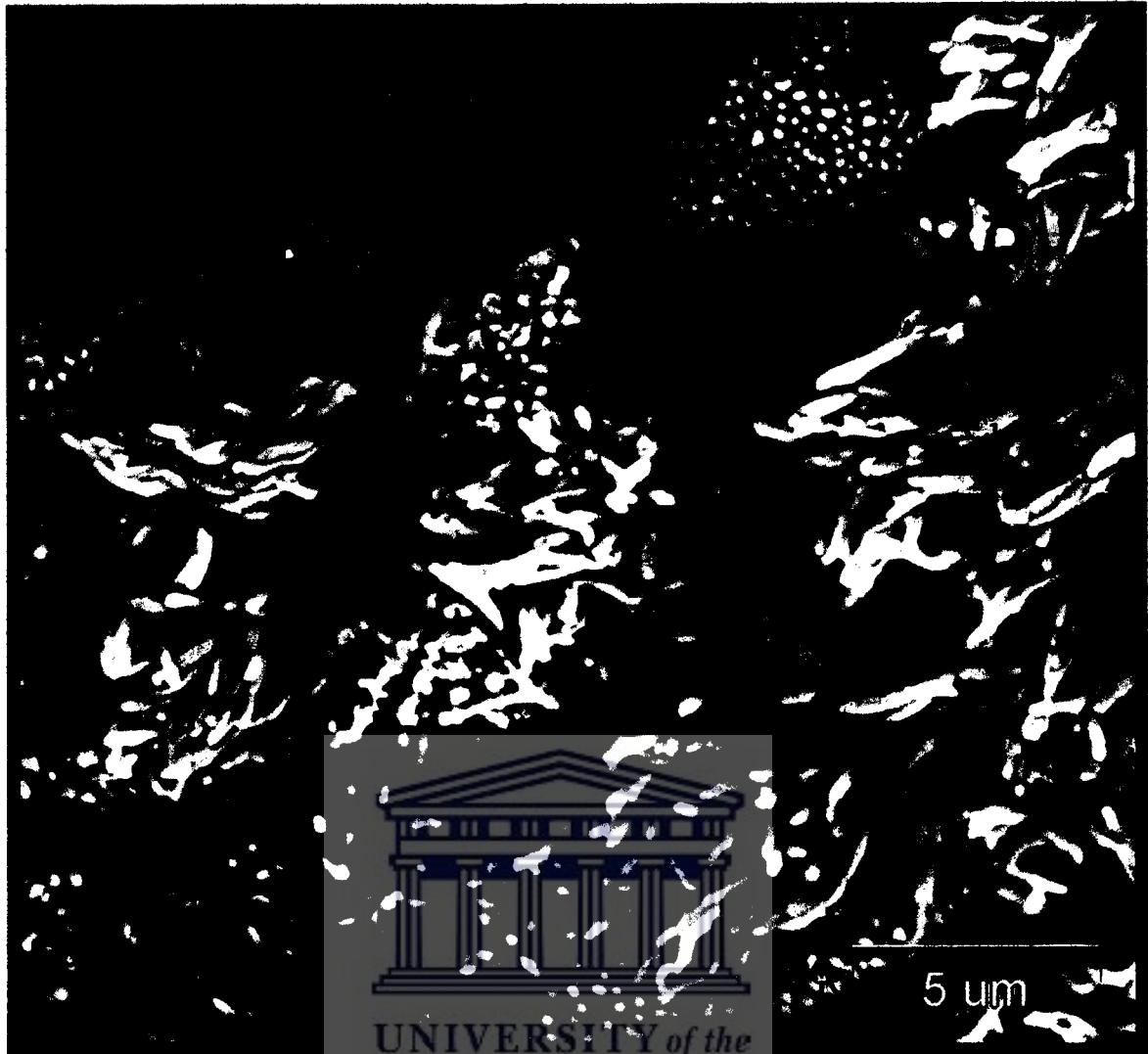


Figure 3.15: Trachea epithelium of a 14 day old control rat.

Bar = 5 $\mu$ m

Epithelium surface of the tracheae illustrating, ciliated cells (Ci) and goblet cells (GC) as

well as microvilli (▶).



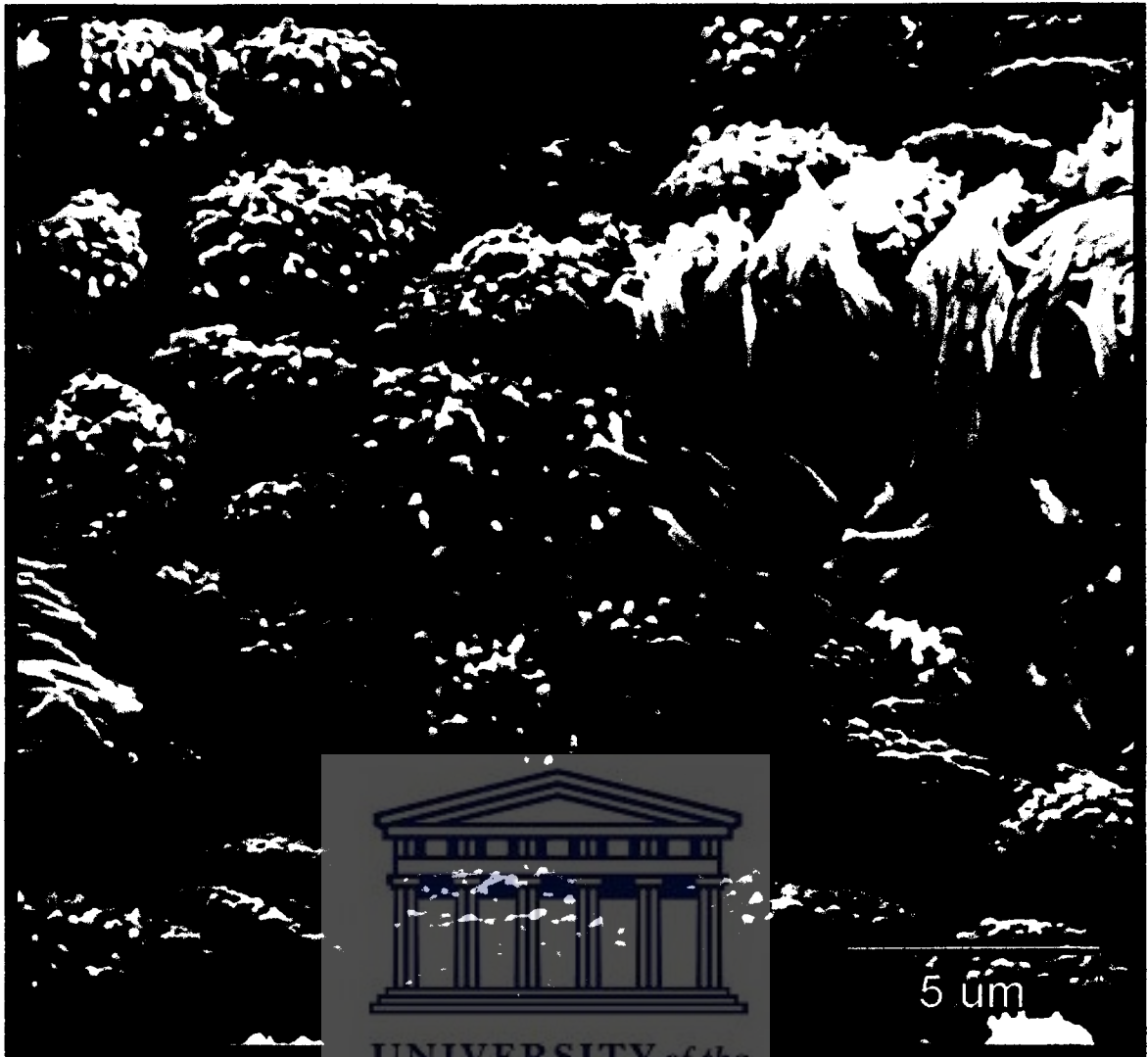


Figure 3.16: Trachea epithelium of a 14 day old nicotine exposed rat. Bar = 5 μm

Epithelium surface of the tracheae illustrating, ciliated cells (Ci) and goblet cells (GC) as well as microvilli (◆).

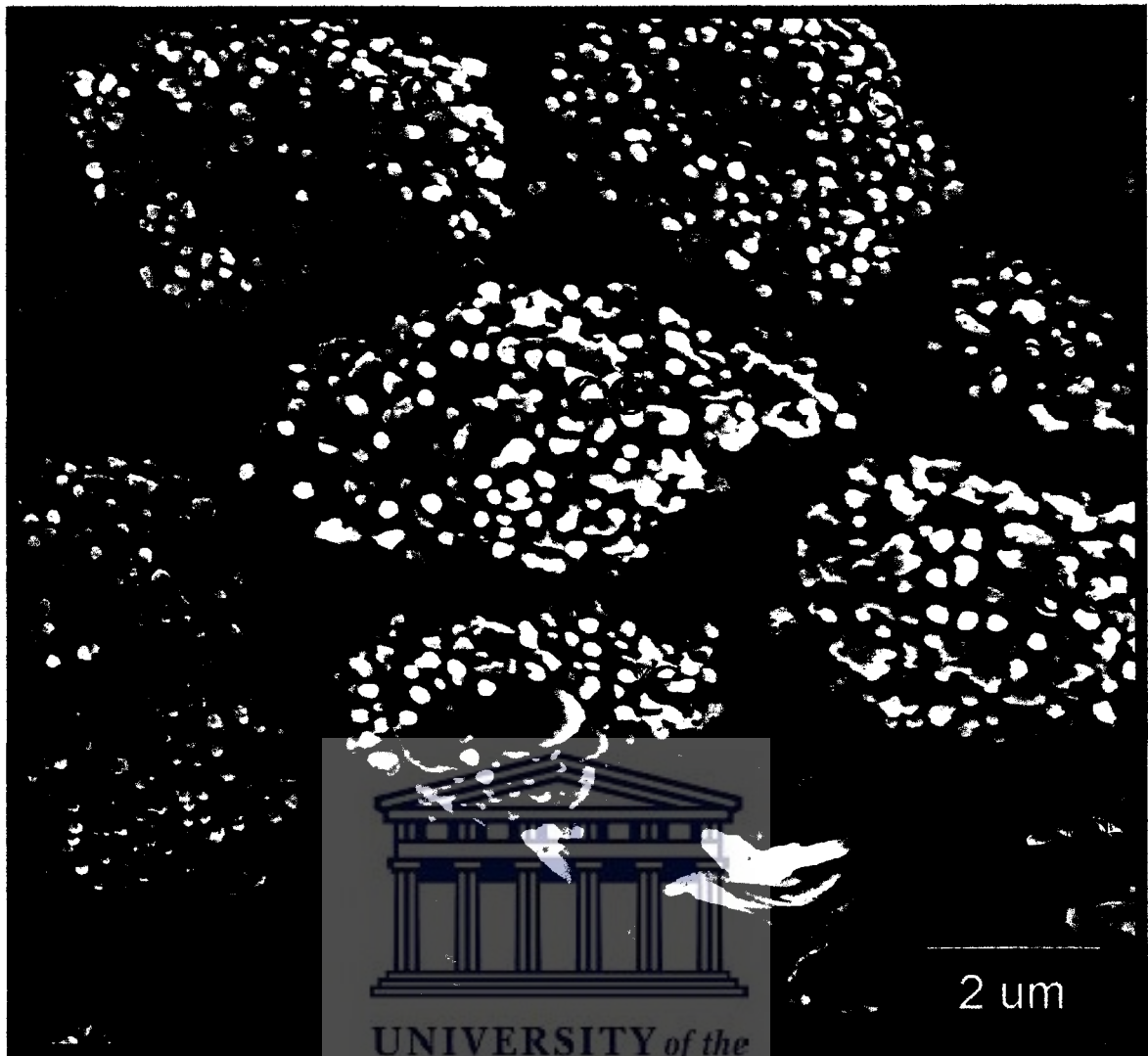


Figure 3.17: Trachea epithelium of a 42 day old control rat.

Bar = 2μm

Epithelium surface of the tracheae illustrating, ciliated cells (Ci) and goblet cells (GC) as well as microvilli (▶).

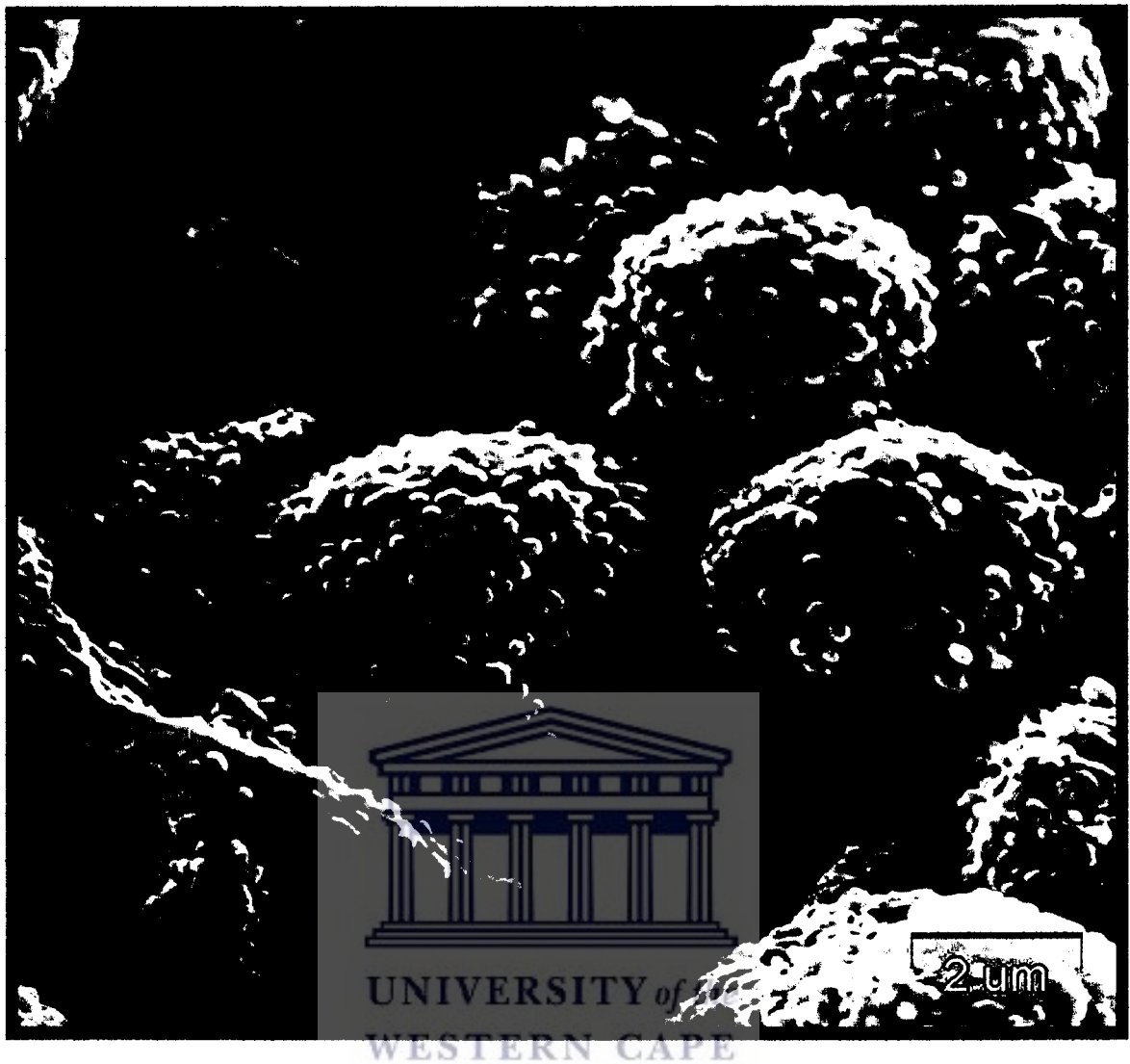


Figure 3.18: Trachea epithelium of a 42 day old nicotine exposed rat. Bar = 2 $\mu$ m  
Epithelium cell surface of the trachea illustrating, nonciliated cells namely goblet cells (GC) with short microvilli (▶).

### 3.2.3 Alveolar Surface

The alveolar surface of 7 day old control (Figure 3.19) and experimental (Figure 3.20) rat pups, are both intact. However, the alveoli of the 7 day old nicotine exposed rat pups were evidently bigger than that of the control rat pups of the same age. This is also evident in the lungs of control rats at postnatal day 42 (Figure 3.21) However, at day 42, the experimental rat lung tissue (Figure 3.22) have widespread damage in the form of alveolar fenestrations, evident within the alveoli.

This means that from postnatal day 7 to postnatal day 42, the alveolar surface of the nicotine exposed rat pups, gradually deteriorated. This observation whereby deterioration occur as the lung matures, corresponds with the observation on changes in the surface morphology of the goblet cells in the trachea epithelium in that it became evident only after lung maturation is completed.



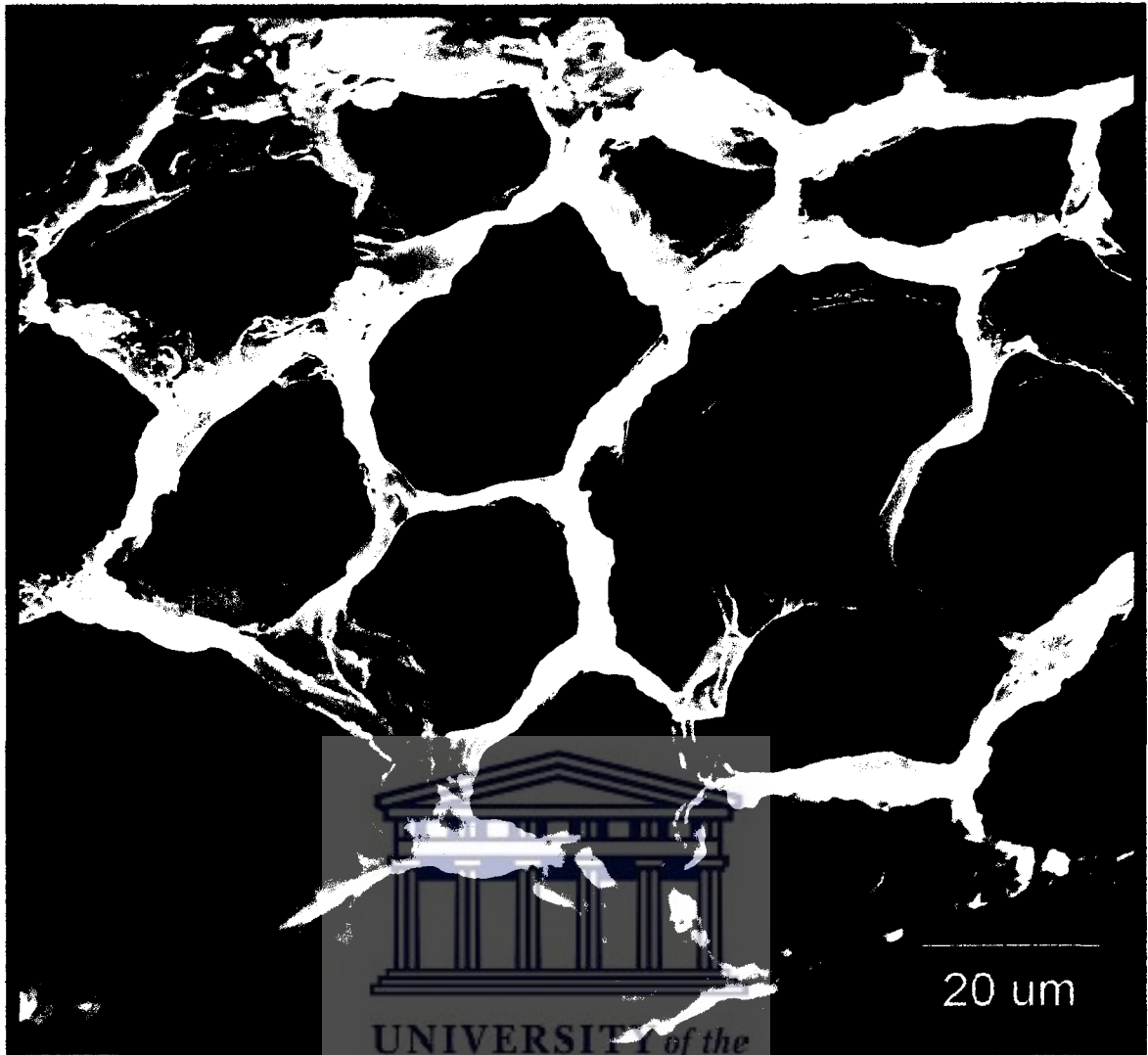


Figure 3.19: Alveolar surfaces of lungs of day 7 old control rat pup.

Bar = 20μm

Alveoli (A).

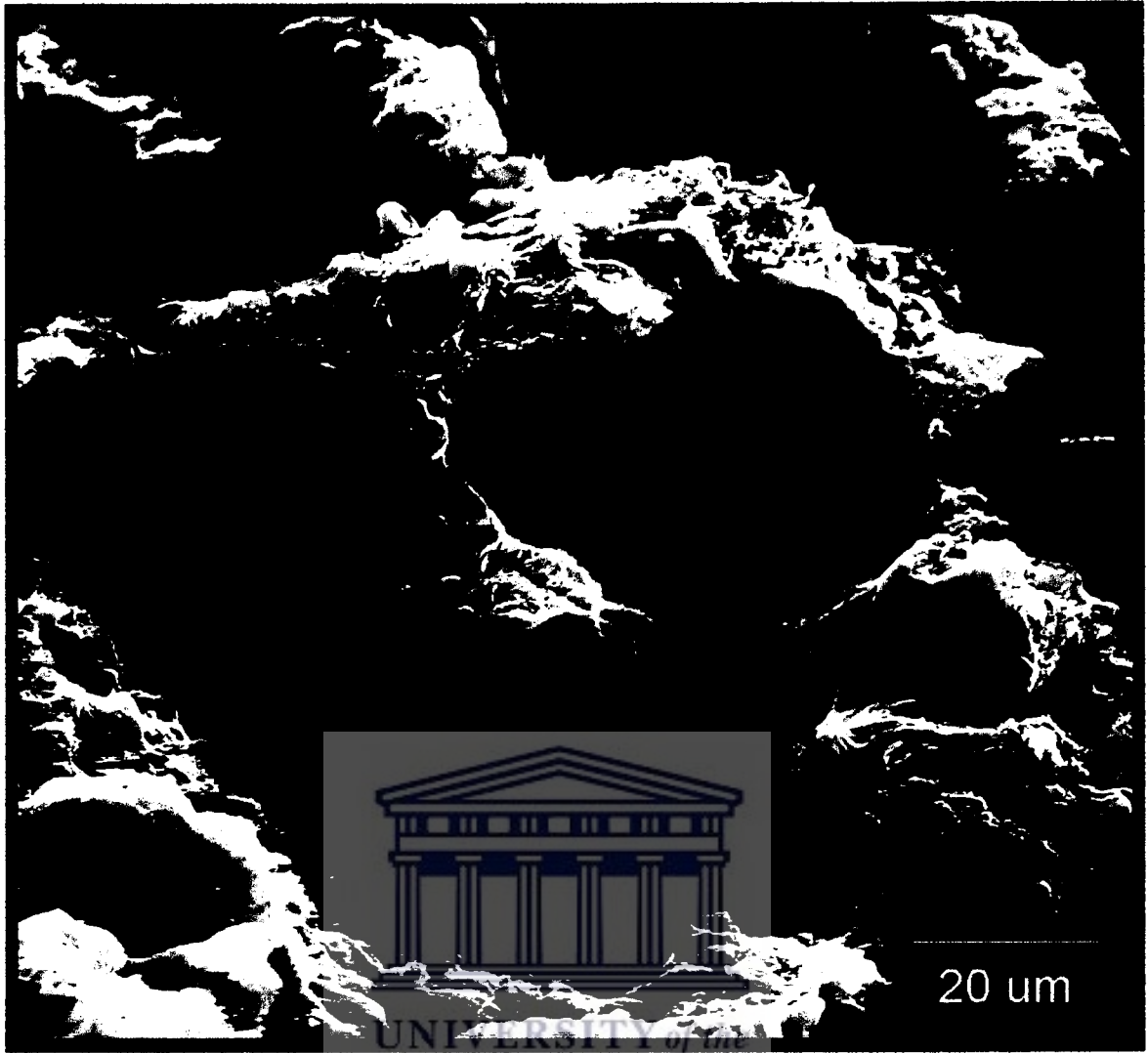


Figure 3.20: Alveolar surfaces of lungs of day 7 old experimental rat pup. Bar = 20 $\mu$ m

Alveoli (A).

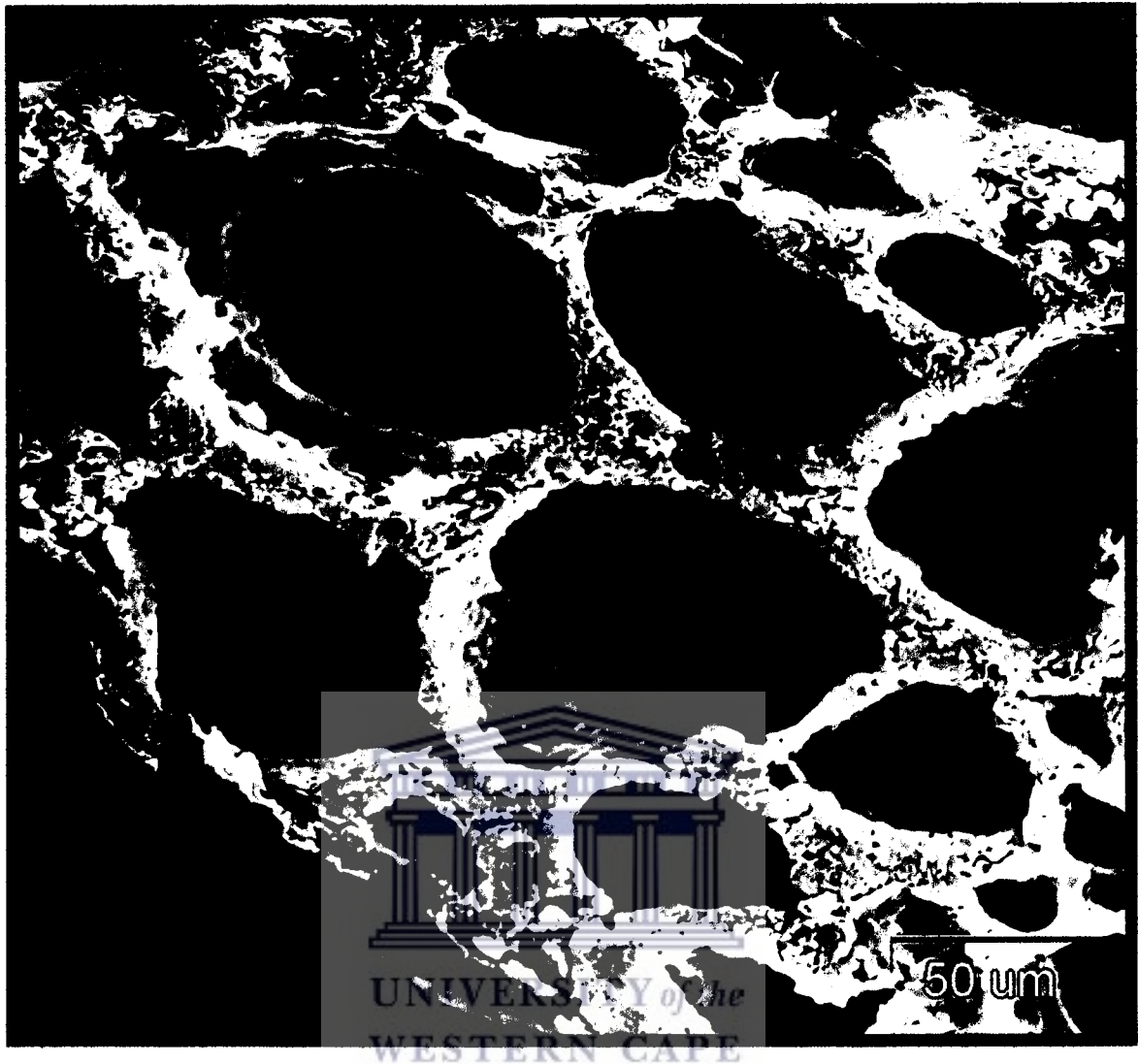


Figure 3.21: Alveolar surfaces of lungs of day 42 old control rat pup.

Bar = 50μm

Alveoli (A).



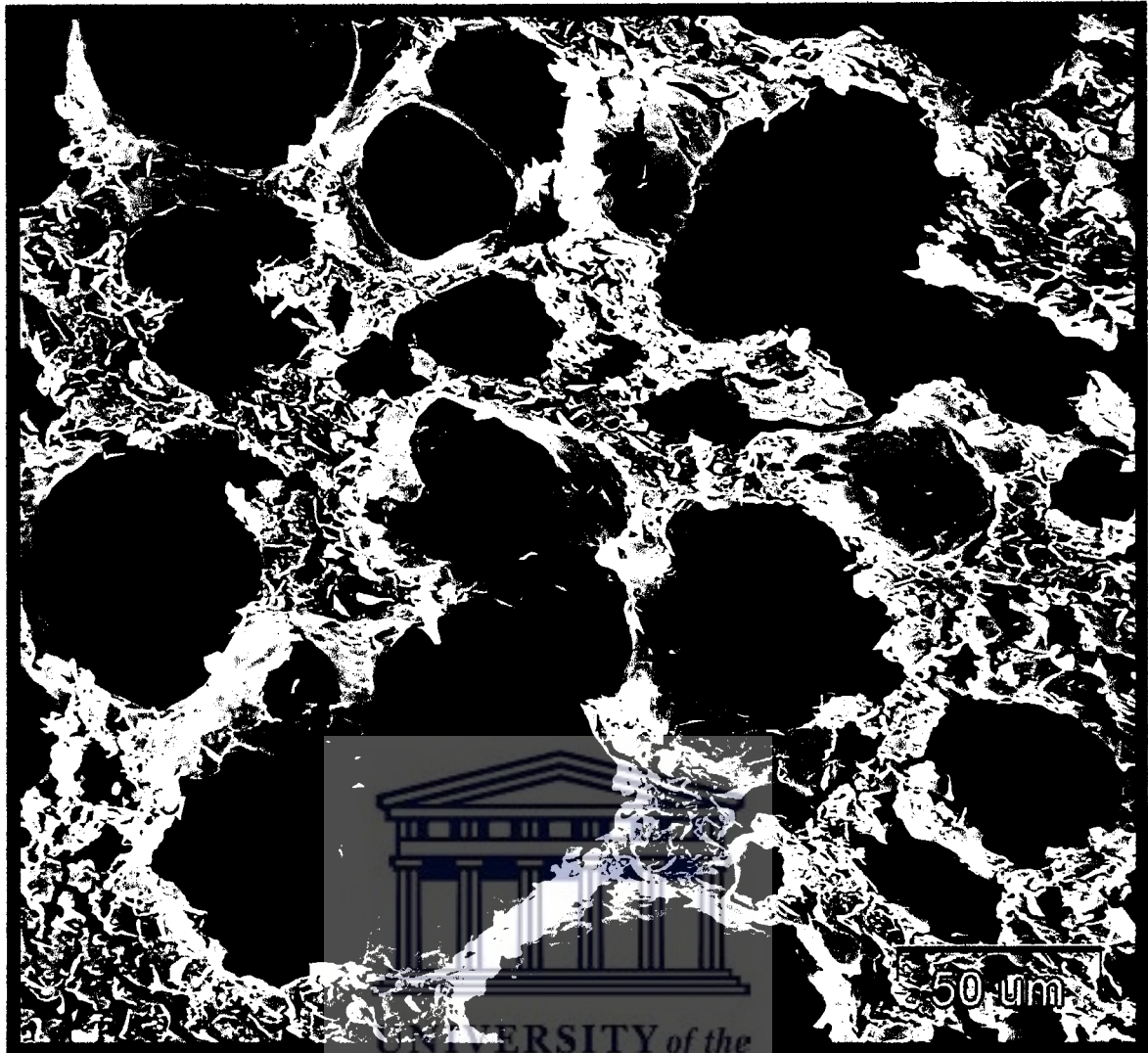


Figure 3.22: Alveolar surfaces of lungs of day 42 old nicotine exposed rat pup.

Damaged alveoli (A) with uneven fenestrations, indicated with arrows (↯).

Bar = 50μm

### **3.3 TRANSMISSION ELECTRON MICROSCOPY**

The morphologic status (Figure 3.23 – 3.28) and morphometric (Table 3.2) data on cells of the trachea of the control and nicotine exposed rat pups of various age groups are described in this section.

#### **3.3.1 Morphology of trachea epithelium of neonatal rats:**

##### **Effects of maternal nicotine exposure.**

Figures 3.23 and 3.24 are electron micrographs of the trachea epithelial cells of 21 day old control and nicotine exposed rat pups, respectively. In both the following structural features of the trachea epithelium, was evident. The trachea epithelium lining were found to be composed of columnar epithelial cells. These include ciliated cells as well as mucous secreting cells or goblet cells. Cell borders are clearly visible. The cytoplasm of the goblet cells is electron dense and contains many large secretory granules (s) near the free surface with sparse mitochondria. The cytoplasm of the ciliated cells (c) is electron lucent compared to the goblet cells. It contains scattered ribosomes and an abundance of mitochondria (m). Well-developed endoplasmic reticulum chains (») as well as a few Golgi (g) complexes are present.

At postnatal day 21, the trachea epithelium of the control rat pups (Figure 3.23) appeared to have an abundance of scattered endoplasmic reticulum throughout the cytoplasm of both the ciliated cells (c) and the goblet cells. The ciliated cells (c) appear to have numerous mitochondria within the cytoplasm. The goblet cells on the other hand, have many secretory granules (s) present as well as short microvilli at the base of cells. In Figure 3.24, the trachea epithelium of the nicotine exposed rat pups, the ciliated cells had

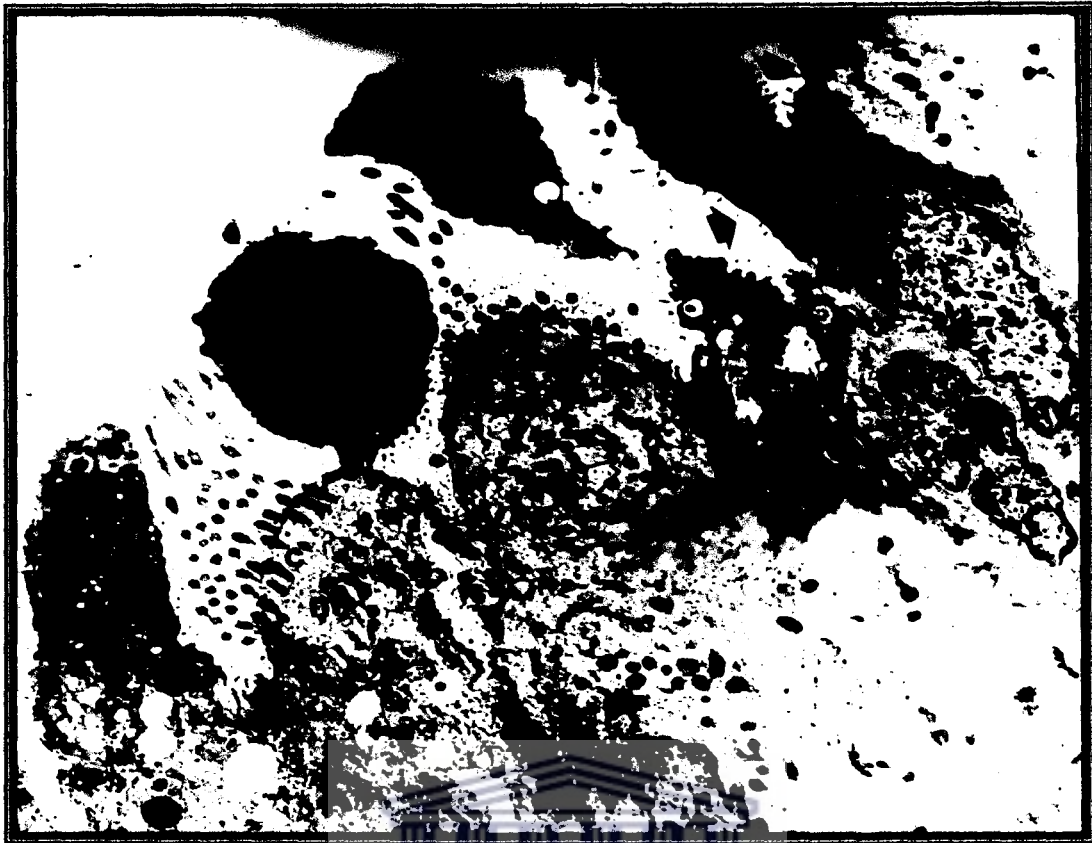


Figure 3.23: Electron micrograph of the epithelial cells of the trachea of day 21 old control rat pup. The trachea epithelium has ciliated cells (c) and goblet cells with secretory granules (s) near the free surface of these cells. The cytoplasm contains cell nuclei (n), mitochondria (m) and endoplasmic reticulum (e). Microvilli indicated with arrows (↕). (3 500X magnification)



Figure 3.24: Electron micrograph of the epithelial cells of the trachea, day 21 old nicotine exposed rat pup. The trachea epithelium has ciliated cells (c) and goblet cells with secretory granules (s) near the free surface of these cells. The cytoplasm contains nuclei (n), mitochondria (m) and endoplasmic reticulum (r). (3 000X magnification)

many mitochondria (m) but fewer endoplasmic reticulum (») present. The goblet cells are electron dense with secretory granules (s) near the surface of these cells with no microvilli being present at the base of these cells.

The microvilli of the goblet cells in the scanning micrographs were observed to be less prominent on the cell surface of the nicotine exposed rat pups of postnatal day 14 (Figure 3.16) and day 42 (Figure 3.18), when compared to the control animals of postnatal day 14 (Figure 3.15) and 42 (Figure 3.17).

### **3.3.2 Morphology of trachea chondrocytes of neonatal rats :**

#### **Effects of maternal nicotine exposure**

The morphological data of 21 day old rats and older are presented because no differences were visible in younger animals. Morphological differences only occur from postnatal day 21. Figures 3.25 and 3.26 are electron micrographs of chondrocytes of trachea hyaline cartilage of 21 day old control (Figure 3.25) and nicotine exposed (Figure 3.26) rat pups. Figures 3.27 (control) and 3.28 (nicotine exposed) are electron micrographs of trachea hyaline cartilage of 42 day old rats.

At postnatal day 21, the chondrocytes of the control rat pups (Figure 3.25) have an electron dense cell nuclei (n) and the cytoplasm contains numerous small mitochondria (m), lipid bodies (l), as well as a well-developed Golgi apparatus (g). An abundance of

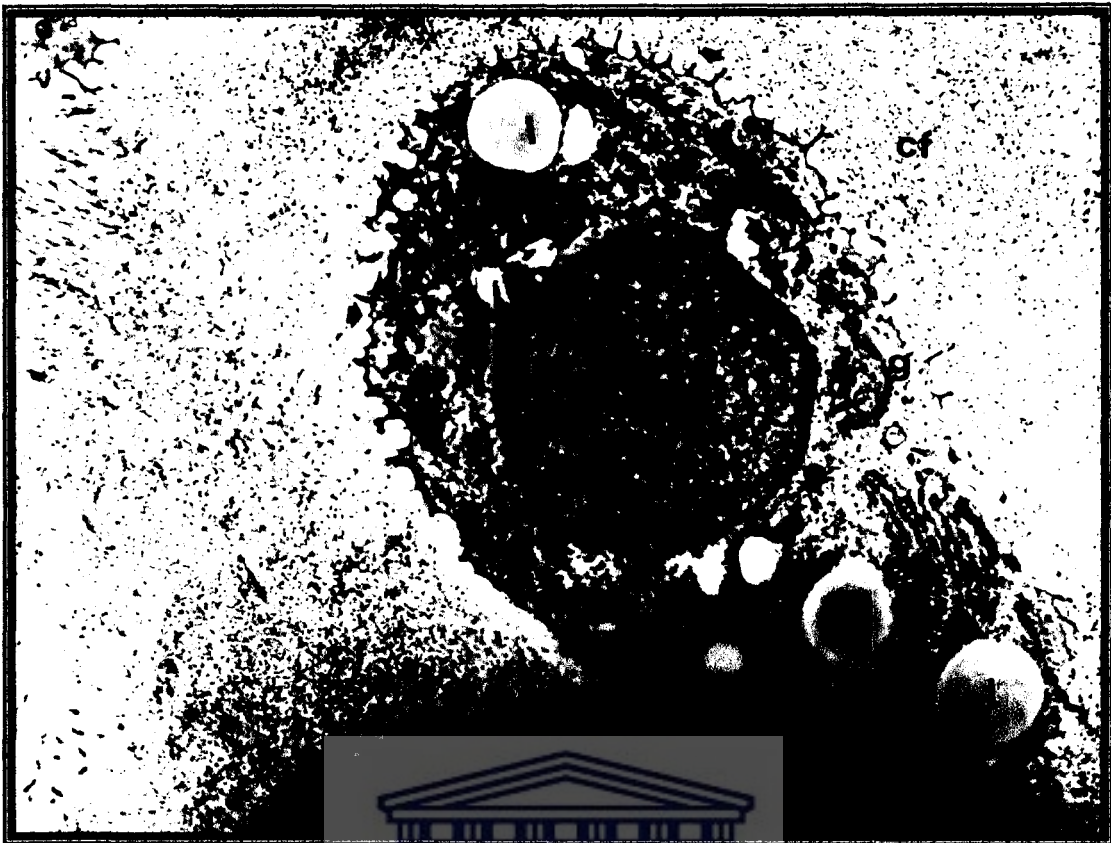


Figure 3.25: Electron micrograph of the chondrocyte, of a 21 day old control rat pup.

Where the cell nucleus (n), mitochondria (m), lipid bodies (l), Golgi apparatus (g) and endoplasmic reticulum (er). Cytoplasmic projections indicated with arrows (b) and collagen fibers (cf) in the matrix. (4 000X magnification)



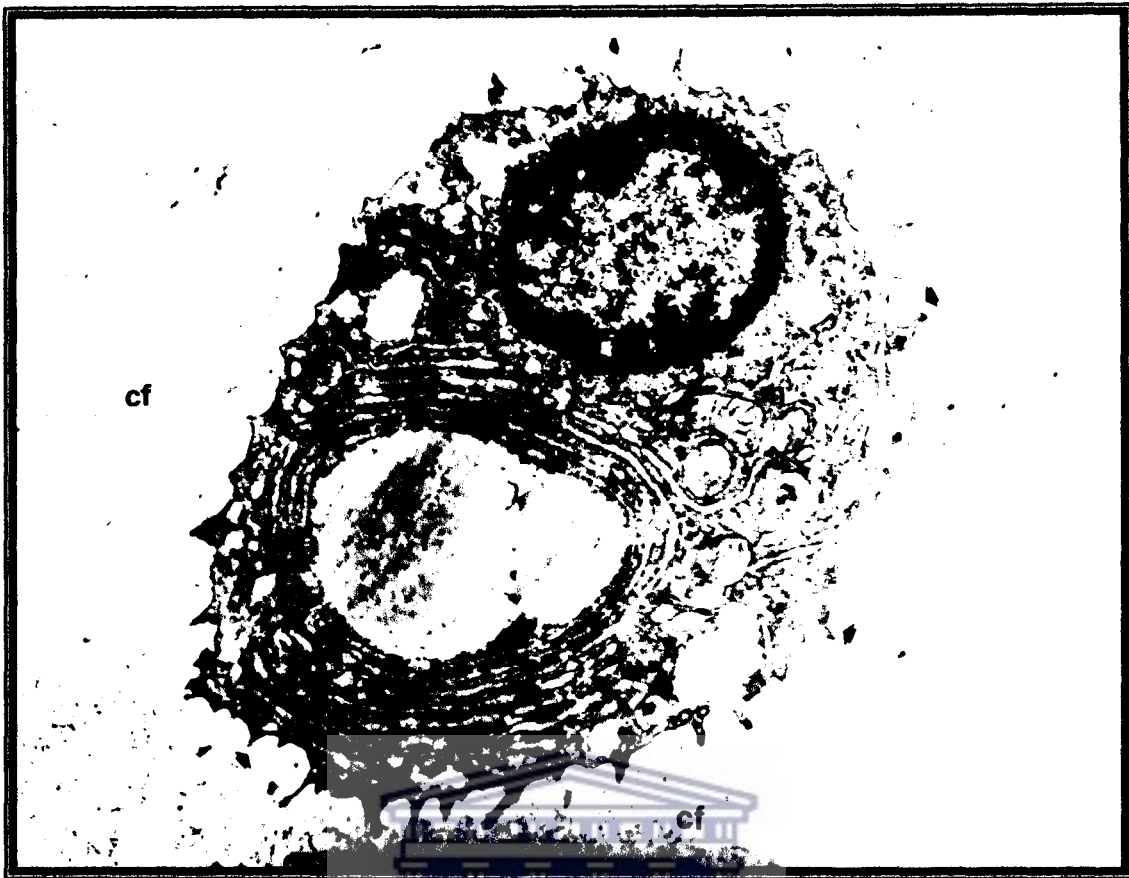


Figure 3.26: Electron micrograph of the chondrocyte, of a 21 day old nicotine exposed rat pup. With a large cell nucleus (n), mitochondria (m), lipid bodies (l) and endoplasmic reticulum (er) chains. Cytoplasmic projections indicated with arrows (♦) and collagen fibers (cf) in the matrix. (10 000X magnification)



endoplasmic reticulum (») are scattered throughout the granular cytoplasm. The chondrocytes of the day 21 old, nicotine exposed (Figure 3.26) rat pups have electron lucent cell nuclei (n) with peripheral arranged chromatin. The cytoplasm appears to contain fewer mitochondria (m) than the control animals of the same age and appears to be swollen. The Golgi apparatus (g) and endoplasmic reticulum (») chains also appears to be less prominent than in chondrocytes of the control animals of the same age.

The cytoplasm of the chondrocytes of the 21 day old nicotine exposed (Figure 3.26) animals displays many electron lucent areas and is not as granular as in the chondrocytes of the 21 day old control (Figure 3.25) animals. In both, the control (Figure 3.25) and experimental (Figure 3.26) animals the cartilage matrix have a very fine, granular appearance. Collagen fibrils (cf) are observed within the surrounding cartilage matrix, the electron-dense particles interspersed between the fibrils are believed to be glycosaminoglycans. The chondrocytes also possess numerous cytoplasmic projections at its surface. These possibly may function to increase the cell surface area available for absorption of nutrients and diffusion of respiratory gases into and out of the cells as well as for the maintenance of the surrounding matrix.

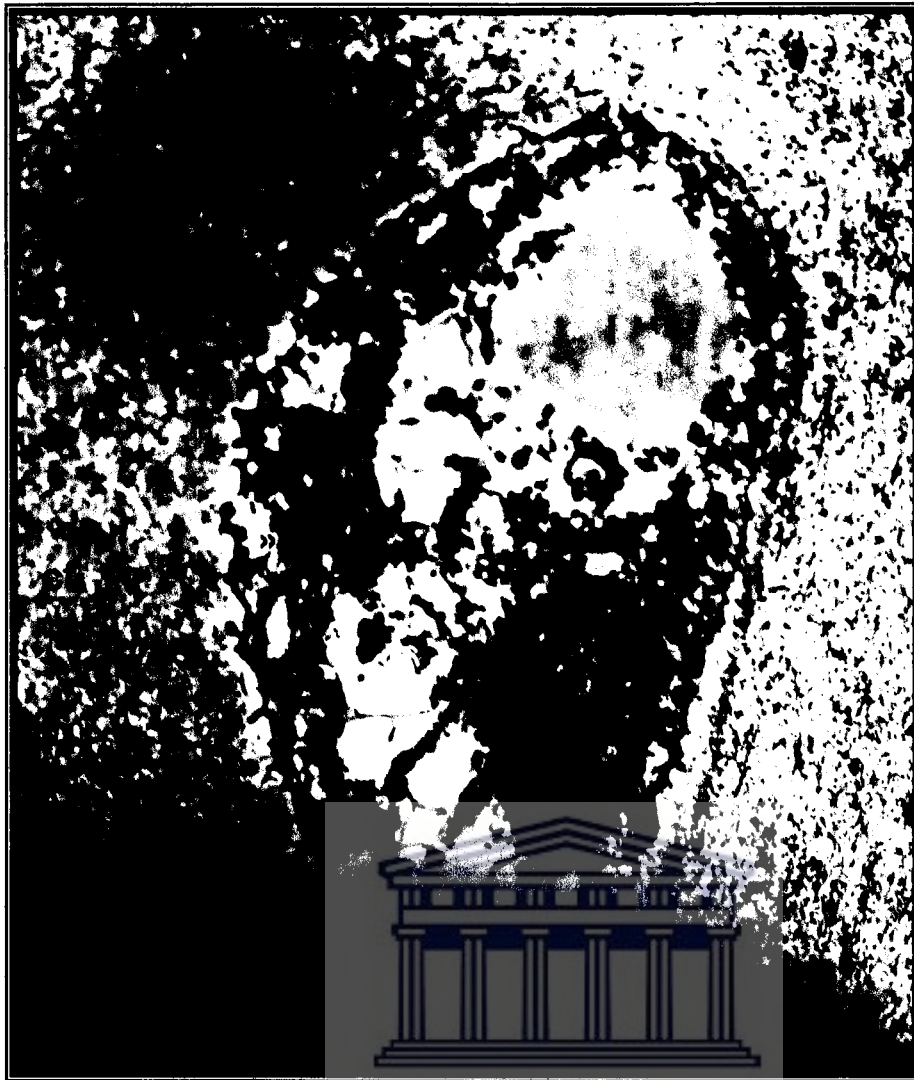


Figure 3.27: Electron micrograph of the chondrocyte, of a 42 day old control rat pup. With an electron dense cell nucleus (**n**), mitochondria (**m**), lipid bodies (**l**) and endoplasmic reticulum («) chains. Cytoplasmic projections indicated with arrows (♦) and collagen fibers (**cf**) in the matrix. (5 000X magnification)

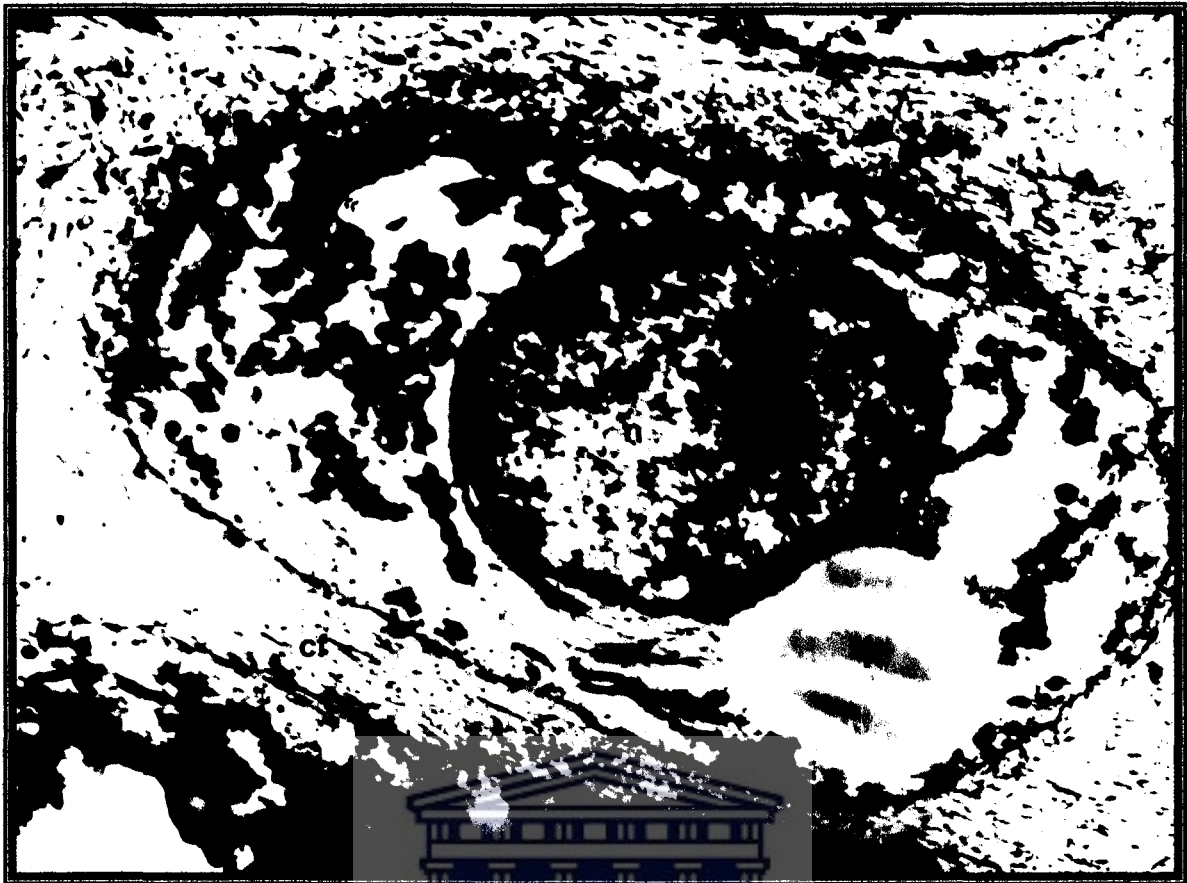


Figure 3.28: Electron micrograph of the chondrocyte, of a 42 day old nicotine exposed rat pup. With an electron dense cell nucleus (n), lipid bodies (l) and endoplasmic reticulum (er). Cytoplasmic projections indicated with arrows (♦) and collagen fibers (cf) in the matrix . (6 000X magnification)

At postnatal day 42, the chondrocytes of the trachea cartilage of the control rats (Figure 3.27) contains electron-dense nuclei. The cytoplasm also have lipid bodies (I) and scattered endoplasmic reticulum (») present. Whilst the cytoplasm of the chondrocytes of the 21 day old rat pups was homogenous, the cytoplasm of the chondrocytes of the trachea hyaline cartilage of the 42 day old control rats showed a cytoplasm with numerous electron lucent areas. The endoplasmic reticulum (») was also not as abundant as in the 21 day old rat pups. The cytoplasmic projections are also less prominent than the chondrocytes of the hyaline cartilage of trachea of 21 day old control rat pups.

In Figure 3.28 the chondrocytes of the trachea cartilage 42 day old nicotine exposed rat pups contains electron-dense nuclei with peripheral arranged chromatin. Lipid bodies (I) and endoplasmic reticulum (») appear to be present within the cytoplasm. The cytoplasmic cell projections are not as well defined as that of the chondrocytes of 21 day old nicotine exposed animals. It is also less prominent than the chondrocytes of the 42 day old control rat pups. The cytoplasm also shows bigger areas that are electron lucent than in the cytoplasm of the trachea chondrocytes of the control animals of the same age.

### 3.3.3 Morphometric Data:

The morphological data showed certain differences between the chondrocytes in the trachea hyaline cartilage of the control animals and the animals that were exposed to nicotine via the placenta and mother's milk. Morphometric techniques were used to quantify some of these observed changes in the chondrocytes of the trachea cartilage chondrocytes of the offspring.

Age (Days)	Volume Density of Chondrocyte components (%) (MEAN ± SEM)							
	Cytoplasm		Nucleus		Endoplasmic Reticulum		Lipid	
	Control	Nicotine	Control	Nicotine	Control	Nicotine	Control	Nicotine
7	69.1 ± 5.1	70.3 ± 6.1	30.9 ± 4.1	29.3 ± 3.7	20.7 ± 3.7*	13.03 ± 1.6*	0.4 ± 0.4*	4.5 ± 0.21*
21	72.7 ± 5.8	67.1 ± 4.1	27.3 ± 3.6	32.9 ± 4.8	19.5 ± 1.9*	13.1 ± 2.03*	12.2 ± 2.9	8.6 ± 0.47
42	69.4 ± 6.1	71.8 ± 5.1	30.6 ± 6.2	29.8 ± 5.13	5.5 ± 0.69	4.9 ± 0.9		4.96 ± 0.38

Table 3.2 (a): The influence of maternal nicotine exposure during gestation and lactation on chondrocytes in trachea cartilage.

Asterisk (\*) indicates significant difference that occur i.e. P<0.05.

The data summarized in Table 3.2(a) clearly shows that the volume density of the endoplasmic reticulum (ER) of the chondrocytes of the trachea cartilage of 7 day old control rats was at  $20.7 \pm 3.7\%$  not different from the  $19.5 \pm 1.9\%$  of the 21 day old control rat pups. The volume density of  $13.03 \pm 1.6\%$  of the 7 day old nicotine exposed pups was also not different from that of the 21 day old nicotine exposed rat pups at  $13.1 \pm 2.03\%$ . However, the volume density of the control rat pups of both age groups were significantly higher ( $P < 0.05$ ) than that of the nicotine exposed rat pups of the same ages.

At day 42 after birth the volume density of the endoplasmic reticulum (ER) of control rat pups was at  $5.5 \pm 0.69\%$ , 71.8% lower ( $P < 0.001$ ) than on day 21 after birth. The volume density of the ER of the trachea cartilage of the 42 day old nicotine exposed rat pups was at  $4.9 \pm 0.9\%$ , 62.6% ( $P < 0.001$ ) lower than the postnatal day 21. However, in contrast to postnatal days 7 and 21, there were no differences in volume density of ER of the trachea cartilage on 42 day old control and nicotine exposed rat pups.

The volume density of the lipid bodies of the 7 day old control rat pups was found to be lower at postnatal day 7 than in the nicotine exposed group of the same age ( $P < 0.05$ ). The volume density of the lipid bodies gradually increased from  $0.4 \pm 0.4\%$  on postnatal day 7, to  $12.2 \pm 2.9\%$  on day 21 after birth in the control group ( $P < 0.05$ ).

The volume density of the lipid bodies of the chondrocytes of day 7 old nicotine exposed rat pups increased with 91.1% from  $4.5 \pm 0.21\%$  to  $8.6 \pm 0.47\%$  at 21 day old ( $P < 0.05$ ). After postnatal day 21, the lipid density decreased with 43.3% from  $8.6 \pm 0.47\%$  to  $4.96 \pm 0.38\%$  ( $P < 0.05$ ). The volume density of the lipid droplets on postnatal day 42 was not different from that on postnatal day 7.

Except for differences in the endoplasmic reticulum (ER) and the lipid bodies, there are no significant differences regarding the other organelle, namely the nucleus and the cytoplasm as tabulated in Table 3.2 (a).

Table 3.2 (b) represents the ratios calculated with the nucleus as a constant between the control and nicotine exposed animals for the cytoplasm, endoplasmic reticulum (ER) and the lipid bodies. Differences in the ratios between the cytoplasm and endoplasmic reticulum were evident at postnatal days 7 and 21 for the nicotine exposed animals. The ER ratio at postnatal day 7 and day 21 decreased for the nicotine exposed group while an increase in the ratio for the cytoplasm was observed at day 21 (0.3:0.5) for the nicotine exposed animals. As for the lipid bodies the ratio indicated an increase at postnatal day 7 (0.01:0.3) for the nicotine exposed animals.





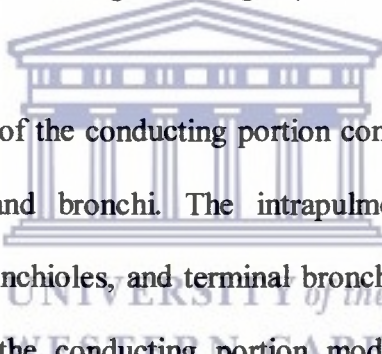
Table 3.2 (b): Results calculated from Table 3.2 (a) indicating the ratio's with the nucleus as a constant between the control and nicotine exposed animals.

<b>RATIO</b>	<b>DAYS</b>	<b>CONTROL</b>	<b>NICOTINE</b>
<b>CYTOPLASM / NUCLEUS</b>	7	0.4	0.4
	21	0.3	0.5
	42	0.4	0.4
<b>NUCLEUS / ENDOPLASMIC RETICULUM (ER)</b>	7	0.7	0.4
	21	0.7	0.4
	42	0.2	0.2
<b>NUCLEUS / LIPID</b>	7	0.01	0.3
	21	0.6	0.7
	42		1

## **CHAPTER 4**

### **DISCUSSION**

The respiratory system functions in exchanging carbon dioxide for oxygen, which will then be distributed to all the tissues of the body. To fulfill this function, air must be brought to that portion of the respiratory system where exchange of gases can occur. The respiratory system, therefore, has a conducting portion and a respiratory portion. Some of the larger airways of the conducting portion are extrapulmonary, while its smaller components are intrapulmonary. The respiratory portion is completely intrapulmonary. The diameters of the various lumina are modified by the presence of smooth muscle cells along their length (Farrell, 1982).



The extrapulmonary region of the conducting portion consists of the nasal cavities, pharynx, larynx, trachea and bronchi. The intrapulmonary region entails the intrapulmonary bronchi, bronchioles, and terminal bronchioles (Helms, 1995). The extrapulmonary region of the conducting portion modifies the inspired air by humidifying, cleansing and adjusting its temperature. Cleansing and humidifying actions are accomplished by the mucosa of the respiratory tract. The mucosa is composed of pseudostratified ciliated columnar epithelium with numerous goblet cells and an underlying connective tissue sheath that is well endowed with serous mucous glands. The conducting portion of the respiratory system, is supported by a skeleton composed of bone and/or cartilage, in order to maintain a patent lumen (Farrell, 1982 & Emery, 1970).

The trachea is a structure supported by 15 - 20 horse-shoe shaped segments of hyaline cartilage. The tracheal lumen is lined by respiratory epithelium composed of various cell types, namely goblet, basal, ciliated, brush cells and hormone-producing cells. The trachea subdivides into the two primary bronchi that lead to the right and left lung (Burri, 1974). It is therefore clear that interference with the development of the cartilage during fetal and neonatal lung growth, or damage to the cartilage will adversely affect the stability of the trachea.

Formation of the hyaline cartilage during lung growth and development and its maintenance is dependent on the chondrocytes that occur within lacunae in the cartilage. Interference with the morphologic and metabolic characteristics of these cells during embryogenesis and organogenesis may have an adverse effect on the development of the hyaline cartilage and thus on the development of the trachea. It is the horse-shoe shaped hyaline cartilage that ensures that the trachea remains open for adequate airflow between the atmosphere and the respiratory portion of the lung. Interference with the role of the chondrocytes in the cartilage to maintain the intactness thereof may have an adverse effect on the tracheal stability and result in limited airflow.

Furthermore, the goblet cells, serous cells, and ciliated cells in the trachea humidify and protect the lungs against the foreign particles that occur in the inhaled air. Malfunctioning of these cells may impair this particular function of these cells. If ciliated cells are impaired it may slow down the mucous escalator system which may result in infection.

### **Trachea Epithelium**

Ciliated cells, with their more than 200 cilia per cell, serve to effectively move the mucous layer, which is produced by the goblet cells, and any entrapped particulate materials toward the larynx by a process referred to as the ciliary beat cycle (Knoll et al, 1995). The mucous production and in particular the ciliary movement requires energy, which is supplied by the mitochondria. It is therefore conceivable that the ciliated epithelial cells will contain many mitochondria. The electron micrographs (Figures 3.22 – 3.27) in the study indeed showed that numerous small mitochondria occur in these cells.

Interference with the maintenance of the structural characteristics of the mitochondria and consequently with the mitochondrial function will thus affect the supply of energy and therefore the ciliary movement of the ciliated epithelial cells of the tracheal epithelium. In the present study it appeared that the number of mitochondria were less in the ciliary epithelial cells of the trachea of the nicotine exposed rat pups. This implies that the ATP production will be less, which again may result in a slower ciliary beat. In addition, studies by Maritz and Burger (1992) showed that maternal nicotine exposure during pregnancy and lactation suppress ATP hydrolysis in neonatal lung. This means that the ATP dependent reactions will be slower than normal. If this is indeed so it may explain the accumulation of mucus on the surface of the tracheal epithelium of the nicotine exposed rat pups seen in this study. The inhibition of ciliary movement by cigarette smoke (Welsh, 1983) could therefore be due to the exposure of the cilia to the nicotine in the smoke.

Cigarette smoke showed clear toxic effects on cilia. Studies by Graf et al., (1999) clearly showed that cigarette smoke and harmful gases in the air such as CO, CO<sub>2</sub>, N<sub>2</sub>, N<sub>2</sub>O, NO<sub>2</sub>, O<sub>3</sub> and SO<sub>2</sub> cause damage to ciliated cells in the human trachea. This may result in compromised ciliary movement. According to Konrad et al., (1995) it is unlikely that the inhibition of ciliary movement in smokers is due to structural changes because impaired mucociliary transport was found to be associated with a loss of cilia rather than ultrastructural abnormalities of cilia. Furthermore, chronic airway diseases shows that squamous metaplasia is associated with more goblet cells and fewer ciliated epithelial cells that may be responsible for compromise of the mucociliary transport (Verra et al., 1995). This implies that compromised mucociliary transport is due to:

1. a loss of cilia and,
2. fewer ciliated cells in the smokers.

In addition to this it is possible that the inhibition of the energy metabolism due to nicotine induced inhibition of ATP catabolism (Maritz et al., 1992) will contribute to a compromised mucociliary transport.

Apart from the effect of cigarette smoke on ciliary beat, Morrison and co-workers (1999) observed that it also increases the permeability of the tracheal epithelial layer. They also reported that there is an increase in the number of neutrophils in the air spaces of cigarette smokers. The reason for the increase in the permeability of the tracheal epithelium induced by cigarette smoke is not clear. Although no evidence is available to support it, it is tempting to speculate that the increased permeability is due to interference with the metabolism of the epithelial cells, which created an

imbalance between synthetic, and degradation processes that are responsible for maintaining the functional and structural integrity of the tracheal epithelium.

In my experiments it was shown that maternal nicotine exposure during pregnancy and lactation had no effect on the morphology of the tracheal epithelium, and no abnormalities in the epithelial cell junctions were observed. This implies that it is unlikely that the nicotine in tobacco smoke will compromise the structural integrity of the tracheal epithelium and thus the permeability thereof. However, it is important to note that in my studies nicotine was administered to the mother during pregnancy and lactation. The rat fetuses and newborns were therefore exposed to nicotine via the mother's blood and milk. Nicotine readily crosses the placenta (Greenberg et al., 1984) and accumulates in the amniotic fluid (Luck and Nau, 1984). This in turn leads to high concentrations of the nicotine in the amniotic fluid. The amniotic fluid provides a reservoir for continued delivery of nicotine to the fetus, even when maternal levels are low (Wonnacott et al, 1990). This implies that the developing fetal trachea and tracheal epithelium is also directly exposed to nicotine. Furthermore, nicotine accumulates in the developing fetal airways. This implies that nicotine can have an effect early during the development of airways. After birth, the offspring receives nicotine via the mother's milk (Svensson, 1987). This implies that the developing lung and thus the trachea is exposed to small quantities of nicotine after birth via the circulation of the neonate. The exposure to nicotine during pregnancy and lactation and thus during the phases of rapid lung development had no apparent effect on tracheal epithelial morphology. Therefore, taking the above into consideration, it is unlikely that the increased epithelial

permeability of the trachea in adult smokers is due to the nicotine in tobacco smoke. However, while no apparent morphological changes were observed in the epithelial cells of the trachea of the nicotine exposed rat pups. It is possible that metabolism could have been affected which could have changed the composition of the extracellular matrix. Studies on the effect of maternal nicotine exposure during gestation and lactation on the extracellular matrix composition is necessary to determine whether nicotine is making the tracheal epithelium of the offspring more susceptible to:

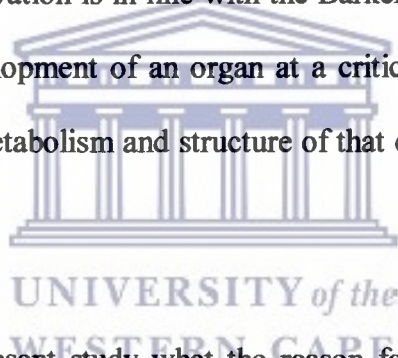
1. an increase in permeability later in life, or
2. more sensitive to the effects of tobacco smoke.

The release of mucus onto the epithelial surface, is a function of the goblet cells, as a means to moisten and act as a protective layer. The morphologic data showed that maternal nicotine exposure had no apparent effect on these cells. It is therefore unlikely that the ability of these cells to produce mucus was affected due to damages in the cell morphology. If this is so, it can be expected that normal mucus production and secretion will occur, unless the synthesis thereof is affected by an inhibition of ATP hydrolysis or by some other metabolic change related to mucous synthesis. More research is required to determine the rate of mucus production, composition and quantity within the airways, when exposed to nicotine.

It is interesting to note that the surface morphology of the goblet cells of the 14 day old neonatal rats that were exposed to nicotine via the placenta and mother's milk, was not different from that of the 14 and 42 day old control animals. In addition, no



changes in organelle structure were apparent at transmission electron microscopy level. However, the scanning electron microscopy showed the microvilli on the surface of goblet cells of the tracheal epithelium of 42 day old nicotine exposed animals were not as prominent as in the trachea of the control animals of the same age, apparently due to mucus covering these cells. Transmission electron microscopy showed that the microvilli were indeed less prominent for these cells in the nicotine exposed animals. Since these changes only developed after postnatal day 21, and thus after nicotine withdrawal, it is conceivable that these changes are irreversible. It is not clear what the consequences of these changes are on goblet cell function and thus its role in protecting the lungs against foreign material in the atmospheric air. This observation is in line with the Barker hypothesis, which states that interference with development of an organ at a critical phase of development may result in changes in metabolism and structure of that organ later in life (Barker et al., 1991).



It is not clear from the present study what the reason for the changes in surface characteristics of the goblet cells are. Studies to investigate for example the microvilli structure and membrane fluidity may give some answers as to the mechanism of action. This may also indicate how changes in goblet cell metabolism may induce changes in the structural and functional characteristics of this all.

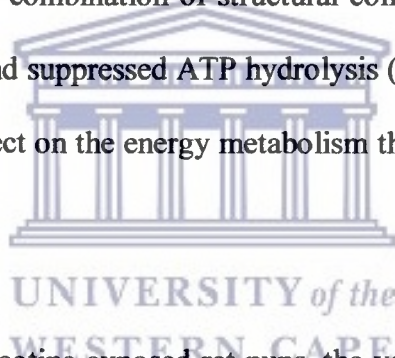
### **Tracheal Cartilage**

In this study it was shown that the cartilage in the trachea of postnatal day 21 and day 42 old rat pups that were exposed to nicotine via the placenta and mother's milk was damaged. This type of cartilage damage is categorized as microdamage, which involves trauma to the chondrocytes and matrix (Buckwalter, 1994 & Mankin, 1982).

However, the morphological and morphometric data indicates that the chondrocytes of the hyaline cartilage of the trachea of the nicotine exposed rat pups contained swollen mitochondria, which may impair mitochondrial function. The volume density of the rough endoplasmic reticulum (RER) was also found to be significantly less than in the chondrocytes of the tracheal cartilage of the control rat pups of the same age. This implies that the total energy yield by the mitochondria of the chondrocytes of the nicotine exposed rat pups will be reduced, where energy is required for the synthetic processes. Furthermore, the lower volume density of the RER also suggests that the synthetic processes will be slower per time unit than in the chondrocytes in the tracheal cartilage of the control animals. Since more energy is required to supply in the growth and development needs of the growing trachea, it is plausible that a reduced energy supply as well as the smaller RER will result in:

1. slower development of the hyaline cartilage and/or,
2. make it more susceptible to damage.

While the swelling of the mitochondria in chondrocytes occur, no swelling of mitochondria was evident in the epithelial cells. No information is available to explain the swelling of mitochondria in chondrocytes of nicotine exposed animals, while that of epithelial cells were apparently unaffected. It is possible that the chondrocytes are more sensitive to the effects of nicotine than the tracheal epithelial cells or that mitochondrial volume is maintained by different mechanisms, where one mechanism is nicotine sensitive and the other not. Despite the fact that the mitochondria are swollen in the chondrocytes, they appear to be still intact. The degree to which this may affect the ability of the mitochondria to produce energy, and thus on energy dependent metabolic processes in these cells is not known. It is however conceivable that a combination of structural compromise of mitochondria as observed in this study, and suppressed ATP hydrolysis (Maritz and Burger, 1992) will have a more severe effect on the energy metabolism than just inhibition of ATP hydrolysis.



At postnatal day 7 of the nicotine exposed rat pups, the volume density of the lipid bodies of the tracheal chondrocytes was significantly higher than compared to the control animals of the same age. Furthermore, the volume density of the RER of the chondrocytes of the 7 to 21 day old rat trachea was significantly less than in the control animals of the same age. This implies that the capacity of these cells to synthesize the components for the matrix of the cartilage will be reduced. At postnatal day 7 of the nicotine exposed rat pups, the volume density of the lipid bodies of the tracheal chondrocytes was significantly higher compared to the control animals of the same age. Furthermore, the volume density of the RER was markedly

less in the chondrocytes of the nicotine exposed rat pups. This implies that the capacity of the chondrocytes of these animals to produce structural proteins, such as collagen, might be reduced. This might explain the increased susceptibility of the tracheal cartilage to damage and thus the damage observed on postnatal days 21 and 42 nicotine exposed rat pups. This also implies that the balance between replacement, growth and degradation is impaired, which could result in the damage seen in 21 and 42 day old rat pups.

It is interesting to note that the volume density of the RER of the chondrocytes of nicotine exposed rat pups were less than that of the control rat pups. Only during the phases of rapid lung growth and development (between days 4 and 13) and equilibrated (after day 14) lung growth. No difference was observed in the volume density of the chondrocytes of 42 day old fully grown mature rats. This implies that the rate of the synthetic processes for the production of extracellular matrix components, such as collagen, is reduced because no further growth occurs. The smaller RER is only to meet the demands of the tissue for maintenance of homeostasis. This also implies that if the synthesis of the extracellular matrix was compromised, that it is unlikely that catch up growth will occur. If the balance between synthesis of the components of the extracellular matrix and the degradation thereof is maintained, no further compromise of structural integrity will occur. However, in this study it appears that structural changes occur late which may point to a faster degradation than synthesis of the matrix. Further studies to investigate this are planned.

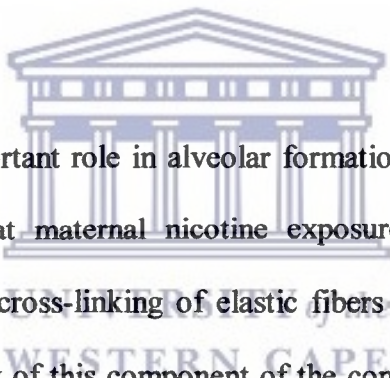
The function of the lipid droplets is not known. However, it is likely that it serves as a source of energy. This may be of special importance during the growth and development phase of the hyaline cartilage of the neonatal rat, since energy is required. This is particularly important since the nutrient supply to these cells is not as efficient as for other cells that are exposed to a good blood supply (Kessel et al., 1979). If the lipid droplets are an important source of energy, any suppression of fat oxidation will result in an accumulation thereof in the cell. It is also conceivable that the lipid content of these cells will be lower during the phase of rapid lung development, which is between postnatal days 4 and 13 in the rat (Vaccaro & Brody, 1978) due to the lipids being used for energy metabolism. If this is so, it indicates that energy metabolism is suppressed in tracheal chondrocytes of nicotine exposed rat pups and might explain the higher volume density of the lipid droplets of the chondrocytes of 7 day old nicotine exposed rats. Between postnatal days 4 and 13, lung growth and development in these rats might be slow which implies that the rate of energy production from carbohydrates and fats will be slower than during the phase of rapid lung growth. This might explain the increase in the volume density of the lipids in the chondrocytes as observed on postnatal day 21. No direct evidence is available to support the above hypothesis. Further studies are therefore required to determine the reason for the differences in volume density of the lipids in the chondrocytes as observed in this study.

In conclusion, the data suggest that maternal nicotine exposure during pregnancy and lactation may induce changes in the tracheal cartilage chondrocytes that may reduce certain metabolic processes, which again may induce permanent changes in

the cartilage. The consequences of this are not known. Maternal nicotine exposure also resulted in the late changes in surface characteristics of goblet cells and it is therefore conceivable that these changes will be permanent.

### **Alveolar Surface**

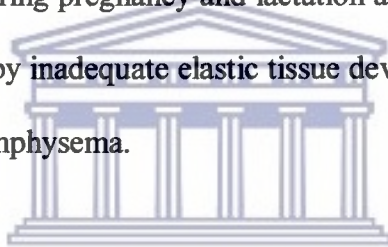
At postnatal day 7, the alveoli surface morphology of both the control and nicotine exposed animals are not different from each other. However, on postnatal day 42, widespread damage occurs in the alveoli of the animals that were exposed to nicotine during pregnancy and lactation. Damage to the alveoli could be in part subscribed to alterations of the connective tissue integrity, elastic tissue in particular (Maritz et al., 2000).



Elastic tissue plays an important role in alveolar formation (Dunnill, 1962). It was shown that it is likely that maternal nicotine exposure during pregnancy and lactation interfere with the cross-linking of elastic fibers (Maritz & Dolly, 1995), thereby lowering the quality of this component of the connective tissue framework of the lung. It was also found that elastic deposition in the lungs of nicotine exposed rat pups was also out of phase with the period of alveolarisation. These findings suggest that the elastic tissue in lungs of nicotine exposed rat pups are more susceptible to stress damage and eventually emphysema. Furthermore, Maritz et al., (1994) showed with scanning electron micrographs that fewer alveoli occurred in those lungs of rat pups exposed to nicotine during gestation and lactation. Damage to the alveolar blood-barrier also occurred and therefore renders the lungs less efficient with regard to gas exchange. As the alveoli are the sites for gas exchange in

the lung, their smaller number in the lungs of nicotine-exposed rat pups indicates that the surface area available for gas exchange is less than in the lungs of control animals (Maritz et al., 1998).

Another important observation is the fenestrations in the alveolar walls of the lungs of the 42 day old rat pups exposed to nicotine via the placenta and mother's milk. According to various reports, these fenestrations are formed due to direct damage to the alveolar walls which can be related to the onset and presence of emphysema (Boren, 1962; Cosio et al., 1986 and Kuhn et al., 1976). It is possible that the nicotine in tobacco smoke induce chronic obstructive lung disease in the offspring of the mothers who smoked during pregnancy and lactation as suggested by Wall et al., (1985). A process initiated by inadequate elastic tissue development that leads to the formation of microscopic emphysema.



The connective tissue framework of the lung is responsible for the stability of the lung. Elastic tissue in particular is associated with alveolar formation and is important for lung compliance. It was indeed shown that suppression of elastic tissue formation result in fewer and bigger alveoli. Damage to the connective tissue framework gives rise to emphysema (Maritz & Woolward, 1993). Recent studies showed that maternal nicotine exposure resulted in damage to the supporting connective tissue skeleton of neonatal lung (Dolley, 1995) and thus induce changes in the structural characteristics of the lung. Although only circumstantial data is available, it appears that nicotine interferes with the metabolism of the connective



tissue component of the lung and thereby initiates slow progressive deterioration of the lung as the animal ages.

In conclusion, maternal nicotine exposure during gestation and lactation induce the formation of fenestrations in the alveolar walls that are considered to be the onset of emphysema. The fact that the fenestrations appear after the exposure to nicotine was terminated, is an indication that a process was started during the exposure to nicotine that is progressive and not reversible. This implies that maternal nicotine exposure during pregnancy and lactation induces progressive lung damage in the offspring, which may result in emphysema even if the offspring never smoke.



## REFERENCES

Arbeille, P., Bosc, M. and Vaillant, M.C. (1992). Nicotine-induced changes in the cerebral circulation in ovine fetus. **Am. J. Perinatol.** 9:270–274.

Ayers, M.M. and Jeffery, P.K. (1988). Proliferation and differentiation in mammalian airway epithelium. **Eur. Respir. J.** 1:58–80.

Aubach, O., Hammond, E.C. and Garfunkl, L. (1979). Changes in bronchial epithelium in relation to cigarette smoking. **N Engl J Med.** 381 - 386.

Bancroft, J.D. and Stevens, A. (1990). Theory and practice of histological techniques (3<sup>rd</sup> ed.) Churchill Livingstone.

Barker, D.J.P., Godfrey, K.M., Fall, C., Osmond, C., Winter, P.D. and Shaheen, S.O. (1991). Relation of birth weight and childhood respiratory infection to adult lung function and death from chronic obstructive airways disease. **Br. Med. J.** 303:671–675.

Bassi, J.A., Rosso, P., Moessinger, A.C., Blanc, W.A. and James, L.S. (1984). Fetal growth retardation due to maternal tobacco smoke exposure in the rat. **Pediatr. Res.** 18:127–38.

Becerra, J.E. and Smith, J.C. (1988). Maternal smoking and low birthweight in the reproductive history of women in Puerto Rico. **Am. J. Public Health** 78:268–272.

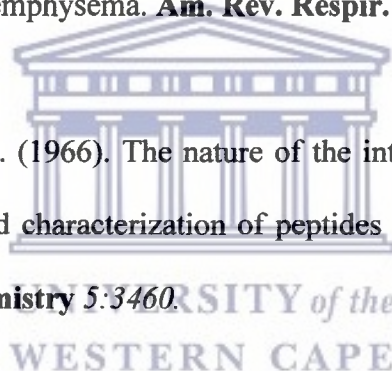
Bindreitter, M., Schuppler, J. and Stockinger, L. (1968). Zell proliferation und differenzierung im trachealepithel der Ratte. **Exp. Cell Res.** 50:377–382.

Bleinkinskopp, W.K. (1967). Proliferation of the respiratory tract epithelium in the rat. **Exp. Cell Res.** 46:144–154.

Bolduc, P. and Reid, L. (1976). Mitotic index of the bronchial and alveolar lining of normal rat lung. **Am. Rev. Respir. Dis.** 114:1121–1128.

Boren, H.G. (1962). Alveolar fenestrae: relationship to the pathology and pathogenesis of pulmonary emphysema. **Am. Rev. Respir. Dis.** 85:328-44.

Bornstein, P. and Piez, K.A. (1966). The nature of the intramolecular cross-links in collagen: The separation and characterization of peptides from the cross-link region of rat skin collagen. **Biochemistry** 5:3460.



Boyden, E.A. and Tompsett, T.H. (1965). The changing patterns in the developing lungs of the infant. **Acta Anat.** 61:164–192.

Bradley, K., McConnell-Breul, S. and Crystal, R.G. (1974). Lung collagen composition and synthesis: Characterization and changes with age. **J. Biol. Chem.** 249:2674.

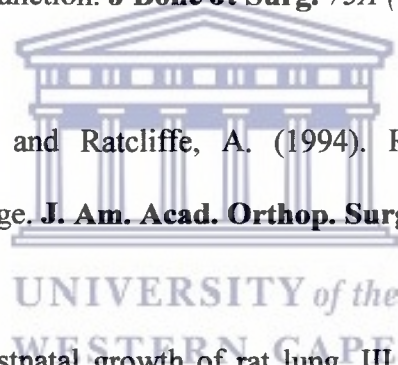
Bradley, K., McConell-Breul, S. and Crystal, R.G. (1974). Lung collagen heterogeneity. **Proc. Natl. Acad. Sci. USA** 71:2828.

Boucher, R.C., Johnson, J., Inuo, S., Hulbert, W. and Hogg, J.C. (1980). The effect of cigarette smoke on the permeability of guinea pig airways. **Lab. Invest.** 43:94.

Bucher, U. and Reid, L. (1961). Development of the mucus secreting elements in human lung. **Thorax** 16:219–225.

Buckwalter, J., Woo, S. and Goldberg, V. (1993). Current concepts review: soft tissue aging and musculoskeletal function. **J Bone Jt Surg.** 75A (10):1533-1548.

Buckwalter, J., Mow, V. and Ratcliffe, A. (1994). Restoration of injured or degenerated articular cartilage. **J. Am. Acad. Orthop. Surg.** 2(4):192-201.



Burri, P.H. (1974). The postnatal growth of rat lung. III. Morphology. **Anat. Rec.** 180:77–98.

Butler, N.R., Goldstein, H. and Ross, E.M. (1972). Cigarette smoking in pregnancy: It's influence on birth weight and perinatal mortality. **Br. Med. J.** 2:127–130.

Campbell, C. (1969). The healing of cartilage defects. **Clin. Orthop.** 64:45-63.

Caro, L.G. and Palade, G.E.(1964). Protein synthesis, storage, and discharge in the pancreatic, exocrine cell. An autoradiographic study. **J Cell Biol.** 20:473.

Chen, F.S., Frenkel, S.R. and Di Cesare, P.E. (1999). Repair of articular cartilage Defects: Part I. Basic Science of Cartilage Healing. **Am. J. Orth. Jan.** 28(1): 31–3.

Condon, W.B. (1941). Regeneration of tracheal and bronchial epithelium. **J. Thorac. Surg.** 11: 33–346.

Cisio, M.G., Shiner, R.J., Saelta, M., Wang, N.S., King, M., Ghezzi, H. and Angus, E. (1986). Alveolar fenestrae in smokers. Relationship with light microscopic and functional abnormalities. **Am. Rev. Respir. Dis.** 133: 126-131.

De Haller, R. (1969). Development of the mucus secreting elements. In: *The Anatomy of the Developing Lung*. Heinemann. pp 94–115.

Di Fiore, M.S.H. (1981). *Atlas of the human histology*. Lea & Febiger, 5<sup>th</sup> ed., Philadelphia. pp 37 & 181.

Di Stefano, A., Capelli, A., Lusuardi, M., Balbo, P., Vecchio, C., Maestrelli, P., Mapp, C.E., Fabbri, L.M., Donner, C.F., and Saetta, M. (1998). Severity of airflow limitation is associated with severity of airway inflammation in smokers. **Am. J. Respir. Crit. Care Med.** 158:1277–1285.

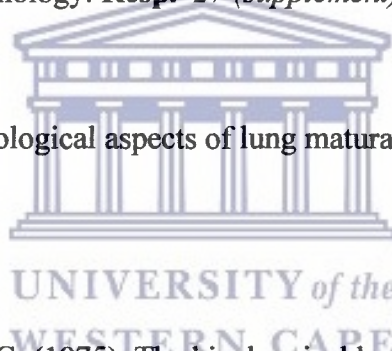
Dolley, L. (1995). The effect of maternal nicotine exposure on the quantity and quality of neonatal rat lung connective tissue. MSc Thesis, University of the Western Cape, Bellville, South Africa.

Dornan, J.C. and Meban, C. (1985). The capillary plexus in the gas exchange zone of human neonatal lung: ultrastructural study. **Thorax** 40: 787–792.

Dunnill, M.S. (1962). Postnatal growth of the lung. **Thorax** 17:329-33.

Emery, J.L. (1970). The postnatal development of the human lung and its implications for the lung pathology. **Resp.** 27 (supplement): 47–50.

Farrell, P.M. (1982). Morphological aspects of lung maturation. **Lung Development** pp 13–24.



Fulmer, J.D. and Crystal, R.G. (1975). The biochemical basis of pulmonary function, In: **The Biochemical Basis of Pulmonary Function**, R.G. Crystal, ed., Marcel Dekker, NY.

Gaillard, D.A., Lallemand, A.V., Petit, A.F. and Puchells, E.S. (1989). In vivo ciliogenesis in human fetal tracheal epithelium. **Am. J Anat.** 185:415–418.

Gallop, P.M., Blumenfeld, O.O. and Seifter, S. (1972). Structure and metabolism of connective tissue proteins. **Annu. Rev. Biochem.** 41:617.

Giddings, J., Griffin, R.L. and Maciwer, A.G. (1982). Demonstration of immunoproteins in araldite embedded tissues. **J. Clin. Path.** 35:111-114.

Graf, W., Graf, H. and Wenz, M. (1999). Tetrahymena pyriformis in the ciliate mobility test. Validation and description of a testing procedure for the registration of harmful substances in the air as well as the effects of cigarette smoke on the human respiratory ciliated epithelium. **Zentralbl Hyg. Umweltmed.** Feb. 201:6:451-72.

Grant, M.E. and Prockop, D.J. (1972). The biosynthesis of collagen. **N Engl. J. Med.** 286:194, 242, 291.

Greenberg, R.A., Haley, N.J, Etzel, R.A. and Loda, F.A. (1984). Measuring the exposure of infants to tobacco smoke: nicotine and cotinine in urine and saliva. **N Engl. J. Med.**, 310:1075-1107.

Hance, A.J. and Crystal, R.G. (1975). Connective tissue of lung. **Am. Rev. Dis.** 112:657-711.

Harding, R. (1991). Fetal breathing movements. In: Crystal R.G., West J.B. et al., eds. *The Lung: Scientific Foundations*, New York: Raven Press, pp 1655-1663.

Helms, P.J. (1995). Lung growth: Implications for the development of disease. **Thorax** 49:440-441.

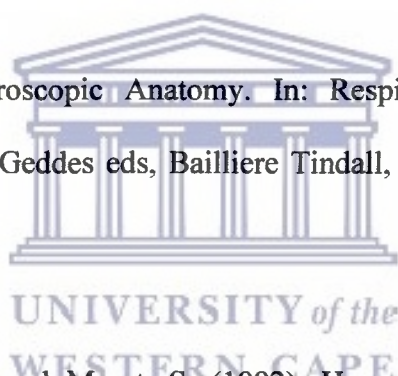


Hislop, A., Wiggelsworth, J.S. and Desai, R. (1986). Alveolar development in the human foetus and infant. **Early Human Development** 13:1–11.

Hubert, W.C., Walker, D.C., Jackson, A. and Hogg, J.C. (1981). Airway permeability to horseradish peroxidase in guinea pigs: the repair phase after injury by cigarette smoke. **Am. Rev. Respir. Dis.** 123:320.

Ito, S. and Mikawa, H. (1987). Defense mechanism of the lung. In: Tinkelman D.G. Falliers C.J., Naspitz C.K., eds. *Childhood Asthma, Pathophysiology and Treatment*, New York: Marcel Dekker, pp 23–38.

Jeffery, P.K. (1990). Microscopic Anatomy. In: *Respiratory Medicine*. R.A.L. Brewis, G.J. Gibson, G.M. Geddes eds, Bailliere Tindall, London/ Toronto. pp 57–78.



Jeffery, P.K., Gaillard, D. and Moret, S. (1992). Human airway secretions cells during development and in mature airway epithelium. **Eur. Respir. J.** 5:93–104.

Jeffery, P.K. and Reid, L. (1975). New observations of rat airway epithelium: A quantitative electron microscope study. **J. Anat.** 120:295–320.

Jeffery, P.K. and Reid, L. (1977). The ultrastructure of the airway lining and its development. In : *The development o/the lung*. W.A. Hodson Ed., Marcell Dekker Inc., NY. pp 87–134.

Jeffery, P.K. and Reid, L. (1981). The effect of tobacco smoke, with or without phenylmethyloxadiazole (PMO), on rat bronchial epithelium: a light and electron microscopic study. **J. Pathol.** 133:341.

Jones, R., Phil, M. and Reid, L. (1978). Secretory cell hyperplasia and modification of intracellular glycoprotein in rat airways induced by short periods of exposure to tobacco smoke and the effect of the anti-inflammatory agent phenylmethyloxadiazole. **Lab. Invest.** 39:41

Kauffman, S.L. (1980). Cell proliferation in the mammalian lung. **Int. Rev. Exp. Path.** 22:131–191.

Kessel, R.G. and Kardon, R.H. (1979). Tissue and organs: A text - Atlas of scanning electron microscopy. W.H. Freeman & Co. San Francisco. pp 19-23.

Koren, G. (1995). Fetal toxicology of environmental tobacco smoke. **Curr. Opin. Pediatr.** 7:128–131.

Knoll, M., Shaoulian, R., Magers, T. and Talbot, P. (1995). Ciliary beat frequency of hamster oviducts is decreased in vitro by exposure to solutions of mainstream and sidestream cigarette smoke. **Biol. Reprod.** July 53(1):29-37.

Mankin, H. (1982). Current concepts review: the response of articular cartilage to mechanical injury. **J. Bone Joint Surg.** 64A(3):460–466.

Mankin, H., Mow, V., and Buckwalter, J. (1994). Form and function of articular cartilage. In: Simon S, ed. **Orthopaedic Basic Science, IL: American Academy of Orthopaedic Surgeons.** pp 1-44.

Maritz, G.S. (1988). Maternal nicotine exposure and carbohydrate metabolism of neonatal lung tissue: response to nicotine withdrawal. **Respir. Dis. Digest** 3:14–16.

Maritz, G.S. (1988). Effects of maternal nicotine exposure on growth in vivo of lung tissue of neonatal rats. **Biol. Neonate** 53:163–170.

Maritz, G.S. and Woolward, K. (1990). Effect of maternal nicotine exposure on the neonatal lung development: a morphological study. **S Afr. J Sci.** 86:537.

Maritz, G.S. and Burger, B. (1992). The influence of maternal nicotine exposure on neonatal lung carbohydrate metabolism. **Cell Biol. International Reports**, 16(12): 1129–1236.

Maritz, G.S. and Woolward, K. (1992). Effects of maternal nicotine exposure on neonatal lung elastic tissue and possible consequences. **S Afr. Med. J.** 81:517–519.

Maritz, G.S. and Woolward, K. (1994). The effect of maternal nicotine exposure on neonatal lung development. A morphological study. **S.A. J. Sci.** 90:249–252.

Maritz, G.S. and Dolley, L. (1995). The influence of maternal nicotine exposure on the status of the connective tissue framework of developing lung. **Pathophysiology** 2:104-9.

Maritz, G.S. and Thomas, R.A. (1995). Maternal nicotine exposure: Response of Type II pneumocytes of neonatal rat pups. **Cell Biol. Intl.** 19:323–331.

Maritz, G.S. and Dennis, H. (1998). Maternal nicotine exposure during gestation and lactation interferes with alveolar development in the neonatal lung. **Reprod. Fertil. Dev.** 10:255–261.

Maritz, G.S., Matthew, H.L. and Aalbers, J. (2000). Maternal copper supplementation protects the neonatal rat lung against the adverse effects of maternal nicotine exposure. **Reprod., Fertil. Dev.** Vol.12 (in Press).

Mayne, R., Schiltz, J.R. and Holtzer, H. (1973). Some overt and covert properties of chondrogenic cells. In: **Biology of Fibroblast**, E. Kulonen and J. Pikkarainen, ed., Academic press, NY. pp 61.

Mc Ateer, J.A. (1984). Tracheal morphogenesis and fetal development of the mucociliary epithelium of the rat. **Scanning Electron Microsc.** IV:1995-2008.

Mc Dowell, E.M., Newkirk, C. and Coleman, B. (1985). Development of hamster tracheal epithelium. I: Quantitative morphologic study in the fetus. II: Cell proliferation in the fetus. **Anat. Rec.** 213:429–456.

Miller, E.J. (1973). A review of biochemical studies on the genetically distinct collagens of the skeletal system. **Clin. Orthop.** 57:260.

Miller, E.J. and Matukas, V.J. (1974). Biosynthesis of collagen: The biochemist's view, **Fed. Proc.** 33:1197.

Miller, W.S. (1932). The epithelium of the lower respiratory tract. In: **Special Cytology**, 2<sup>nd</sup> ed. E.V. Cowdry, ed., Hafner, NY. pp 133–150.

Morrison, D., Rahman, I., Lannan, S. and MacNee, W. (1999). Epithelial permeability, inflammation and oxidant stress in the air spaces of smokers. **Am J Respir. Crit. Care Med.** Feb. 159(2):473-9.

Morrow, R.J., Ritchie, J.W. and Bull, S.B. (1988). Maternal cigarette smoking: The effects on umbilical and uterine blood flow velocity. **Am. J. Obstet. Gynecol.** 159:1069–1071.

Morse, D.E., Gattone, V.H. and McCann, P. (1979). Surface features of the developing rat lung. **Scanning Electron Microsc.** III:899-904.

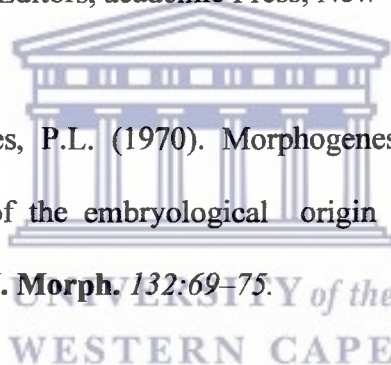
Motoyama, E.K., Brody, J.S., Colten, H.R. and Warshaw, J.B. (1988). Postnatal lung development in health and disease. **Am. Rev. Respir. Dis.** 137:742–746.

Murrin, L.C., Ferrer, J.R., Wanyun, Z. and Haley, N.J. (1987). Nicotine administration to rats: Methodological Considerations. **Life Sci.** 40:1699–1708.

Murray, J.F. (1986). The normal lung: The basis for diagnosis and treatment of pulmonary disease. 2<sup>nd</sup> ed., Philadelphia, W.B. Saunders Company. pp 1–59.

Novikoff, A.B. (1961). Lysosomes and related particles. In **The Cell**, Vol. II, J.Brachret and A.E.Mirsky, Editors, academic Press, New York, pp 723.

O' Hare, K.H. and Townes, P.L. (1970). Morphogenesis of albino rat lung: an autoradiographic analysis of the embryological origin of the type I and type II pulmonary epithelial cells. **J. Morph.** 132:69–75.



Otto–Verberne, C.J.M, Ten Have–Opbroek, A.A.W., Balkema, J.J. and Franken, C. (1988). Detection of the type II cell or its precursor before week 20 of human gestation, using antibodies against surfactant – associated proteins. **Anat. Embryol.** 178:29–39.

Pack, R.J., Al-Ugaily, L.H. and Morris, G. (1981). The cells of the tracheobronchial epithelium of the mouse: A quantitative light and electron microscope study. **J. Anat.** 132:1: 71-84.

Piez, K.A. and Miller, A. (1974). The structure of collagen fibrils. **J. Supramol Struct.** 2:121.

Phipps, R.J. and Denas, S.M. (1982). Epithelial water fluxes in sheep trachea. **Physiologist** 25:224.

Plopper, C.G., Alley, J.L. and Weir, A.J. (1986). Differentiation of tracheal epithelium during foetal lung maturation in the rhesus monkey *Macaca mulatta*. **Am. J Anat.** 175:59–71.

Plopper, C.G., Hill, L.H. and Mariassy, A.T. (1980). Ultrastructure of the nonciliated bronchiolar epithelial Clara cell of mammalian lung. III. A study of man with comparison of 15 mammalian species. **Exp. Lung Res.** 1:171–180.

Porter, K.R. (1961). The ground substance: Observations from electron microscopy. **In The Cell**, Vol. II, J. Brachet and A.E. Mirsky, Editors, Academic Press, New York, pp 621.

Pras, M. and Glynn, L.E. (1973). Isolation of a noncollagenous reticulin component and its primary characterization. **Br. J. Exp. Pathol.** 54:449.

Reith, E.J. and Roos, M.H. (1965). Atlas of descriptive histology. 2<sup>nd</sup> Edition. Harper Row, Publishers. Medical Department, New York, London & Evanston. pp 23-28



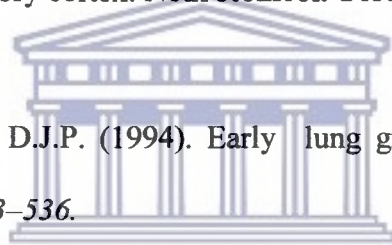
Rhodin, J. and Dalhamn, T. (1956). Electron microscopy of the tracheal ciliated mucosa in rat. **Z Zelforsch.** 44:415.

Rhodin, J. (1966). The ciliated cell: ultrastructure and function of human tracheal mucosa. **The American Review of Respiratory Diseases** 93(3): 114.

Rhodin, J.A.G. (1975). An atlas of histology. Oxford University Press, London. pp 99-105.

Roy, T.S. and Sabherwal, U. (1994). Effects of prenatal nicotine exposure on the morphogenesis of somasensory cortex. **Neurotoxicol. Teratol.** 16:411-421.

Shaheen, S.O. and Barker, D.J.P. (1994). Early lung growth and chronic airflow obstruction. **Thorax** 49:533-536.



UNIVERSITY of the  
WESTERN CAPE

Smolich, J.J. Startford, B.E., Maloney, J.E. and Ritchie, B.C. (1976). Postnatal development of the epithelium of larynx and trachea in the rat: Scanning Electron Microscopy. **J. Anat.** 124(3): 657-673.

Strawich, E. and Nimni, M.E. (1971). Properties of a collagen molecule containing three identical components extracted from bovine articular cartilage. **Biochem.** 10:3905.

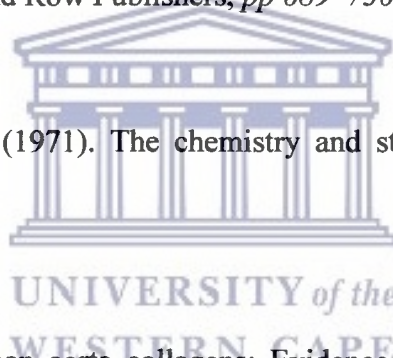
Sturgess, J.M. (1985). Ontogeny of the bronchial mucosa. **Am. Rev. Respir. Dis. (Suppl.)** 131:4-7.

Svensson, C.V. (1987). Clinical Pharmacokinetics of nicotine. **Clin. Pharmacokin.** 12:30 - 40.

Thurlbeck, W.M. (1975). Postnatal growth and development of the lung. **Am. Rev. Resp. Dis.** 11:803.

Tortora, G.J. and Anagnostakos, N.P. (1990). Principles of anatomy and physiology, 6<sup>th</sup> ed. New York, Harper and Row Publishers, pp 689-730.

Traub, W. and Piez, K.A. (1971). The chemistry and structure of collagen. **Adv. Protein Chem.** 25:243.



Trelstad, R.L. (1974). Human aorta collagens: Evidence for three distinct species. **Biochem. Biophys. Res. Commun.** 57:717.

Vaccaro, C. and Brody, J.S. (1978). Ultrastructure of developing alveoli. I. The role of the interstitial fibroblast. **Anat. Rec.** 192:467-480.

Verra, F., Escudier, E., Lebargy, F., Bernaudin, J.F., De Cremoux, H. and Bignon, J. (1995). Ciliary abnormalities in bronchial epithelium of smokers, ex-smokers, and nonsmokers. **Am. J. Respir. Crit. Care Med. March** 151(3) Pt 1: 630-4.

Wall, M.A., Thurlbeck, W.M., Wohl, M.E.B., Taussig, L.M., Brody, J.S., Buist, A.S. and Burrows, B. (1985). Lung growth and development. **Am. Rev. Respir. Dis.** *131:191-92.*

Walsh, R.A. (1994). Effects of maternal smoking on adverse pregnancy outcomes: Examination of the criteria of causation. **Human Biol.** *66:1059–1092.*

Wang, N., Schraufnagel, D.E. and Chen, M.F. (1983). The effect of maternal oral intake of nicotine on the growth and maturation of fetal and baby mouse lungs. **Lung** *161:27–38.*

Weibel, E.R. (1963). *Morphometry of the human lung.* (Springer:Berlin).

Welsh, M.J. (1983). Cigarette smoke inhibition of ion transport in canine tracheal epithelium. **J. Clin. Invest** *71:1614.*

Wharton, J., Polak, J.M. and Bloom, S.R. (1978). Bombesin – like immunoreactivity in the lung. **Nature** *273:769–770.*

Wigglesworth, J.S. (1987). Pathology of the lung in the fetus and neonate, with particular reference to problems of growth and maturation. **Histopath.** *11:671–689.*

Willems, L.M.A., Kramps, J.A., Jeffery, P.K. and Dijkman, J.A. (1988). Antileucoprotease in the developing fetal lung. **Thorax** *43:784–786.*

Witschi, E. (1962). Development in rat growth, Altman, L and Dittmer, D.J. (eds.), **Fed. Am Soc. Exp. Biol.**, Washington DC, *pp 304-314*.

Wonnacott, S., Russell, M.A.H., Stoteman, I.P. (1990). Nicotine sychopharmacology: Molecular, cellular and behavioral aspects. Oxford University Press. New York, USA. *pp 1 – 37, 112 – 157, 374 – 418*.

Woolf, N. (1977). Cell, Tissue and Disease. The Basis of Pathology. 2<sup>nd</sup> ed., Bailliere Tindall, *pp 1- 24*.



## **APPENDIX A**

### **2.1 LIGHT MICROSCOPY**

#### **Mayer's Heamatoxylin and Eosin stain (Bancroft and Stevens, 1990)**

##### **a) Reagents**

- 1) Absolute alcohol (absolute ethanol). This can be diluted to appropriate concentrations using distilled water.
- 2) Xylene: use as supplied by the manufacturer.
- 3) DPX: use as described by the manufacturer.
- 4) Buffered neutral formaldehyde: Dissolve 4 grams sodium dihydrogen phosphate ( $\text{NaH}_2\text{PO}_4$ ) and 6,5 grams disodium hydrogen phosphate ( $\text{Na}_2\text{HPO}_4$ ) in a solution containing 100 ml 40% formaldehyde and 800 ml distilled water. Make this solution up to a final volume of 1L in a volumetric flask.
- 5) Eosin. Dissolve 5,0 grams in 1L of distilled water.
- 6) Mayer's haemalum. Dissolve 1 gram of heamatoxylin in 1L of distilled water. Add 50 grams of potassium ammonium alum and shake to dissolve fully. Then add 0,2 grams of sodium iodate, 1,0 gram of citric acid and 50,0 grams of chloral hydrate.
- 7) Scott's water. Dissolve 4 grams of sodium bicarbonate and 40 grams of magnesium sulphate in 2 L of distilled water.

## **b) Procedure**

- 1) Fix the sections to the glass slide by placing in a hot-air oven at 80°C for 20 minutes.
- 2) Dewax in xylol for 2 minutes, then hydrate by placing the sections for 30 seconds in each of 100%, 96%, 80% and 70 % alcohol, in that order.
- 3) Fully hydrate and remove all traces of alcohol by placing the sections in running tap water for 1 minute.
- 4) Stain in Haemalin for 10 minutes.
- 5) Blue in Scott's water for 1 minute and wash in tap water for 30 seconds.
- 6) Stain in Eosin for 1 minute.
- 7) Wash in tap water for 30 seconds.
- 8) Dehydrate through graded alcohols of 70%, 80%, 96% and 100% respectively for 10 seconds in the first and 30 seconds each in the remaining two alcohols.
- 9) Dip the sections in xylene to clear, using two changes for 30 seconds, and mount in DPX.

## **c) Photography and printing**

All the colour photography was done on a Carl Zeiss D-7082 Oberkochen microscope with MC63 photomicrographic camera attachment and automatic exposure setting. Fujifilm HG100, 36 exposure film was used. Developing and printing of photographs was done through photolab, Bellville.

## **APPENDIX B**

### **2.2 SCANNING ELECTRON MICROSCOPY**

#### **2.2.1 Preparation for scanning ultramicroscopy**

##### **a) Reagents and Equipment**

1. Hitachi HPC – 2 critical point dryer.
2. Edwards S150B sputter coater.
3. Hitachi model X650 scanning electron microscope.
4. Acetone (analytical grade).
5. Xylene (analytical grade).
6. Absolute alcohol (absolute ethanol). This can be diluted to appropriate concentrations using distilled water.
7. Pill bottles.



UNIVERSITY of the  
WESTERN CAPE

##### **b) Procedure**

1. Methods for the operation of each instrument was according to the manufacturers specifications.
2. Tissue samples were obtained from the remaining wax blocks that were used for light microscopic examination as described in chapter 2.  
The respective tissue samples in the wax block was cut into pieces approximately 3 mm with a sharp scalpel. The wax blocks provided support thus minimal tissue damage occurred.



3. These tissue pieces that was cut were placed in a new labeled cassette and the wax removed in a Shandon tissue processor using the protocol in

Table 3.1:

Table 3.1: Protocol for dewaxing of embedded trachea tissue.

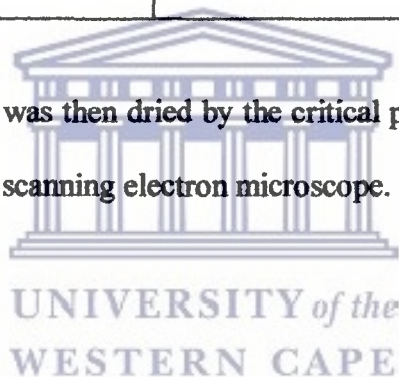
	<b>SOLVENT</b>	<b>TIME</b>
<b>1.</b>	<b>Xylene</b>	<b>1 hour</b>
<b>2.</b>	<b>Xylene</b>	<b>30 minutes</b>
<b>3.</b>	<b>100 % alcohol</b>	<b>30 minutes</b>
<b>4.</b>	<b>95% alcohol</b>	<b>15 minutes</b>
<b>5.</b>	<b>90% alcohol</b>	<b>15 minutes</b>
<b>6.</b>	<b>80 % alcohol</b>	<b>15 minutes</b>
<b>7.</b>	<b>70 % alcohol</b>	<b>15 minutes</b>
<b>8.</b>	<b>Distilled water</b>	<b>30 minutes</b>
<b>9.</b>	<b>Distilled water</b>	<b>Overnight</b>

Tissue samples were gradually dehydrated from distilled water to 100% acetone as indicated in Table 3.2.

Table 3.2: Protocol for acetone dehydration of trachea tissue prior to critical point drying and sputter coating.

	<b>SOLVENT</b>	<b>TIME</b>
<b>1.</b>	<b>70 % acetone</b>	<b>30 minutes</b>
<b>2.</b>	<b>80 % acetone</b>	<b>30 minutes</b>
<b>3.</b>	<b>90 % acetone</b>	<b>15 minutes</b>
<b>4.</b>	<b>95 % acetone</b>	<b>15 minutes</b>
<b>5.</b>	<b>100% acetone</b>	<b>15 minutes</b>
<b>6.</b>	<b>100 % acetone</b>	<b>15 minutes</b>

This dehydrated tissue was then dried by the critical point method, sputter coated and examined with the scanning electron microscope.



## APPENDIX C

### **a) Reagents**

1. 2,5% Gluteraldehyde (pH = 7,4). Add 90 ml of Working buffer to 10 ml of 25% Gluteraldehyde.

Working buffer (Phosphate Buffer). Add 210 ml of Solution A to 40 ml of Solution B. Make up 500 ml distilled water

**Solution A:** Make 1L of 0,2 M  $\text{Na}_2\text{HPO}_4$ , pH = 7,4 . Dissolve 28,39 grams of  $\text{Na}_2\text{HPO}_4$  in 500 ml heated distilled water then make up 1L.

**Solution B:** Make 500 ml of 0,2 M  $\text{NaH}_2\text{PO}_4 \cdot \text{H}_2\text{O}$  (hydrous), pH = 7,4 .

Dissolve 13,78 grams of  $\text{NaH}_2\text{PO}_4 \cdot \text{H}_2\text{O}$  in 500 ml distilled water.

2. Palade's Buffer (Veronal Acetate Buffer ):

Dissolve 2,89 grams of barbital sodium and 1,15 grams of anhydrous sodium acetate ( or 1,90 grams of hydrous sodium acetate ) in 70 ml of distilled water.

Make up to 100 ml.

3. 0,1 Normal HCl. Used as supplied by manufacturer.
4. 2% Osmium Tetroxide. Use ampules as supplied by manufacturer.
5. Palade's 1% Osmium Fixative Solution. Add 12,5 ml of 2% Osmium Tetroxide, 5ml Palade's Buffer, 5 ml of 0,1 Normal HCl and 2,5 ml distilled water.
6. 2% Uranyl acetate. Dissolve 2 grams of uranyl acetate in 100 ml of 70% alcohol. Uranyl acetate is light-sensitive and should be kept in the dark.
7. Absolute alcohol. Use distilled water to dilute to the various concentrations.
8. Acetone. Use concentrated or diluted to the appropriate concentrations with distilled water where required.

9. Spurr's Epoxy Resin. The standard embedding medium is formulated as follows:  
Add 10,0 grams ERL 4206 resin, 6,0 grams DER 736 (flexibiliser), 26,0 grams NSA hardener and 4,0 grams S1 accelerator together and mix with a magnetic stirrer until all air bubbles are released from the resin mixture. All work were done in a fume cupboard since many of the chemicals are toxic.
10. 2 mM Sodium Methoxide. Dissolve 10 grams of sodium (solid metal) in 200 ml methanol. Evaporation will occur, therefore solution must be made up to 200 ml after fuzzing has stopped. Add 10 ml benzene.
11. Reynold's Lead Citrate. Add 1.33 grams of lead nitrate and 1.76 grams of sodium citrate to 30 ml of distilled water (freshly boiled to remove carbon dioxide) and shake vigorously for 1 minute. A heavy white precipitate will be formed. Shake the solution every 5 minutes over 30 minutes period to facilitate conversion of lead nitrate to lead citrate. Add 8 ml of 1N sodium hydroxide with agitation and dilute to 50 ml with distilled water. The white precipitate of lead citrate will dissolve during this step.
12. 1% Toluidine Blue. Dissolve 1 gram Toluidine Blue in 100 ml distilled water.

**b) Program for primary fixation**

**Program for standard secondary tissue fixation and embedding**

1. Post – fixation in 1% osmium tetroxide for 45 minutes – 1 hour.
2. Rinse twice with distilled water over 20 minutes.
3. Place in 2% uranyl acetate for 30 minutes (enhances general contrast and aids as tertiary fixatives).

4. Dehydrate through 2 changes of 80% alcohol over 10 minutes.
5. Dehydrate through 2 changes of 95% alcohol over 10 minutes.
6. Dehydrate through 3 changes of 100% alcohol over 30 minutes.
7. Rinse in 2 changes of 100% acetone over 30 minutes.
8. Impregnate in a 1:1 mixture of 100% acetone/Spurr's resin overnight, at least for 12 hours, at room temperature.
9. Impregnate with fresh Spurr's resin for 1 hour under vacuum.
10. Impregnate with fresh Spurr's resin for 2 – 5 hours under vacuum.
11. Embed with fresh Spurr's resin in oven-dried embedding capsules and polymerize in an incubator for 16 hours at 60°C.
12. Remove capsules from incubator and allow setting for 2 hours.
13. Microtomy.

**c) MICROTOMY**

**Steps to follow in Microtomy**

The following steps are followed in cutting ultra-thin sections:

1. Trimming the resin blocks. The blocks that are embedded in capsules have a flat base, which are trimmed with a wax free blade to form a pyramid with the tissue situated at the apex of the pyramid. The block are then stabilized within the ultra-microtome and trimmed until the tissue is exposed. The face of the block being the shape of a trapezium is then suitable for 1µm thick sectioning (Figure 4.1).



2. Preparation of glass knives. Before thin sections can be cut, a glass knife has to be prepared to serve as the cutting edge. For this purpose, a LKB Bromine 7800 knifemaker was used. This instrument combines the functions of scoring and breaking the glass into squares or rhombi and then into knives of various angles. When properly set up, the knifemaker scores the 25 mm wide glass strip at a preset position and applies controlled pressure on the glass to form a break. The rhombus produced is then positioned diagonally in order to form a 45° cutting edge, which will produce two knives, from a square (Figure 4.2).
  
3. An ideal knife-edge should be very thin, straight across or slightly convex and should have no nicks or irregularities. This assessment is carried out by examining the knife with a stereomicroscope. For cutting thicker sections a thin strip of dental wax 1 mm across the knife is sufficient. A trough or boat for holding the liquid onto which the sections are floated must be attached to the face of the knife below the cutting edge. The form of a trough is made with adhesive aluminum tape, which is attached to each side of the cutting edge to form a water container on the diagonal side of the cutting edge. Dental wax is used as a sealant to close the small gap left at the bottom of the trough (Figure 4.3).

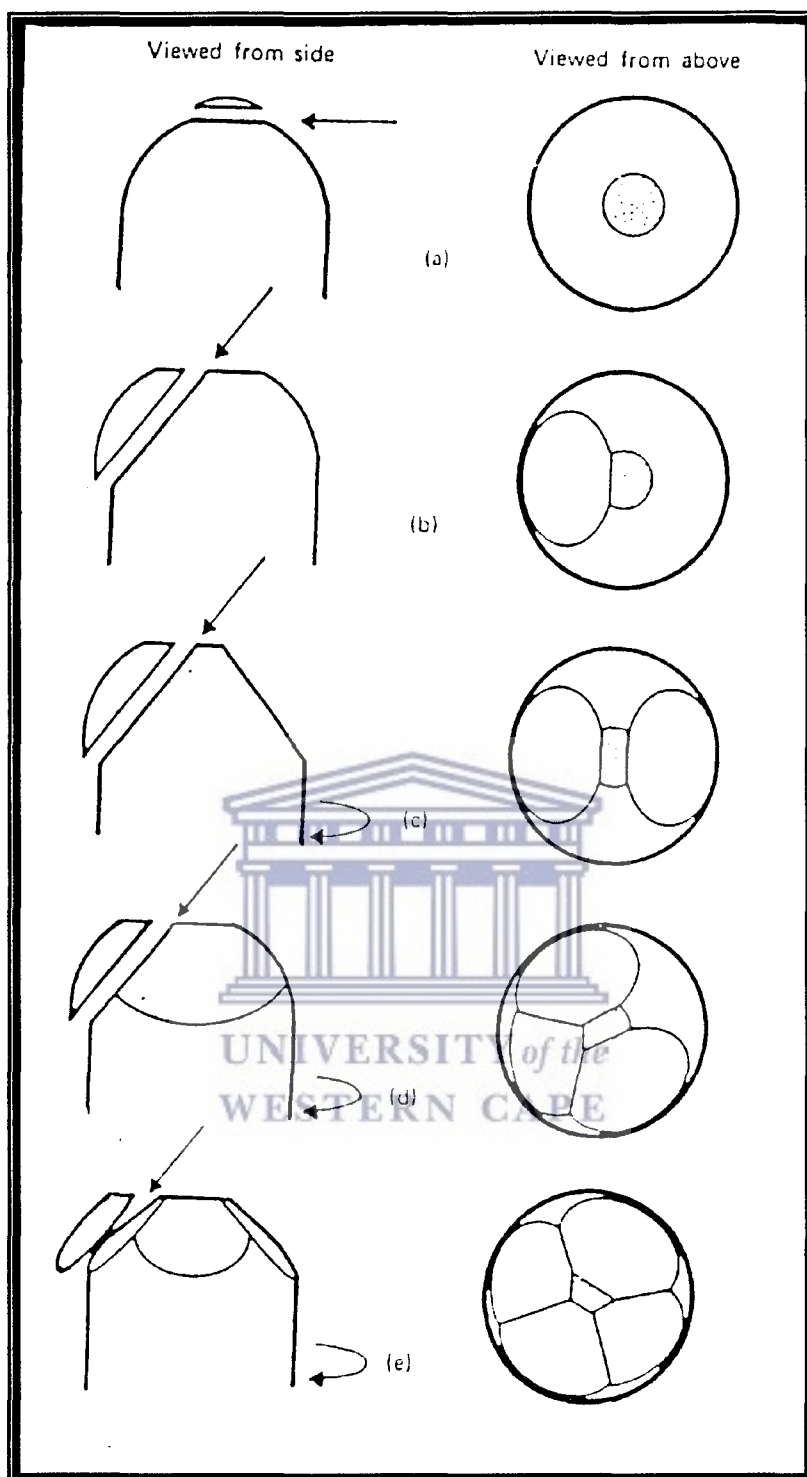
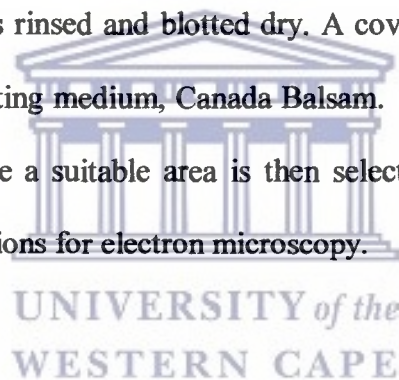


Figure 4.1: The stages in the trimming of a specimen block. The straight arrows indicate the directions of the cutting with the trimming blade.



4. Thin sectioning. One micron sections are cut with a glass knife on a Sorvall MT – 5000 Ultra – Microtome, picked up with a orange stick and transferred onto a drop of water on a clean, labeled slide. The slide is placed on a hotplate in order for excess water to evaporate as well as to adhere the sections to the slide. Thereafter the slide is placed into a jar containing 2mM Sodium Methoxide which facilitates penetration of the dye used (1% Toluidine Blue) (Giddings et al., 1982), after which it is rinsed twice in absolute alcohol thus ensuring the removal of the Sodium Methoxide and also facilitates penetration of the stain. The slide is placed on to a staining rack and a few drops of 1% Toluidine Blue are poured over the sections. The slide is then placed on the hotplate until the vapour is given off from the dye, after which it is rinsed and blotted dry. A coverslip is then placed on the slide by using the mounting medium, Canada Balsam. The sections are viewed by using a light microscope a suitable area is then selected which will be used for obtaining ultra–thin sections for electron microscopy.



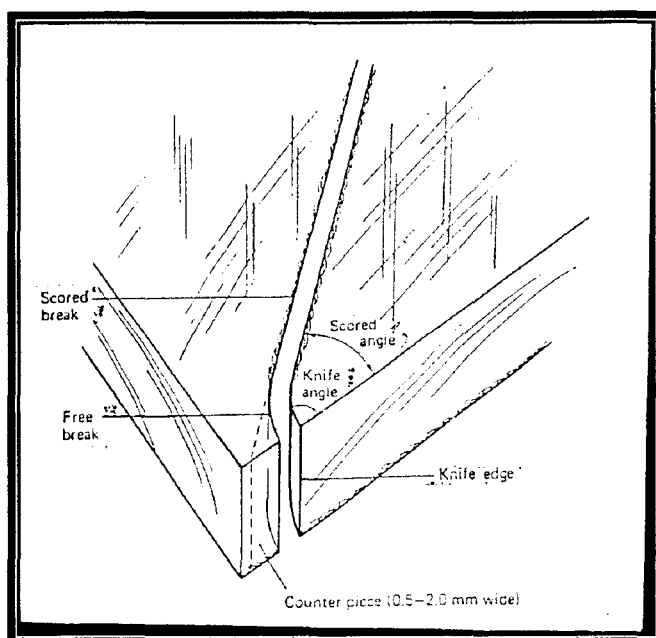


Figure 4.2: Enlargement of the corner of a glass square showing the knife angle is greater than the scored angle because the free break curves away from the corner.

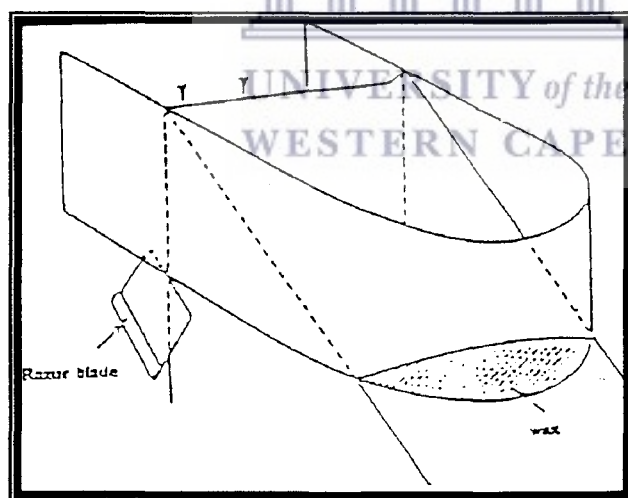


Figure 4.3: Adhesive tape applied to a glass knife to form a trough. The cutting edge is marked with arrows.

5. Ultra-microtomy. The face of the sectioned block is retrimmed to a size suitable for ultramicrotomy after examination of the 1  $\mu\text{m}$  sections. The size of the face depends on the consistency of the resin, the type of tissue and the quality of the knife being used. The ultra-microtome is set to advance at 60 nm intervals and will subsequently advance automatically and cut sections of the specified thickness. For a straight and coherent ribbon of sections to be formed during sectioning the two parallel edges of the trapezium must be cut as precisely as possible. The sections are picked up using a 400 mesh copper grid which is then placed on filter paper in closed petri dishes to dry. By using heavy metal salts stains the contrast of these sections are further enhanced.

6. Staining ultra-thin sections. Two dental wax strips are used as staining blocks. These are placed in both halves of a clean, wet piece of blotting paper with a petri dish covering the blotting paper. Uranyl acetate droplets, equivalent to the number of grids being stained are placed on the first strip of wax. These drops are filtered through a millipore filter to prevent sedimented crystals from being deposited onto the specimens. The grids are then placed onto the drops for 5 minutes and then rinsed with distilled water by rapid dipping into the filled beakers. Each grid is placed on a filtered drop of Reynold's lead citrate for 10 minutes in a covered petri dish. The grids are again rinsed by rapid dipping of it in two beakers of distilled water respectively. The grids are again rinsed by rapid dipping of it in two beakers of distilled water respectively. The grids are then dried on filter paper and placed into a closed petri-dish, ready for viewing.